

A cellular automaton model of *Eldana saccharina* Walker infestation in sugarcane to improve the spatio-temporal planning of sugarcane planting and harvesting



Thesis presented in partial fulfilment of the requirements for the degree of
Master of Commerce
in the Faculty of Economic and Management Sciences at Stellenbosch University

Declaration

By submitting this thesis electronically, I declare that the entirety of the work contained therein is my own, original work, that I am the sole author thereof (save to the extent explicitly otherwise stated), that reproduction and publication thereof by Stellenbosch University will not infringe any third party rights and that I have not previously in its entirety or in part submitted it for obtaining any qualification.

Date: December 1, 2020

Abstract

Farmers are being increasingly challenged to use management techniques that reduce the negative impacts of farming. One of the main areas where the environment is negatively impacted by farming practices is pest management when using chemical pesticides. The manipulation of harvesting schedules has long been recognised to impact pest populations in agricultural crops and plays an important role in establishing an integrated pest management (IPM) system.

In this study, the impact of differently configured sugarcane agricultural landscapes in terms of crop age, and the resulting different harvesting times, on the infestation dynamics of *Eldana saccharina* Walker, were considered. The dynamics of *Eldana saccharina* Walker infestation in sugarcane were simulated using a cellular automaton approach. The main objective was to identify generic field configurations (in terms of crop age) where infestation levels are minimised, and subsequently sucrose yield was maximised.

The results obtained indicate that larger groupings of same aged crops tend to provide higher sucrose yields, compared to configurations where many same aged small fields were scattered across the landscape. It was also determined that harvesting spread over the entire harvesting season with various aged crops tended to outperform scenarios with bulk harvesting of crops only at certain times during the harvesting season. In addition, an earlier harvesting age was found to be better, indicating that if possible, sugarcane should not be carried over during the period when sugarcane mills are closed.

Uittreksel

Boere word toenemend uitgedaag om bestuurstegnieke wat die negatiewe gevolge van die boerdery sal verminder, te gebruik. Die gebruik van chemiese plaagdoders is een van die hoof redes waarom die omgewing negatief beïnvloed word deur boerderypraktyke. Die invloed wat die manipulerings van oestye op plaagpopulasies in landbougewasse het, is lankal reeds erken en speel 'n belangrike rol in die instelling van 'n geïntegreerde plaagbestuurstelsel (IPM).

In hierdie studie, word die impak van verskillende konfigurasies van 'n suikerrietlandskap in terme van plant ouderdom, en die gevolglike verskillende oestye, op die infestasië dinamika van *Eldana saccharina* Walker, ondersoek. Die infestasië dinamika van *Eldana saccharina* Walker in suikerriet word gesimuleer deur gebruik te maak van 'n sellulêre outomaat. Die hoofdoel is om generiese veld konfigurasies (in terme van gewas ouderdom) te identifiseer waar infestasië vlakke geminimeer word, en sodoende suikrose opbrengs gemaksimeer word.

Die resultate wat verkry is, dui aan dat groter groeperings van dieselfde gewas ouderdom geneig is om hoër suikrose opbrengste te lewer, in vergelyking met konfigurasies waar baie van dieselfde ouderdom klein velde oor die landskap versprei was. Daar is ook vasgestel dat die verspreiding van die oestye oor die hele oesseisoen met verskillende gewas ouderdomme geneig is om beter te presteer as scenarios met grootmaat oes van gewasse slegs op sekere tye gedurende die oesseisoen. Verder is daar gevind dat 'n vroeëre oes ouderdom beter was, wat daarop dui dat suikerriet, indien moontlik, nie oorgedra moet word gedurende die periode waarin suikerriet meule gesluit is nie.

Acknowledgements

The author wishes to acknowledge the following people for their various contributions towards the completion of this work:

- Thanks to my supervisor, Dr. Linke Potgieter, for the continued support and guidance. I know my progress was frustrating at times, but you never lost faith that I could reach the finish line.
- My fiancée, Anneri van Zyl, for keeping me motivated and helping me through the rough times. Your patience with me during this time is greatly appreciated.
- My parents for all the love and support through the years and giving me the opportunity to pursue my studies.
- The Department of Logistics for the use of their facilities and all the open doors with a well full of wisdom, guidance and life lessons.
- The South African Sugarcane Research Institute for their financial support for this research and for sharing with me their expert knowledge on all things Eldana.
- To all my friends and family for all the words of encouragement throughout all my studies.

Table of Contents

List of Acronyms	xiii
List of Figures	xv
List of Tables	xix
1 Introduction	1
1.1 Background	1
1.2 Problem Description	2
1.3 Scope and Objectives	2
1.4 Thesis Organization	2
2 Literature Review	5
2.1 Sugarcane	5
2.1.1 Agricultural	6
2.1.2 Production	6
2.2 <i>Eldana sacharina</i> Walker	7
2.2.1 Physical Description	7
2.2.2 Habitat	7
2.2.3 Dispersal	9
2.2.4 Sugarcane Damage	9
2.3 Pest Management Strategies	10
2.4 Cellular Automata	11
2.4.1 Characteristics	12
2.4.2 Neighbourhood	12
2.4.3 Boundary Conditions	13
2.5 Chapter Summary	13

3	Simulation model	15
3.1	Model Description	15
3.2	Assumptions	16
3.3	Model formulation	17
3.3.1	Infestation state	17
3.3.2	Crop state	18
3.3.3	Boundary conditions	18
3.3.4	Initial conditions	19
3.4	Parameterisation	21
3.5	Model output	22
3.6	Solution evaluation	23
3.7	Computer implementation	24
3.7.1	Initialisation phase	24
3.7.2	Main phase	26
3.7.3	Output phase	28
3.8	Model verification	28
3.8.1	Infestation spread	29
3.8.2	Harvesting and planting process	30
3.9	Chapter Summary	32
4	Results	33
4.1	Statistical validation	33
4.2	Agricultural landscape structures	34
4.2.1	Harvesting age	34
4.2.2	Field sizes	35
4.2.3	Age groups	35
4.3	Simulation results	36
4.3.1	Maturity functions	37
4.3.2	Harvesting age	38
4.3.3	Initial allocation pattern	38
4.3.4	Field size	40
4.3.5	Age groups	42
4.4	Sensitivity Analysis	46
4.4.1	Maturity function value	46
4.4.2	Alpha value	47
4.5	Recommendations	48

Table of Contents	xi
4.6 Chapter Summary	49
5 Decision support tool	51
5.1 Description of the decision support tool	51
5.1.1 Initial allocation	51
5.2 GIS incorporation	51
5.3 User interaction	53
5.3.1 Shapefile	53
5.3.2 Initial structure	55
5.4 Model output	55
5.4.1 Infestation state	55
5.4.2 Sugarcane growth	56
5.4.3 Sugarcane yield	56
5.5 Chapter Summary	56
6 Conclusion	57
6.1 Thesis Summary	57
6.2 Main Contributions	58
6.3 Possible Future work	59
References	61
Appendices	65
A Initial infestation probabilities	65
B Field size analysis	69
B.1 Increasing maturity function	69
B.2 Decreasing maturity function	72
B.3 Shaped maturity function	75
C Age group analysis	79
C.1 Increasing maturity function	79
C.2 Decreasing maturity function	82
C.3 Shaped maturity function	85
D Sensitivity analysis: Maturity function	89

List of Acronyms

GIS: Geographic Information System

CA: Cellular Automata

SASRI: South African Sugarcane Research Institute

SASTA: South African Sugar Technology Association

IPM: Integrated Pest Management

EGT: Effective Growth Time

List of Figures

2.1	Sugarcane fields	6
2.2	The life cycle of Eldana	7
2.3	The different life stages of Eldana	8
2.4	Damage to sugarcane done by Eldana	10
2.5	CA neighbourhood structures	13
3.1	Infestation curves for maturity functions	22
3.2	The simulation process	24
3.3	Initial allocation patterns	26
3.4	Process to update a cell	27
3.5	Process for updating crop state	28
3.6	Infestation spread within the simulation	29
3.7	Observed harvesting yields	30
3.8	Visualisation of the harvesting process	31
3.9	Visualisation of the planting process	32
4.1	Illustration of different field sizes	35
4.2	Illustration of different age groups	36
4.3	Maturity function comparison	39
4.4	Effect of harvesting age	39
4.5	Field size yield trend for 8 month harvesting age	41
4.6	Field size yield trend for 10 month harvesting age	41
4.7	Field size yield trend for 12 month harvesting age	42
4.8	Field size yield trend for 14 month harvesting age	42
4.9	Field size yield trend for 16 month harvesting age	43
4.10	Field size yield trend for 18 month harvesting age	43
4.11	Age group yield trend for 8 month harvesting age	44
4.12	Age group yield trend for 10 month harvesting age	44

4.13	Age group yield trend for 12 month harvesting age	45
4.14	Age group yield trend for 14 month harvesting age	45
4.15	Age group yield trend for 16 month harvesting age	46
4.16	Age group yield trend for 18 month harvesting age	46
4.17	Analysis of maturity factor	47
4.18	Analysis of alpha value	48
5.1	Visualisation of shapefile	52
5.2	Grid overlay of shapefile	52
5.3	Visual of simulation based of shapefile	53
B.1	Field size comparison for increasing function and 8 months harvesting age	69
B.2	Field size comparison for increasing function and 10 months harvesting age . . .	70
B.3	Field size comparison for increasing function and 12 months harvesting age . . .	70
B.4	Field size comparison for increasing function and 14 months harvesting age . . .	71
B.5	Field size comparison for increasing function and 16 months harvesting age . . .	71
B.6	Field size comparison for increasing function and 18 months harvesting age . . .	72
B.7	Field size comparison for decreasing function and 8 months harvesting age	72
B.8	Field size comparison for decreasing function and 10 months harvesting age . . .	73
B.9	Field size comparison for decreasing function and 12 months harvesting age . . .	73
B.10	Field size comparison for decreasing function and 14 months harvesting age . . .	74
B.11	Field size comparison for decreasing function and 16 months harvesting age . . .	74
B.12	Field size comparison for decreasing function and 18 months harvesting age . . .	75
B.13	Field size comparison for shaped function and 8 months harvesting age	75
B.14	Field size comparison for shaped function and 10 months harvesting age	76
B.15	Field size comparison for shaped function and 12 months harvesting age	76
B.16	Field size comparison for shaped function and 14 months harvesting age	77
B.17	Field size comparison for shaped function and 16 months harvesting age	77
B.18	Field size comparison for shaped function and 18 months harvesting age	78
C.1	Age group comparison for increasing function and 8 months harvesting age . . .	79
C.2	Age group comparison for increasing function and 10 months harvesting age . . .	80
C.3	Age group comparison for increasing function and 12 months harvesting age . . .	80
C.4	Age group comparison for increasing function and 14 months harvesting age . . .	81
C.5	Age group comparison for increasing function and 16 months harvesting age . . .	81
C.6	Age group comparison for increasing function and 18 months harvesting age . . .	82
C.7	Age group comparison for decreasing function and 8 months harvesting age . . .	82

C.8	Age group comparison for decreasing function and 10 months harvesting age . . .	83
C.9	Age group comparison for decreasing function and 12 months harvesting age . . .	83
C.10	Age group comparison for decreasing function and 14 months harvesting age . . .	84
C.11	Age group comparison for decreasing function and 16 months harvesting age . . .	84
C.12	Age group comparison for decreasing function and 18 months harvesting age . . .	85
C.13	Age group comparison for shaped function and 8 months harvesting age	85
C.14	Age group comparison for shaped function and 10 months harvesting age	86
C.15	Age group comparison for shaped function and 12 months harvesting age	86
C.16	Age group comparison for shaped function and 14 months harvesting age	87
C.17	Age group comparison for shaped function and 16 months harvesting age	87
C.18	Age group comparison for shaped function and 18 months harvesting age	88

List of Tables

3.1	Initial infestation level probability lookup table	20
3.2	Expected sucrose yields	23
3.3	Infestation state colour scale	25
3.4	Crop state colour scale	27
3.5	Crop age colour scale	27
4.1	Statistical validation results - Part 1	34
4.2	Statistical validation results - Part 2	34
4.3	Crop ages at model initialisation	37
4.4	Highest yields obtained	38
4.5	Analysis of initial allocation patterns	40
4.6	Yields obtained for each maturity function factor	47
4.7	Yields obtained for each alpha value	48
A.1	Probability lookup table for Decreasing maturity function.	66
A.2	Probability lookup table for Increasing maturity function.	67
A.3	Probability lookup table for Shaped maturity function.	68
D.1	Yields for maturity factors - Part 1	89
D.2	Yields for maturity factors - Part 2	89

CHAPTER 1

Introduction

Contents

1.1	Background	1
1.2	Problem Description	2
1.3	Scope and Objectives	2
1.4	Thesis Organization	2

In recent years, there has been a global move to research and the establishment of environmentally friendly farming practices, especially within the context of pest management. As a result, a number of integrated pest management (IPM) systems in a variety of agricultural ecosystems have been developed that combines biological control of pest species, varietal resistance, appropriate farming practices and minimises the use of chemical pesticides. In South Africa, the sugarcane industry has been using an IPM system developed by the South African Sugarcane Research Institute (SASRI) that includes a number of good farming practices. This include, the use of more resistant sugarcane varieties, the removal of old stalks in the field, pre-trashing, improved soil management and the use of uninfested seedcane. The current sugarcane IPM system does not yet include newer interventions such as the use of biological control or habitat management, and ways to incorporate these approaches are under consideration. [30]

Land management is the process of managing the use and development of land resources. Habitat management in particular is a land management practice that seeks to restore habitat areas for wild plants and animals. In the context of sugarcane, the restoration of important natural habitat areas of sugarcane pest species may reduce infestation within sugarcane fields. Furthermore, the use of push and pull plants reduces *Eldana saccharina* Walker (hereafter referred to as Eldana) damage to sugarcane and may even lead to a reduction in the development of resistance towards insecticides. In this thesis, the configuration of the sugarcane landscape in terms of the crop age is considered as an alternative land management practice. [30]

1.1 Background

The history of Eldana as a sugarcane pest in South Africa started in 1939 when it was found in sugarcane on the Umfolozi flats. The outbreak was confined to the area until 1953, after which the pest died out due to the advent of harder varieties of sugarcane. Further outbreaks followed in 1972, with the pest found at Empangeni as well as northern Swaziland. These infestations increased in 1973 and infestations were also noted at Mtunzini, Gingindhlovu and in the eastern

Transvaal. The following year also led to a reappearance of the pest in the Umfolozi flats, 20 years after the first outbreak in this area. [4, 7]

Eldana has since established itself as a pest in the sugarcane industry of South Africa, leading to great losses in sucrose yields and sugarcane quality. Extensive research has been done on how to combat the pest, as well as numerous research on the behaviour of Eldana to inform more biological friendly strategies of pest management.

1.2 Problem Description

In a previous study by Potgieter et al. [29] the existence of an optimally diversified sugarcane habitat in terms of crop age, which may contribute to lower infestation levels, was hypothesized, and investigated using a mathematical model. The study employed a reaction-diffusion model to simulate the population dynamics of Eldana in sugarcane on differently configured sugarcane fields in terms of crop age. Experimental simulation runs were performed on four ha sugarcane spatial domains, however, only regular shapes were considered for the simulated sugarcane habitats which is an unrealistic representation of a sugarcane landscape. The study by Potgieter et al. [29] found that more diversified field configurations, in terms of crop age, with boundaries between different ages as small as possible led to lower average infestation levels. The primary aim of this thesis is to test the hypothesis presented in the research by Potgieter et al. [29] by developing an alternative simulation model of Eldana infestation in sugarcane in which larger sugarcane spatial domains as well as irregular field shapes typical of a sugarcane landscape are considered by incorporating GIS information, and that captures the stochastic nature of the problem better than the deterministic approach followed by Potgieter et al. [29].

1.3 Scope and Objectives

The scope of this thesis will be restricted to Eldana infestations in sugarcane. The effect of variations in the configuration of the agricultural landscape will be inspected, with these variations limited to the age of sugarcane. The following main objectives will be pursued:

1. Review literature regarding pests in sugarcane and the pest management strategies applied.
2. Use a cellular automaton approach to develop a simulation model that describes Eldana infestation in sugarcane as a function of crop age.
3. Compare various agricultural landscape configurations in terms of crop age by considering sugarcane yield and Eldana infestation levels in different simulation runs.
4. Expand the model to incorporate GIS data regarding the landscape.
5. Elaborate on the limitations of the research and provide direction for future studies.

1.4 Thesis Organization

This thesis consists of six chapters, of which the first is this introductory chapter. In Chapter 2, a literature review of previous research done related to Eldana are presented, as well as an introduction to the methodology that is used in the model development in this research study.

The chapter provides the reader with sufficient knowledge regarding the biological aspects of sugarcane and Eldana, to understand the implementation of Eldana infestation in sugarcane in the simulation model. The chapter also provides the reader with a basic understanding of cellular automaton methodology.

The simulation model is described in Chapter 3, together with the GIS implementation of the model that is used for simulations on different landscape structures. The chapter includes the model assumptions, input and output parameters and the computer implementation of the model. This is followed by Chapter 4, where the results of the various simulation scenarios are provided along with various insights and recommendations based on these results.

In Chapter 5, a decision support tool is presented, showing how the simulation model can practically be utilised. An expansion on the model is also included, with the additional functionality to incorporate GIS data in the underlying landscape structure used by the model. Finally, a short summary of the thesis is presented in Chapter 6 together with the main contributions made by the thesis. Possible future directions for research are also provided in this final chapter.

CHAPTER 2

Literature Review

Contents

2.1	Sugarcane	5
2.2	Eldana sacharina Walker	7
2.3	Pest Management Strategies	10
2.4	Cellular Automata	11
2.5	Chapter Summary	13

For the purpose of providing the reader with a basic knowledge of the research work presented in this thesis, both biological and simulation literature are reviewed in this chapter. Firstly, sections §2.1 & §2.2 will familiarise the reader with sugarcane and the Eldana moth and the influence that Eldana has on the sugarcane yield. Secondly, information regarding current pest management strategies are provided in §2.3, along with a brief overview of previous research regarding these and other strategies.

In §2.4, the Cellular Automata simulation methodology used in this study is explained in detail, providing all the information required by the reader to understand how the simulation model is constructed. This section also highlights previous research that support the relevance of the methodology for this study. Lastly, the chapter concludes with a summary of the chapter in §2.6.

2.1 Sugarcane

Sugarcane (*Saccharum officinarum*), is a perennial grass, cultivated primarily for its juice that is used in the processing of sugar. Sugarcane is primarily grown in subtropical and tropical areas. Sugarcane forms lateral shoots at the base to produce multiple stems. The stems are typically three to four meters in height with a diameter of approximately five centimetres and bear long sword-shaped leaves. The stems grow into cane stalk, which makes up about 75% of the entire mature sugarcane plant. The stalks have many segments, with a bud at each joint. As the cane matures, a slim arrow bearing a tuft of tiny flowers develop at the upper end of the stalk. The mature stalk consists of 11-16% fibre, 12-16% soluble sugar, 2-3% non-sugar and 63-73% water. [15, 36]

A picture of sugarcane fields is provided in Figure 2.1, showing how sugarcane is usually planted for agricultural purposes.

FIGURE 2.1: *Sugarcane fields*

2.1.1 Agricultural

Numerous varieties of sugarcane are produced and specifically designed to suit the agroecological conditions of the South African industry. Varieties are purposefully selected in order to maximise the sucrose yield and improve productivity and profitability in order to counter the pressures of pests and diseases. Depending on the management practices, the crop can be ratooned up to seven times, following planting. A grower is expected to replant 10% of the farm annually. [31]

In most parts of South Africa, harvesting is a manual process, with mechanical harvesting conducted in some parts of Mpumalanga and the Midlands. Cane stalks are cut at the base with the top of the cane stalks cut off to remain in the field [31].

2.1.2 Production

The main reason for sugarcane production is the sucrose that the crop yields. A hectare of sugarcane will, on average, yield between 60 and 70 tonnes of sugarcane per year. This number does however vary depending on climate, farming practices, sugarcane variety and damage from pest species. [15, 36]

A previous study by Stray [32] fitted regression models to historical data received from farms. A first-order as well as a second-order model was fitted, with the second order model performing best. This lead to a base yield model of

$$y = 11.7x - 0.29x^2,$$

where x is the effective growth time (EGT) of the crops. The EGT is determined by the number of months where environmental factors are sufficient for sugarcane growth, with the colder months of June, July and August deemed as no-grow months and do not add to the EGT. This study also makes use of the equation derived by Stray to determine the simulated yields.

2.2 *Eldana sacharina* Walker

Eldana forms part of the Pyralidae family, comprising of only one species, namely the African sugarcane borer, commonly found in Equatorial Guinea, Ghana, Mozambique, Sierra Leone and South Africa. The larvae are a pest to sugarcane, sorghum and maize, with some other host plants recorded as cassava, rice and *Cyperus* species. The pest is quite resilient, as it can survive crop burnings [35].

2.2.1 Physical Description

The complete *Eldana* life cycle is illustrated in Figure 2.2, consisting of an egg, larval, pupal and moth stage. The larvae are insatiable feeders that hollow out the sugarcane stem and pushes out frass through holes in the stem. The hatching larva does not enter the stem immediately after hatching and initially feeds on the sugarcane leaves or bits of organic matter. Once the larva is strong enough to enter the plant tissue, it enters the cane stem to spend the rest of its emergent active live as a borer in the stem. There is great variability in the development time of the *Eldana* larval stage [6]. The larval period varies by season from 20 days during the summer months and up to 60 days during the winter months. During this time the male moult five or six times and the female will typically moult between six or seven times. The quality and the nitrogen levels of the food supply was found to influence the development time of the larvae. [5, 13, 34]

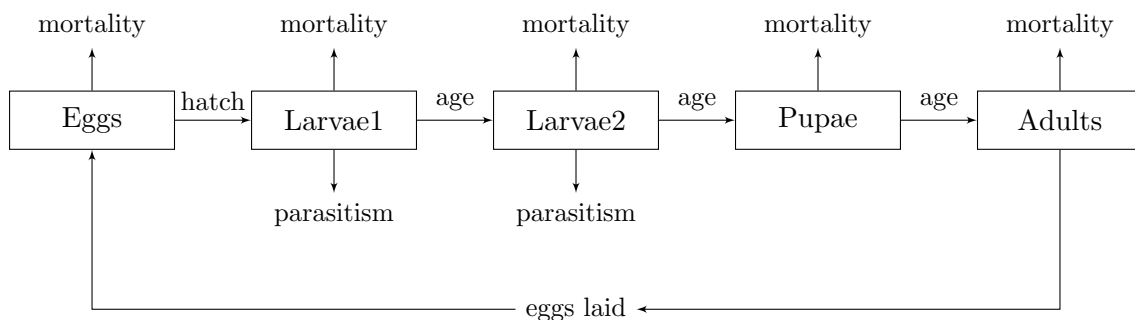


FIGURE 2.2: *The life cycle of Eldana*

Once a larva matures, it spins a protective cocoon to pupate within. The pupa will either be located within the hollowed stem or it can be found covered by a leaf sheath on the outside of the stalk. The adult moth will emerge after approximately 10 days, usually shortly after sunset to mate. The female will start oviposition approximately 24 hours after mating and is known to travel up to 200m before laying her eggs. It is however more common for the eggs to be laid close to the emergence site. The female lays approximately 450 eggs in batches of 20 each. The eggs hatch in 8 to 10 days. [7]

A picture of the various life stages of *Eldana* is given in Figure 2.3, showing the eggs, larvae, pupae and adult moth.

2.2.2 Habitat

Eldana is native to Africa and predominantly lives in sedges and wild grasses amongst riverine vegetation. Recently, the borers have extended their range to graminaceous crops in the eastern and southern parts of Africa. The species is not as widespread in the sandier soil areas [35]. The

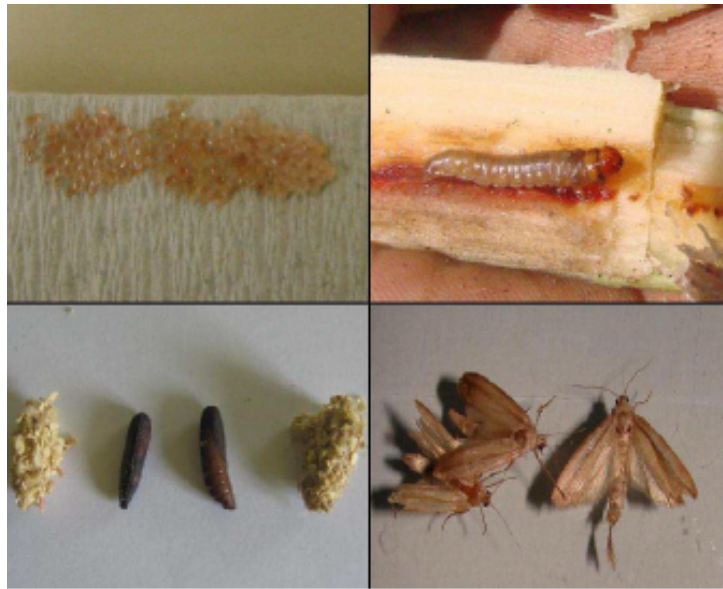


FIGURE 2.3: *The different life stages of Eldana*

polyphagous borer favours monocots as host plants. It originally infested maize and sorghum, but has since gained pest status in sugarcane as well [10].

Eldana distribution is not uniform across Africa, with recent studies showing that in South Africa the pest is moving inland from the warmer coastal regions. This poses an increased threat to sugarcane and it also poses a renewed threat to maize. From the first outbreak on the Umflozi flats in KwaZulu-Natal in the 1940s, where Eldana was first identified as a sugarcane pest, the incidence of the pest decreased up until the 1970s with the second outbreak. Now, the pest is known as one of the most harmful pest to sugarcane in South Africa, with direct economic loss due to damage caused by the insect estimated at R60 million per annum [10]. The area most affected by the insect in South Africa stretches along the coast from Richards Bay to the Umvoti River mouth. The natural host plant of the insect is *Cyperus immensus* C.B.Cl. The Eldana host plant species, excluding sugarcane, reduces from ten hosts in the northern parts of Natal to five within the region along the coast. South of the Umvoti River, the number of host species reduces to one. The infestation of sugarcane in this region is heavier than the rest of the Natal cane belt. The host plant species that extend further south are not heavily infested by Eldana, with numerous occurrences of *Cyperus prolifer*, *C. sexangularis*, *C. fastigiatus*, *Kyllinga spp.* and *Pymeus polystachyus* south of the Umvoti river not attacked. Infestation decreases slightly when moving inland, which could be attributed to the cooler conditions. Sugarcane infestation increases with the decrease in natural hosts in the Empangeni and Amatikulu areas. Further south the insect is more frequently found in the natural host than in sugarcane [3].

The insect prefers dead leaf material and rarely uses green tissue, with no eggs found in the flowers of *Cyperus immensus*. Although sugarcane is not the preferred host for the insect, the abundance of dead leaf material makes sugarcane a favourable host. The oviposition frequency in sugarcane is twice the oviposition frequency in *C. latifolius*. Sugarcane is thus actively selected by the insect for oviposition [3].

The preferred oviposition sites are under the leaf sheaths or in the area between the stem and soil. Eggs are also laid on clods or plant residue [7]. During certain stages of the insects development, it is well protected from both natural and applied controlling factors. The larvae feed internally and the pupae is protected by the frass embedded cocoon. The more exposed stages are thus the

neonate larvae that disperse from the oviposition sites and the dispersal, mating and oviposition stages of the adult moth [24].

Primary feeding sites on sugarcane is the middle and base of mature tillers. With the node as the most common penetration site, feeding starts at the node and extend toward the internode. Feeding of 2cm to 8cm is required to produce mature larvae [3].

2.2.3 Dispersal

The female is known to travel up to 200m before laying her eggs. It is however more common for the eggs to be laid close to the site of emergence [7]. Leslie [24] studied the dispersal behaviour on the sugarcane stalks as well as dispersal in litter of the neonate larvae on three varieties of sugarcane with differing susceptibility to the *Eldana* borer. The three varieties NI1, NC0376 and N8 used as part of the study range between susceptible, intermediate and resistant respectively. [24].

The dispersal of larvae on sugarcane was measured at daily intervals. One day after hatching, the majority of the larvae moved up to 300mm away from where it has hatched. Dispersal up to 1000mm, mostly upward, was recorded on the second day after hatching, with dispersal on the most resistant sugarcane varietal occurring at a noticeably slower pace. This dispersal pattern continued for the third and fourth day after hatching, with the larvae moving further and further away from the hatching site. The movement toward the root bands and internodes was at a slightly slower pace on the most resistant varietal tested. On the susceptible and intermediately resistant varietals, the preferred boring sites were the cracks and buds, where the preferred boring site on the most resistant varietal was the internodes. Very few larvae were found to penetrate the most resistant varietal during the trials [24].

2.2.4 Sugarcane Damage

Up to 12 larvae can be found in a single joint. The borers extend into the underground parts of the stool as well, attacking all parts of the stalk [7]. As soon as the pest is present in an infested sugarcane field, it increases rapidly as the crop ages [10].

The assessment done by King [22] has shown that the recoverable sucrose yield decreases with the increase in damage to the stalks. This results in a decrease in cane quality and mass, although the quality decrease is of greater concern. Sugarcane quality is measured by the percentage sucrose yield and the sugarcane juice purity (which is the percentage of sucrose in total solids in the juice). The lower the sucrose yield and juice purity, the lower the cane quality. As the level of damage increase the brix percentage decreases while the fibre percentage is only affected at the highest level of damage, due to a reduction in water uptake [17]. The moisture levels are unaffected by the damage and shows a tendency to increase with the increase in damage. In King's assessment, the major effects on the quality of the cane could be directly associated with the level of damage and seem to be more severe mid-season [22]. The reduction in quality of the sugarcane could also be attributed to the fungus associated with the *Eldana* borings. This fungus is known to cause deterioration of sucrose molecules. In Figure 2.4, a sugarcane stalk that was bored by *Eldana* is shown, where the red areas are the fungus associated with *Eldana*. [25, 26]

The reduction in the cane mass cannot be directly attributed to the level of damage, suggesting that *Eldana* has a negative influence on the plant growth with a significant reduction in the stalk length rather than the diameter [17]. The effect on the cane mass was more apparent on



FIGURE 2.4: *Damage to sugarcane done by Eldana*

samples taken later in the season and the yield losses are thus greater in cane harvested late in the season [22].

King's findings conclude that there is a 1% loss in the yield of recoverable sucrose per 1% internode damage, in 11 to 12 month old cane. Seasonal effects are significant with losses varying from 0.7% in the early season to 1.3% toward the end of the season [22].

2.3 Pest Management Strategies

The hatching larvae are a very suitable target for applied control measures, such as pre-trashing [8] and the application of insecticide [20]. The knowledge gained from their behaviour aids in the development of control measures [24]. As soon as the larvae enters the plant tissue, it is well protected from control measures. The cocoon protects the pupa from control measures. Certain insecticides are not recommended due to the effect of the insecticides on ants. Ants are known to destroy the eggs as well as the hatching larvae before the larvae are able to start the boring process [7].

The most important measure of control is in harvesting the sugarcane as early as possible as well as the reduction or avoidance of stand-over cane. Crop age therefore plays an important role in infestation levels. By cutting cane below ground level, the chances of borers remaining in the stubble and surviving into the next ratoon is reduced. All remaining stubble should be covered with soil and no plant material should be left over in the field after harvesting to ensure that no borers or moths move to the ratooning cane [7].

The environmental risks associated with pesticide use, the resistance and increased cost of fossil fuel has renewed the interest in the more sustainable control methods, such as habitat management [10]. Habitat management is part of the conservation biological control approach to pest management. These controls include the manipulation of the agroecosystem to protect

and enhance the natural, locally occurring enemies and in turn reducing the effect of Eldana on the crop [14]. Push-pull is a specific type of habitat management used as part of the IPM approach to control Eldana in sugarcane. With the push-pull method, certain components in the agroecosystem attract the pests and other deter the pests [12, 18]. A habitat management system designed to increase the efficiency of the natural enemies of Eldana is required based on the constraints in establishing biological control agents for Eldana in sugarcane [10].

Eldana naturally favours indigenous host plants over sugarcane. The reason for the shift from the preferred host plants to sugarcane can be attributed to the rapid expansion of sugarcane in KwaZulu-Natal in South Africa. A decrease due to natural predation in the new crop environment was as a result of the natural enemies of Eldana not following into the sugarcane fields. With the natural enemies no longer present in the new environment, Eldana was no longer under natural control and the insect population started increasing. The natural enemies, particularly parasitoids ensures an equilibrium in the Eldana population in the natural host as the parasitoids population will peak just after the Eldana population and as soon as the parasitoids reach high numbers, the Eldana population decreases. Parasitism of Eldana is extremely low in sugarcane. Establishment of parasitoids have been very poor when released in sugarcane fields, due to a lack of kairomones or herbivore-induced plant volatiles released when Eldana feeds on sugarcane. Parasitoids use kairomones to find a suitable host. [10]

The current Eldana control recommendations form part of an IPM framework, providing a complete approach to pest management under the four main focus areas of host plant resistance, chemical, cultural and biological control. The following definition by Kogan [23], incorporates the most common understandings of IPM: “IPM is a decision support system for the selection and use of pest control tactics, singly or harmoniously coordinated into a management strategy, based on cost/benefit analyses that take into account the interests of and impacts on producers, society, and the environment.”

Good cultural control is emphasized in the current control measures. Crop health, soil moisture and nutrient levels, field hygiene, planting of the correct varieties of sugarcane as well as the age at which the sugarcane is harvested all play a very important role in the management of Eldana. Chemical control is recommended in cases where older crops with high levels of infestation need to be carried over, due to the sugar mills closing before completion of the harvesting process. Currently, the only registered insecticide for use against Eldana is alpha-cypermethrin [10]. IPM recommends limited use of insecticides in order to prevent any build-up or resistance and reduce the negative effects that insecticides have on the environment.

Biological control is not currently included in the Eldana management guidelines, although SASRI has been involved in biological control measure research since 1975. Although numerous biological control agents have been identified and tested in the Insect Unit at SASRI, very few parasitisms have been successfully established [10, 11].

2.4 Cellular Automata

Cellular automata (CA) are mathematical models for the explicit simulation of a system in which many simple components act together in a pre-defined manner to produce complicated patterns of behaviour [27]. According to Ermentrout [16], CA models are an appropriate methodology for modelling biological systems, with the CA able to represent various spatial and temporal patterns. Although CA are simplified models, they are capable of modelling very complicated behaviour and are useful for examining larger parameter ranges. CA are regularly used as alternatives to diffusion equations or partial differential equations (PDEs), mostly due to being

computationally cheaper [16, 19, 37].

There are various other examples of CAs applied to real world problems. Karafyllidis [21] developed a CA to simulate the spread of forest fires, for the ease of incorporating weather conditions and land topography. Arai [2] also made use of a CA for the ability to integrate with Geographic Information System (GIS) data, once again using it to model the spread of forest fires. The use of CAs has become more and more popular as may be seen in the numerous applications shown in the review by Ermentrout [16] and the book by Adamatzky et al [1] as well as the other studies cited within this study [1], spanning both physical and biological systems.

In the context of this study, a CA is used to describe the dynamics of an Eldana infestation in a sugarcane landscape, with each cell representing a small sugarcane patch and corresponding infestation level and being influenced by the infestation pressure placed upon it by the cells in its neighbourhood. A CA is used due to the ease of incorporating the underlying GIS data, while maintaining relatively low runtime for larger spatial domains in comparison to the reaction-diffusion model used in the study of Potgieter et al [28].

2.4.1 Characteristics

A CA is defined as an n -dimensional grid of cells, each having a finite number of states in which it can be. Although in practice, most CA models are constructed for one- or two-dimensional spaces. The CA is initialised by setting each cell to a starting state, after which time progresses in discrete time steps. During each time step, every cell updates their state according to a rule that specifies the new value according to the values of a neighbourhood of cells around it at the previous time step. [37]

Chopard [9] defined a CA as having three requirements:

1. a regular lattice of cells covering a portion of a d -dimensional space
2. a set $\Phi(\vec{r}, t) = \{\Phi_1(\vec{r}, t), \Phi_2(\vec{r}, t), \dots, \Phi_m(\vec{r}, t)\}$ of Boolean variables attached to each cell \vec{r} of the lattice and giving the local state of each cell at the time $t = 0, 1, 2, \dots$
3. a rule $\mathbf{R} = \{R_1, R_2, \dots, R_m\}$ which specifies the time evolution of the states $\Phi(\vec{r}, t)$ in the following way

$$\Phi_j(\vec{r}, t + 1) = R_j(\Phi(\vec{r}, t), \Phi(\vec{r} + \vec{\delta}_1, t), \Phi(\vec{r} + \vec{\delta}_2, t), \dots, \Phi(\vec{r} + \vec{\delta}_q, t))$$

where $\vec{r} + \vec{\delta}_k$ designate the cells belonging to a given neighbourhood of cell \vec{r} .

2.4.2 Neighbourhood

Two of the most widely used neighbourhood structures for a two-dimensional CA are shown in Figure 2.5. The nine-neighbour square demonstrated in Figure 2.5(a) is referred to as the Moore neighbourhood, and the five-neighbour square in Figure 2.5(b) is referred to as the Von Neumann neighbourhood. There is no restriction on the size of the neighbourhood as long as it is consistent for all cells. However, only adjacent cells is mostly used in practice. [9, 27]

A totalistic rule indicates that the centre cell only depends on the sum of the values of the cells in the neighbourhood, while outer totalistic rules include the previous value of the centre cell as well as the sum of the values of the neighbouring cells. It is also possible to have triangular or hexagonal cells. [27]

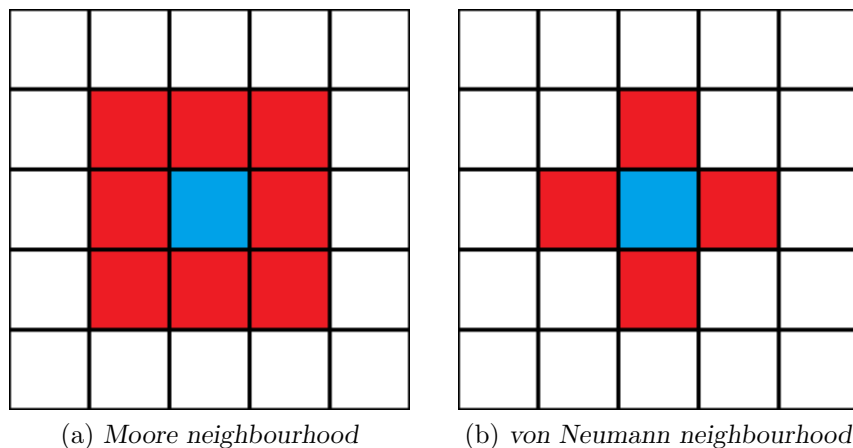


FIGURE 2.5: The neighbourhood (red) of the selected (blue) cell.

2.4.3 Boundary Conditions

It is not possible to model an infinite area with a CA, therefore a boundary must exist. The boundaries of the simulated area depend on the geometry of the CA, which can be separated into two categories: toroidal and non-toroidal. Toroidal geometry assumes that the boundaries are connected, with anything crossing an edge immediately emerging on the opposite edge. Non-toroidal geometry implies the boundaries are fixed, and can be either reflective or dispersive. Reflective boundaries act like a wall which cannot be crossed and is used for modelling enclosed spaces, while dispersive boundaries allows movement across the edges into areas that do not form part of the simulation. [9, 16]

It is clear that cells that form the boundary of the simulated area will not have the same neighbourhood as other cells. Therefore, a different rule is required that considers the appropriate neighbourhood. It is also possible to define several rules for various boundaries, thus it is required to include in the code information regarding which cells are on the boundary and which rule should be applied. [9]

In the case where a toroidal boundary is used, it is also possible to apply a constant rule, independent of whether a cell is on the boundary or not. The neighbourhood of boundary cells will then extend to the cells on the edge of the opposite boundary. [9]

2.5 Chapter Summary

In this chapter, information regarding sugarcane and the pest Eldana was provided. Sugarcane was explained from an agricultural viewpoint, along with the physical description, growth and expected sucrose yields. Information on the life cycle of Eldana was provided, including how infestation growth takes place and the resulting damage to sugarcane that it causes.

Various pest management strategies were explained together with previous research done relating to management of Eldana on sugarcane. The CA simulation methodology was described, providing the reader with information to understand the various aspects of the model.

CHAPTER 3

Simulation model

Contents

3.1	Model Description	15
3.2	Assumptions	16
3.3	Model formulation	17
3.4	Parameterisation	21
3.5	Model output	22
3.6	Solution evaluation	23
3.7	Computer implementation	24
3.8	Model verification	28
3.9	Chapter Summary	32

In this chapter, a detailed description of the CA simulation model is presented, with the model also forming the basis for the GIS simulation approach used. A brief description of the model is given in §3.1, followed by the model assumptions in §3.2. These simplifying assumptions were needed to be able to incorporate the complexities associated with biological modelling into the cellular automaton model. The mathematical formulation of the model is given in §3.3, comprising of the various probability calculations required. The model input parameters are discussed in §3.4, followed by the model output parameters in §3.5. In §3.6, the computer implementation of the model formulation is described as well as the iterative simulation process followed by the model. The verification and validation of the model is presented in §3.7 and §3.8 respectively. The chapter concludes with §3.9, where a summary of the chapter is provided.

3.1 Model Description

In this chapter, a CA model is developed to simulate the spread of an Eldana infestation and resulting damage in a heterogeneous sugarcane environment. The sugarcane environment is diversified in terms of the age of each sugarcane patch, represented with the different cells of the CA. At each time step of the simulation, each cell is assigned an infestation state, with the cell's state an indication of the level of Eldana infestation found in the corresponding patch of sugarcane.

Multiple levels of infestation are incorporated, representing various percentages of damage done to the cane. Each level is also associated with a maturation rate indicating the likelihood of

progressing to the next infestation level due to a natural increase of infestation in the cell. The likelihood of infestation spreading between neighbouring cells is also incorporated.

In addition to the infestation state, a crop state is also assigned to each cell at each time step, namely *growing*, *ready to harvest*, *harvested*, *ready to plant* and *planted*. This state is updated according to the sugarcane age in each cell.

3.2 Assumptions

A number of simplifying assumptions with respect to the environment, sugarcane growth and the behaviour of the pest species are made to allow for a CA representation of the population dynamics:

1. *Neighbourhood.* The Moore neighbourhood is used in the model, as described in Chapter 2. In addition, the spread of Eldana infestation is allowed in any direction. Due to Eldana being known as a lazy flyer [7], with larvae also not dispersing over great distances as discussed in Chapter 2, it is assumed that the dispersal of the pest would not cover great distances in a single iteration of the model. Therefore, an infested cell's infestation can only spread to the neighbouring cells and a radius of 1 is used for the neighbourhood.
2. *Boundary conditions.* A closed domain, like a farm, is considered in this study, leading to the use of a reflective boundary. This boundary ensures pest do not leave the simulated domain and thus no assumptions needs to be made regarding the neighbouring cells outside the domain. Additional conditions is required on the boundary cells, as they would have a reduced neighbourhood compared to cells that are not on the boundary.
3. *Eldana.* All members of the species are homogeneous, meaning that there is no distinction between two members of the same species. This removes the need to simulate individuals, and allows the simulation to aggregate and model levels of infestation.
4. *Infestation level.* The model makes use of infestation levels rather than actual infestation numbers. During each time step, a cell's infestation can only remain the same or increase to the next infestation level. A decreased infestation is only possible once the crop is harvested. This assumption is fair, based on the problem considered of cumulative damage in the sugarcane crop.
5. *Crop age.* A maximum crop age of 18 months was assumed. The harvesting age of crops was variable, but also constraint with between 8 and 18 months, with the default harvesting age of 12 months used for most verification examples.
6. *Temperature.* The effect of temperature is incorporated in a very simplified manner, only making use of an average monthly temperature. Furthermore, temperature was only used to determine sugarcane growth and corresponding yield, with sugarcane growing slower during colder winter months. The effect of temperature was excluded as a factor of Eldana growth.
7. *Variety.* The damage done by Eldana depends on the sugarcane variety, where some varieties are more resistant towards the pest than others. However, this model does not make a distinction between different sugarcane varieties.

8. *Sugarcane yield.* The yield of sucrose from harvested sugarcane is estimated based on the age of the cane at the time of harvest and the month it was planted. This will be one of the main drivers used to compare various agricultural landscape structures.
9. *Soil composition.* No difference in soil composition was considered, therefore it was assumed that every cell contained similar soil and that sugarcane growth would be the same for every cell.
10. *Harvesting.* It was assumed that harvesting would take place at any age, as long as the crop has reached maturity. However, the number of cells that may be harvested per time period is limited. Therefore, simulated crops will be ready for harvesting as soon as they reach the chosen harvest age and will then go into a queue of cells to be harvested. They will stay in the harvesting queue until there is harvesting capacity available, upon which time they will be harvested. It is also assumed that harvesting does not result in all pests being removed and therefore newly planted crops has a small probability of starting as infested crops.
11. *Planting.* Planting of new crops can only occur the month after harvesting of the previous crops. They will then go into a planting queue and be planted as soon as capacity is available.

3.3 Model formulation

Consider a habitat of finite size containing patches of sugarcane infested by Eldana, where infestation levels increase over time as the crop matures. Set a grid \mathcal{G} as a two-dimensional array with $m \times n$ cells, m and n being non-negative integers to represent the infested sugarcane habitat. Let each cell in \mathcal{G} be in one of N infestation states where these states refer to a level of yield loss caused by the Eldana infestation within the specific cell. Let the infestation states be a set $\mathcal{E} = \{0, 1, \dots, N - 1\}$, with these states updated by a totalistic rule set. The model runs in daily time steps t , where t is a non-negative integer, and has a total number of time periods T such that $t \leq T$. Each cell will also be in one of five crop states depending on the age of the sugarcane represented by the cell, with the crop states all belonging to the set $\mathcal{S} = \{1, 2, 3, 4, 5\}$.

3.3.1 Infestation state

The infestation state of a cell, $g_{i,j,t}$, at position (i, j) during time t is updated according to the rule

$$g_{i,j,t+1} = \begin{cases} g_{i,j,t} + 1 & \text{with probability } p \\ g_{i,j,t} & \text{with probability } 1 - p \end{cases} \quad (3.1)$$

where p is the probability of an increase in infestation during time t . In the case when the final infestation level has been reached, the probability of an increase will be zero.

The probability p is calculated according to the rule

$$p = \alpha p_d + (1 - \alpha) p_g \quad (3.2)$$

where the weighted average, as determined by $\alpha \in [0, 1]$, of the probability p_d of an increase in infestation as a result of pest dispersal within the neighbourhood of a cell during time t , as

well as the probability p_g of a natural increase in infestation experienced within the cell due to population growth of Eldana. The probability p_d is calculated by

$$p_d = \frac{\sum_{i-1}^{i+1} \sum_{j-1}^{j+1} g_{i,j,t} - g_{i,j,t}}{8(N-1)(g_{i,j,t} + 1)} \quad (3.3)$$

which is a summation of the values in the neighbourhood of a cell, divided by the value of the next infestation state of the cell. The summation of the values in the neighbourhood of a cell can range from zero to $8(N-1)$, therefore, a further division by $8(N-1)$ is required to ensure that p_d falls within the range between 0 and 1.

The probability p_g is determined according to the infestation state at time t for each position $(i, j) \in \mathcal{G}$, denoting the probability that a cell will enter the next infestation state given the cell's current infestation state. This probability will differ depending on the maturity probability function used, with the various options explained in §3.4.

3.3.2 Crop state

Five crop states are defined: growing (1), ready to harvest (2), harvested (3), ready to plant (4) and planted (5), where these states all belong to the set \mathcal{S} . The crop state of a cell at time t is $c_{i,j,t} \in \mathcal{S}$. Each cell will also have a crop age at each time t , providing the number of months that the crop has been growing and is denoted by $a_{i,j,t} \in \mathcal{A}$.

The updating of a cell's crop state to 2 & 4 can only occur at the start of a month, therefore once a cell has been harvested the crop can only be replanted starting the first day of the next month. Crops can also only be harvested during certain months of the year when the mills are open, sometimes leading to decisions regarding harvesting the cane earlier or letting the cane carry over until the mills reopen a few months later. If harvesting is allowed at the current period in the model, a cell's states can progress to 2 based on

$$c_{i,j,t+1} = \begin{cases} 1 & \text{if } c_{i,j,t} = 1 \text{ and } a_{i,j,t+1} < H_a \\ 2 & \text{if } c_{i,j,t} = 1 \text{ and } a_{i,j,t+1} \geq H_a \end{cases} \quad (3.4)$$

where the crop age of the cell, $a_{i,j,t}$, needs to reach its harvesting age, H_a , before it can be harvested. Once a cell's crop state is updated to 2 (ready to harvest), it goes into a harvesting queue and will be harvested during the next time step of the model. When harvested, the cell's crop state updates to 3 (harvested). At the start of the next month after harvest in the simulation, the crop state is updated to 4 (ready to plant). Once the crop state has been updated to 4, it will go into a planting queue for the next period and will be further updated to 5 (planted) when planting is completed during the following period. After planting, the cell gets updated to state 1 (growing) and the process starts over again. This process will continuously loop until the simulation has come to an end.

3.3.3 Boundary conditions

There are some cells that make up the boundary of the simulated area that requires adjustments to their probability calculations. These cells won't have the same size neighbourhood, with cells that are located in the corner of the simulated area having only 3 neighbours and the cells located on the sides only having 5 neighbours. Therefore, if the cell is in the corner the formula for p_d changes to

$$p_d = \frac{\sum_{i-1}^{i+1} \sum_{j-1}^{j+1} g_{i,j,t} - g_{i,j,t}}{3(N-1)(g_{i,j,t} + 1)} \quad (3.5)$$

where the summation of the values in the neighbourhood of a corner cell can range from zero to $3(N-1)$. If the cell is on the border the formula changes to

$$p_d = \frac{\sum_{i-1}^{i+1} \sum_{j-1}^{j+1} g_{i,j,t} - g_{i,j,t}}{5(N-1)(g_{i,j,t} + 1)} \quad (3.6)$$

where the summation of the values in the neighbourhood of a border cell can range from zero to $5(N-1)$. The formula for p_g will stay the same.

3.3.4 Initial conditions

On initialisation of the simulation, detailed information regarding each cell is required. All cells need to be initialised with an initial crop age, initial crop state and initial infestation state.

The age of the crop at $t = 0$ is provided by the user and must adhere to the rule

$$0 \leq a_{i,j,0} \leq 18 \quad (3.7)$$

where the age must be a positive integer and represents the monthly age of the crop. In the case of an initial age greater than the harvesting age of the crop, the crops will already have reached maturity. The initial crop state of a cell then gets assigned based on the initial crop age, where

$$c_{i,j,0} = \begin{cases} 1 & \text{if } a_{i,j,0} < H_a \\ 2 & \text{if } a_{i,j,0} \geq H_a \end{cases} \quad (3.8)$$

indicates that any cell initialised with mature age will immediately be ready for harvesting. It is assumed that all cells representing sugarcane will have planted crops at the start of the simulation and therefore no cell will be initialised with either of the planting crop states.

After a cell at position (i,j) has been allocated the age of the sugarcane patch it represents, an appropriate initial infestation state $g_{i,j,0}$ according to the age of the sugarcane is also assigned. The initial infestation state is based on the probability that the cell is in a specific infestation at a specific age if it was simulated. A probability lookup table is required to determine which infestation state to assign, with different probability tables generated for different maturity probability functions. One such probability lookup table is provided in Table 3.1, where the crop infestation uses the linear maturity probability function. The rest of the lookup tables may be found in Appendix A.

These probabilities are calculated through 100 simulation runs for each maturity probability function, with only newly planted crop initially. As a starting point in determining these values, it was assumed that the newly planted crops had a 0.9 probability of not being infected (infestation state 0) and a 0.1 probability of being infected (infestation state 1). During each simulation run data regarding the infestation probabilities are gathered. At the start of every month in the simulation the proportion of cells in each infestation state is calculated and saved, thus collecting information about the infestation probabilities for every month. These values are then averaged over the 100 simulation runs to obtain the probabilities that certain aged crops will be in the respective infestation states.

Age	Initial infestation state ($g_{i,j,0}$)																	
	0	1	2	3	4	5	6	7	8	9	10	11	12	13	14	15	16	
0	0.9	0.1	0	0	0	0	0	0	0	0	0	0	0	0	0	0	0	0
1	0.826	0.112	0.048	0.012	0.002	0	0	0	0	0	0	0	0	0	0	0	0	0
2	0.699	0.149	0.092	0.042	0.014	0.004	0.001	0	0	0	0	0	0	0	0	0	0	0
3	0.53	0.18	0.141	0.085	0.041	0.016	0.005	0.001	0	0	0	0	0	0	0	0	0	0
4	0.351	0.184	0.179	0.134	0.082	0.043	0.018	0.007	0.002	0.001	0	0	0	0	0	0	0	0
5	0.202	0.152	0.182	0.172	0.131	0.084	0.044	0.021	0.009	0.003	0.001	0	0	0	0	0	0	0
6	0.1	0.103	0.153	0.176	0.164	0.13	0.084	0.048	0.024	0.011	0.004	0.002	0.001	0	0	0	0	0
7	0.044	0.059	0.104	0.15	0.168	0.159	0.128	0.086	0.053	0.027	0.013	0.005	0.002	0.001	0	0	0	0
8	0.017	0.028	0.061	0.105	0.144	0.162	0.154	0.128	0.089	0.056	0.031	0.015	0.007	0.003	0.001	0	0	0
9	0.007	0.012	0.03	0.061	0.102	0.138	0.156	0.151	0.126	0.092	0.059	0.034	0.018	0.008	0.004	0.001	0.001	0.001
10	0.003	0.005	0.013	0.031	0.062	0.098	0.133	0.152	0.146	0.126	0.093	0.063	0.038	0.02	0.01	0.004	0.003	0.003
11	0.001	0.002	0.005	0.014	0.033	0.062	0.097	0.129	0.145	0.143	0.123	0.095	0.066	0.041	0.023	0.012	0.009	0.009
12	0	0.001	0.002	0.006	0.015	0.034	0.062	0.094	0.122	0.14	0.139	0.124	0.096	0.069	0.044	0.026	0.026	0.026
13	0	0	0.001	0.002	0.006	0.017	0.034	0.062	0.092	0.118	0.136	0.135	0.122	0.099	0.07	0.047	0.06	0.06
14	0	0	0	0.001	0.003	0.007	0.017	0.035	0.06	0.09	0.115	0.13	0.133	0.12	0.098	0.074	0.116	0.116
15	0	0	0	0	0.001	0.003	0.008	0.018	0.035	0.059	0.087	0.113	0.127	0.13	0.117	0.099	0.202	0.202
16	0	0	0	0	0	0.001	0.003	0.008	0.019	0.036	0.058	0.085	0.108	0.124	0.128	0.116	0.312	0.312
17	0	0	0	0	0	0.001	0.001	0.004	0.009	0.019	0.036	0.058	0.083	0.106	0.121	0.124	0.438	0.438
18	0	0	0	0	0	0.001	0.001	0.004	0.01	0.02	0.036	0.059	0.081	0.103	0.118	0.118	0.567	0.567

TABLE 3.1: Probability lookup table for the Linear maturity function with $N = 17$.

Many other factors would also affect the infestation state during simulation, like the pressure from older sugarcane patches close by or the combination of parameters used for the simulation. Unfortunately it would be impossible to determine lookup tables for every possible instance of the simulation and thus the default parameter combination is used to determine the initial infestation states. New probability lookup tables would have to be generated if changes to the parameter values are required.

3.4 Parameterisation

The model defined in §3.3 has only two parameters, namely the weight α , and the maturity parameter p_g .

The value of α determines the weighting of the two probabilities used in Equation (3.2), with the default value of 0.3 implemented. Eldana is assumed to be a weak flyer, thus α was chosen such that the natural increase in the population in a cell would be weighted higher than the population growth caused by a dispersal in the neighbourhood.

The maturity parameter, p_g , refers to the likelihood that a cell's infestation state will increase based solely on its current infestation state. This forms part of Equation (3.2) that is used to determine the probability of infestation increasing to the next level. Four different maturity functions are investigated in this thesis, namely: Linear, Increasing, Decreasing and Shaped.

The values used for the linear maturity function are

$$p_g = \begin{cases} 0 & \text{if } g = 0 \\ 0.025 & \text{if } 1 \leq g \leq 15 \\ 0 & \text{if } g = 16 \end{cases} \quad (3.9)$$

where g is the current infestation state and p_g is the probability that the cell will increase to the next infestation without considering the neighbourhood. The values for the increasing function are

$$p_g = \begin{cases} 0 & \text{if } g = 0 \\ 0.005(g + 1) & \text{if } 1 \leq g \leq 15 \\ 0 & \text{if } g = 16. \end{cases} \quad (3.10)$$

The decreasing function is defined by

$$p_g = \begin{cases} 0 & \text{if } g = 0 \\ \min(0.04 - 0.003(g - 1), 0.001) & \text{if } 1 \leq g \leq 15 \\ 0 & \text{if } g = 16 \end{cases} \quad (3.11)$$

and lastly the shaped function is defined by

$$p_g = \begin{cases} 0 & \text{if } g = 0 \\ 0.01 + \sum_{x=1}^g 0.003(x - 1) & \text{if } 1 \leq g \leq 8 \\ 0.01 + \sum_{x=g}^{15} 0.003(15 - x) & \text{if } 9 \leq g \leq 15 \\ 0 & \text{if } e = 16 \end{cases} \quad (3.12)$$

The linear function makes use of a fixed probability regardless of the current infestation level, while the increasing and decreasing functions has a fixed value by which the probability increases

or decreases for each increment of the infestation level, respectively. The final function follows an S-shaped curve, which has a low probability of increase at lower infestation levels that gradually increases as the infestation level increases, but then also starts decreasing again at higher levels of infestation. All of these functions have been calibrated such that a cell with infestation level 1 at age 0 will reach infestation level 10 at 12 months of age on average, resulting in a 5% loss of sucrose if harvested at that age. It is important to note that all cells with infestation level 0 cannot increase in infestation on its own and will only increase to level 1 if a sufficient neighbourhood pressure is achieved. The four functions are also shown as graphs in Figure 3.1 to illustrate the various growth curves.

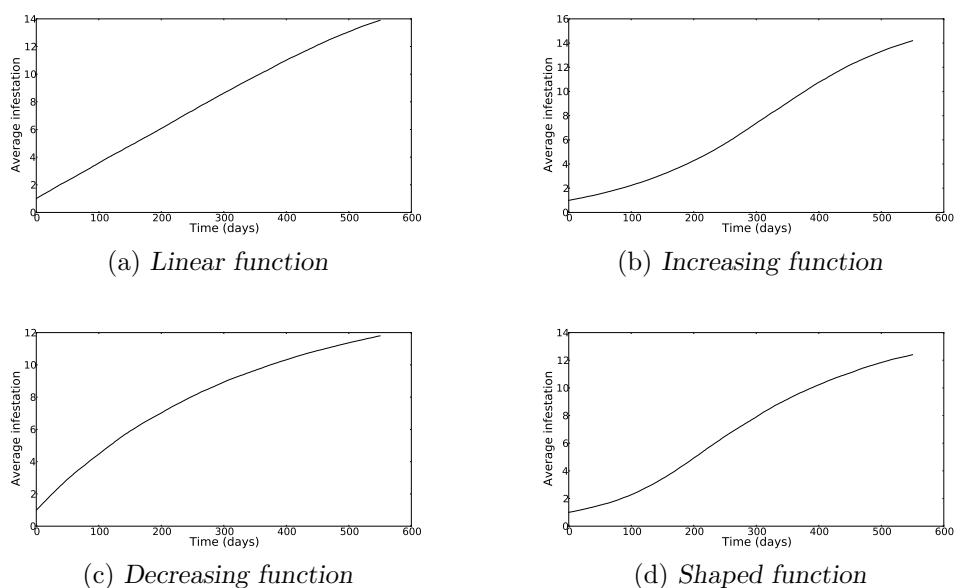


FIGURE 3.1: *The various maturity probability functions*

Due to the infestation level limited at 16, the increasing function as shown in Figure 3.1(b) seems to be decreasing when some of the cells start to reach the maximum infestation level and therefore reducing the potential growth of the infestation.

3.5 Model output

The base yield regression model determined by Stray [32] is used for this study. The model makes use of an EGT to determine the yield, with the colder months of June, July and August deemed as no-grow months and do not add to the EGT. The yield can then be calculated according to the function

$$y = 11.7x - 0.29x^2 \quad (3.13)$$

where y is the sucrose yielded in tons per hectare and x is the EGT of the crop at the time of harvesting. Table 3.2 provides the expected yield for each possible harvest age and harvest month, with the yield based on the month the crop would have been planted. The harvesting ages are limited to between 8 and 18, with crops younger than 8 months assumed to not have any sucrose yield worth harvesting and crops older than 18 months assumed to not produce more sucrose than that of 18 month old crops when the risk of increased damage is considered.

Month	Sucrose yield for each harvest age										
	8	9	10	11	12	13	14	15	16	17	18
Jan	51.25	59.76	67.69	75.04	81.81	88.00	93.61	98.64	103.09	103.09	103.09
Feb	51.25	59.76	67.69	75.04	81.81	88.00	93.61	98.64	103.09	106.96	106.96
Mar	59.76	59.76	67.69	75.04	81.81	88.00	93.61	98.64	103.09	106.96	110.25
Apr	67.69	67.69	67.69	75.04	81.81	88.00	93.61	98.64	103.09	106.96	110.25
May	75.04	75.04	75.04	75.04	81.81	88.00	93.61	98.64	103.09	106.96	110.25
Jun	75.04	81.81	81.81	81.81	81.81	88.00	93.61	98.64	103.09	106.96	110.25
Jul	67.69	75.04	81.81	81.81	81.81	81.81	88.00	93.61	98.64	103.09	106.96
Aug	59.76	67.69	75.04	81.81	81.81	81.81	81.81	88.00	93.61	98.64	103.09
Sep	51.25	59.76	67.69	75.04	81.81	81.81	81.81	81.81	88.00	93.61	98.64
Oct	51.25	59.76	67.69	75.04	81.81	88.00	88.00	88.00	88.00	93.61	98.64
Nov	51.25	59.76	67.69	75.04	81.81	88.00	93.61	93.61	93.61	93.61	98.64
Dec	51.25	59.76	67.69	75.04	81.81	88.00	93.61	98.64	98.64	98.64	98.64

TABLE 3.2: Sucrose yields in tons per hectare for different harvesting ages, based on the month of harvesting, as calculated using equation (3.13)

Yield reduction due to Eldana infestation is not incorporated in Equation (3.13). An adjustment of yields are therefore done at harvest time by reducing the yield with a percentage loss depending on the level of infestation. The percentage of sucrose loss per infestation level in cell (i,j) at harvest time t' is given by

$$L_{i,j,t'} = 0.5g_{i,j,t'}/100. \quad (3.14)$$

If the infestation level is 10 at harvesting, a 5% loss will be applied, resulting in only 95% of the yield calculated with Equation (3.13) being realised. The updated sucrose yield equation in cell (i,j) at harvest time t' assumed in this thesis is given by

$$y_{i,j,t'} = (1 - L_{i,j,t'})(11.7x_{i,j,t} - 0.29x_{i,j,t}^2) \quad (3.15)$$

and the accumulated total yield at the end of a simulation run for the entire grid is given by

$$Y = \sum_{i=1}^m \sum_{j=1}^n \sum_{t'=1}^T y_{i,j,t'}. \quad (3.16)$$

3.6 Solution evaluation

For the purpose of comparing different agricultural landscape structures, we define a performance measure to quantify and evaluate the effectiveness of each landscape structure in minimising infestation levels. The performance measure used is the average yield over a total number of q simulation runs and given by

$$\bar{Y} = \frac{\sum_{k=1}^q Y_k}{q}, \quad (3.17)$$

where Y_k is the calculated yield value from Equation (3.16) associated with the agricultural landscape structure for simulation k , and q is the total number of simulations performed for a landscape structure. This value is used to compare various landscape structures, with a higher average yield indicating a better solution. Due to the randomness associated with the simulation model, multiple simulations of the same agricultural landscape structure might be required.

3.7 Computer implementation

The CA was implemented in the open source programming language Python 3.3. The simulation process is shown in Figure 3.2, with the process divided into three phases: the initialisation phase, main phase and output phase. Each phase will be explained in the sections that follow.

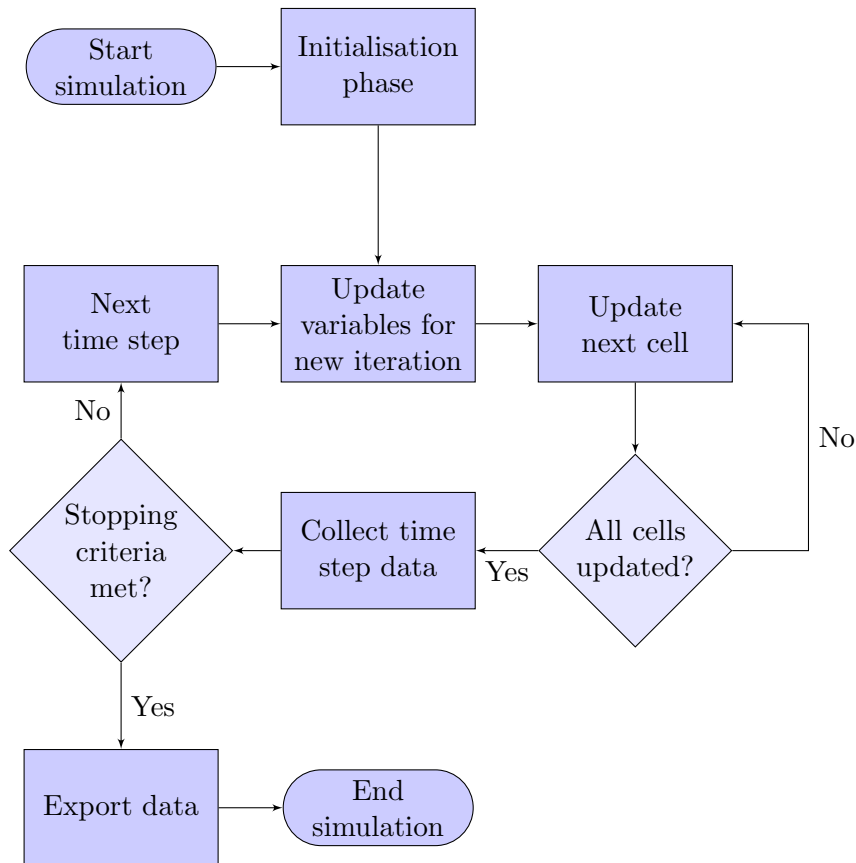


FIGURE 3.2: Flow diagram of the process followed during the simulation

3.7.1 Initialisation phase

During the initialisation phase the sugarcane environment is constructed and all the input parameters provided. To construct the environment, information about the size of the simulated area and that of each cell is firstly needed. The simulated area is represented with a rectangle and therefore both the length and width (in meters) of the area needs to be given. For the purposes of this study, each cell has a default size of $10\text{m} \times 10\text{m}$, from where the required number of cells can be calculated. A change in cell size would require an adjustment made to the probability of an increase in infestation due to dispersal.

After all the parameters have been assigned values for the simulation, the final step is to assign each cell with the information regarding the sugarcane patch it represents. The assigning of the sugarcane age is done according to an initial allocation structure, after which the initial infestation state is determined for each cell. The harvesting age of each cell must also be provided after which the simulation is ready to start.

Initial allocation

The initial distribution of sugarcane among the cells (in terms of age) are assigned according to one of four initial allocation structures. A visual representation of the four structures used by the model is given in Figure 3.3, together with the assigned initial infestation states. Each infestation state from 1 to 16 is represented in the CA by the colours ranging from blue to red, with the full colour scale provided in Table 3.3. The infestation state 0 does not have a colour, as no infestation is present and the full cell will be the colour of the crop state.








Infestation level	1	2	3	4	5	6	7	8	9	10	11	12	13	14	15	16	
Colour																	

TABLE 3.3: Colour scale indicating level of infestation.

To determine the sugarcane allocation for each cell, two user input parameters are used. The user must provide the number of different ages of sugarcane present in the simulation as well as the maximum age the crops are allowed to be. The initial ages of crops are then chosen at even intervals between 0 and the maximum crop age according to the provided numbers. The user must also provide a value for the number of cells that needs to be grouped together. Cells will be grouped together in square groups, where every cell in this group would then have the same initial cane age. The four allocation structures are explained further, including how the user defined parameters are used.

Homogeneous allocation

In this allocation all the cells forms part of a singular group, thus all cells will have the same age of sugarcane. This allocation is mostly used for verification and validation purposes, as well as to determine the initial infestation states as explained previously. This allocation also forms the basis of the other allocations, where other allocations are a set of heterogeneous groups of patches, with homogeneous allocation in the cells of each set of homogeneous patch.

Uniformly random allocation

For the uniformly random allocation, each field will be assigned one of the cane ages randomly. In the example of Figure 3.3(b), the field size is five and thus every 5×5 cells are grouped together in it's own field.

Column allocation

The column allocation does not make use of square groups as in the other allocations, but instead a group is made of an entire column as the name suggests. The size of the groups is still used to determine the width of a column. Each column would then be assigned one of the chosen crop ages in a repeating order, as seen in Figure 3.3(c) where the columns are given a crop age in the order 0,4,8,12,0,4,8,12. in the illustration, a harvesting age of 16 was assumed with 4 ages chosen, the sequence would continue for larger simulation areas.

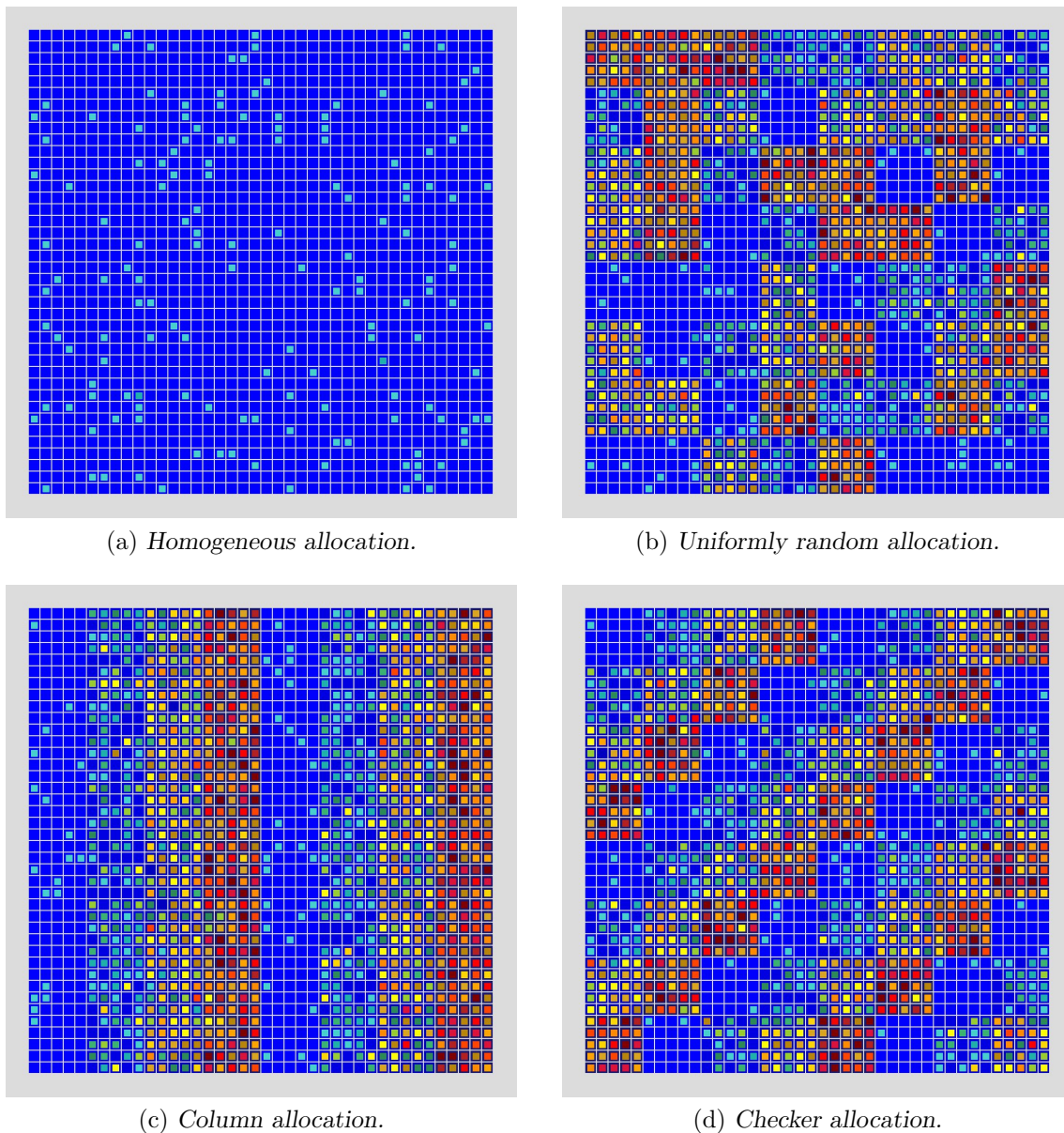


FIGURE 3.3: Four different initial allocation structures in terms of crop age used in the basic model. With an older crop age, higher infestation levels are assumed.

Checker allocation

The checker allocation structure considers the position of each group with respect to row and column placement when allocating a crop age, forming a diagonal checkers pattern as shown in Figure 3.3(d). This example having the same inputs as the column allocation presented.

3.7.2 Main phase

Once the initialisation phase is completed, the main phase is entered in which cells are iteratively updated until a stopping criteria is met. At the start of each iteration, the variables that influence the entire simulated area must be updated before the individual cells can be updated. Firstly, the simulation timestep as well as the day of the year simulated are incremented.

During each iteration, the infestation state as well as the cane age within each individual cell are updated according to the process shown in Figure 3.4. The cane age is updated on a monthly basis, with the age increased only if it is the start of a new month. Depending on the cane age within each cell, the cell can be in either of the five statuses as described previously.

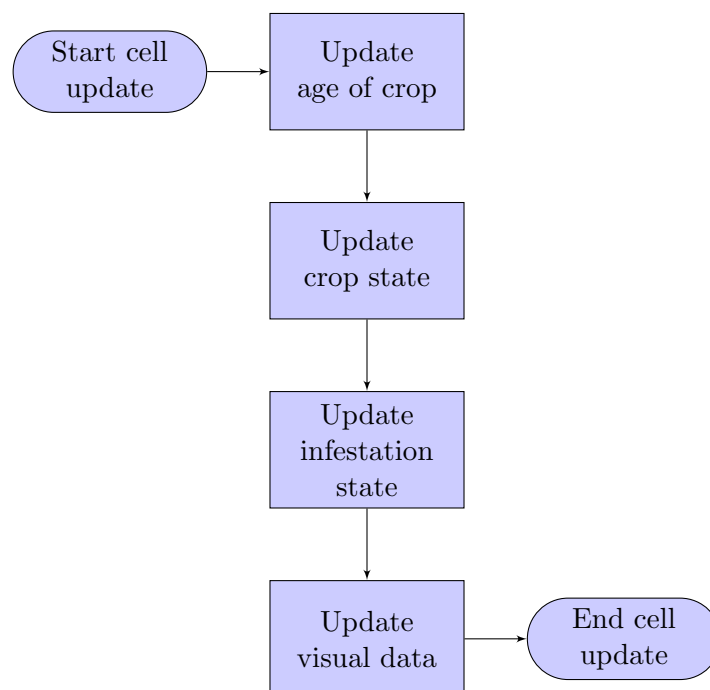


FIGURE 3.4: Flow diagram of process involved during the update of a cell.

The process for updating the crop state is provided in Figure 3.5, where the initial status is *growing*. The figure highlights the decisions made to determine what the crop state of the cell should be in the next time step of the model. It first considers if the appropriate harvesting age, H_a , has been reached, after which it determines if the cell can be harvested and eventually if new crops can be planted. The process ends with the *planted* crop state, which will change back to the *growing* status at the next time step and thus restarting the process.

Various colours are used to represent the crop state of the cell, with these colours provided in Table 3.4. Furthermore, while the cell has the *growing* crop state, the blue colour is associated with it and the shade of blue will change according to the age of the crop. This is shown in Table 3.5, where the corresponding colour for each possible crop age is provided.

Crop State	1	2	3	4	5
Colour					

TABLE 3.4: Colours indicating different crop states.

Crop age	0	1	2	3	4	5	6	7	8	9	10	11	12	13	14	15	16	17	18
Colour																			

TABLE 3.5: Colour scale indicating age of the crop during the growing crop state.

Once the crop state of the cell has been updated, the updating of the infestation state is done according to (3.1). A random number r is generated such that, if $r < p$ the infestation state will

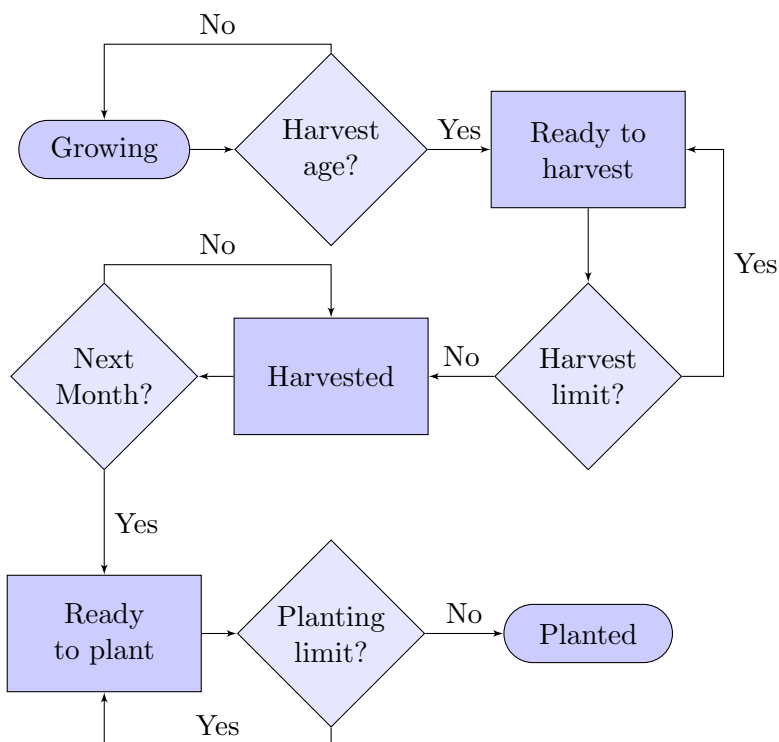


FIGURE 3.5: Flow diagram of the process followed during status updating

be increased to the next infestation state. Finally, the visual data for each cell is updated. The visual data is used for the visualisation of the simulation and linked with the colour representing the cell's infestation state. It is also possible to remove the visualisation of the model. This may be used if multiple simulation runs needs to be performed and the user only requires the collected data obtained from the output phase for each simulation run.

3.7.3 Output phase

The output phase is where data is collected regarding the Eldana infestation for a simulation scenario. During each time step of the simulation, data regarding the infestation state of each cell is available for collection. However, to collect all the available data would not be feasible for simulations on large spatial areas. Therefore, only data described in §3.5 is saved.

The data can be obtained for the entire simulated area or otherwise can be collected for each cane age if needed. After completion of the simulation, the obtained data is summarised for analysis purposes. The main output provided by the simulation that are used for analysis is the sucrose yield obtained from harvesting along with a growth curve of Eldana infestation levels. An example of such a growth curve can be seen in Figure 3.1. If needed, the model also provides the user with an Excel worksheet containing the information required.

3.8 Model verification

Verification of the model was done by testing whether the model reacts as expected for instances where initial infestation are varied. All simulations were done on an Intel(R) Core(TM) i7-3770 CPU @ 2.40GHz with 8.00 GB (7.88 GB usable) installed RAM and a 64-bit operating system.

3.8.1 Infestation spread

Firstly, the way in which infestation spreads over the simulated area was verified. Under the assumptions of the model, the infestation state of an uninfested cell can only be influenced by the infestation pressure provided by the cell's neighbourhood. Therefore, a cell can only become infested if a neighbouring cell is already infested. Figure 3.6 provides a two-dimensional view of an infestation spreading over time given that only the centre four cells were initially infested. During the first 100 days, a few additional cells has been infested but none that are disjoint from the rest of the infested cells. At day 200 the infestation has spread some more and the center of the infestation has increased in terms of infestation level, and a few more cells have become infested. Once day 300 was reached, the infestation pressure on the centre cells have caused them to reach relatively high infestation levels, while it is clear that the infestation state of cells is generally lower the further they are from the centre. This is in line with the underlying assumption that infestation can only occur should a cell's neighbours be infested causing a diffusion-like spread over the domain. Similar behaviour was observed in the studies of Potgieter [28] and Van Vuuren [33].

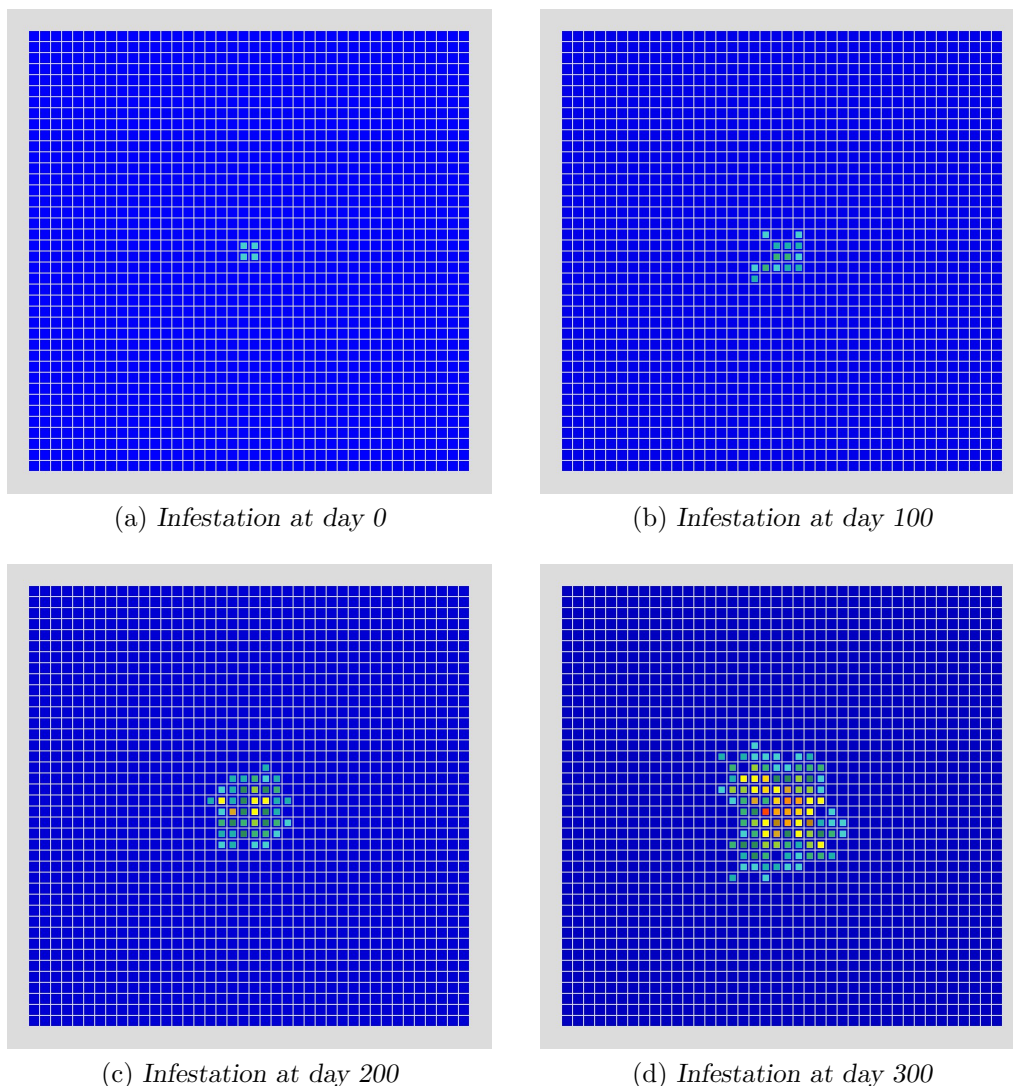
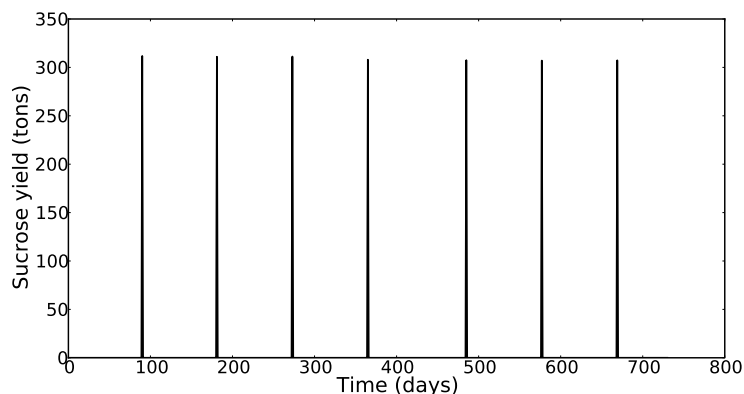


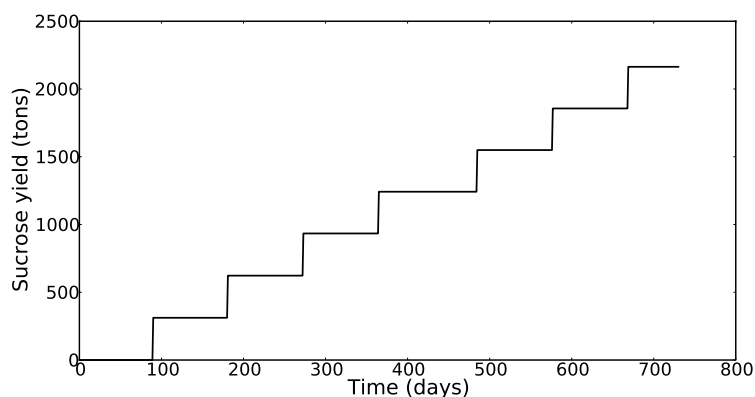
FIGURE 3.6: *Two-dimensional view of the infestation spread over time in a verification test.*

3.8.2 Harvesting and planting process

Secondly, an important aspect of the model that was verified for correct behaviour was the harvesting and planting process. A checkers configuration with 4 age groups, a field size of 5×5 cells and a harvesting age of 12 months was used to test the required behaviour. The crop ages at initialisation were 0, 3, 6 and 9 months, with each represented equally in the simulated area. A two-year simulation was run, with Figure 3.7 showing the yields obtained in the simulation.



(a) Daily sucrose yield



(b) Cumulative yield

FIGURE 3.7: Observed harvesting yields during the simulation, with an increase in cumulative yield after each field's harvesting cycle is completed.

In Figure 3.7(a) the additional yields obtained each day is presented, where it is seen that yields are only achieved every three months during the first year, corresponding to the harvesting of the four age groups used. It then takes another 13 months after initial harvesting before the crops are harvested again due to the 1 month waiting period before new sugarcane is planted. This also causes that the newly planted sugarcane at model initialisation only gets harvested once in the two year simulation, with the second harvesting taking place on month 25. The cumulative yield is also tracked in Figure 3.7(b), clearly corresponding to the daily yields and providing an accurate value of the total sucrose yield over the simulation period.

The visual representation of the process can be seen in Figures 3.8 and 3.9, showcasing the first harvesting event at day 90 and the first planting event at day 119. All colours are updated according to the colour scale provided in Table 3.4.

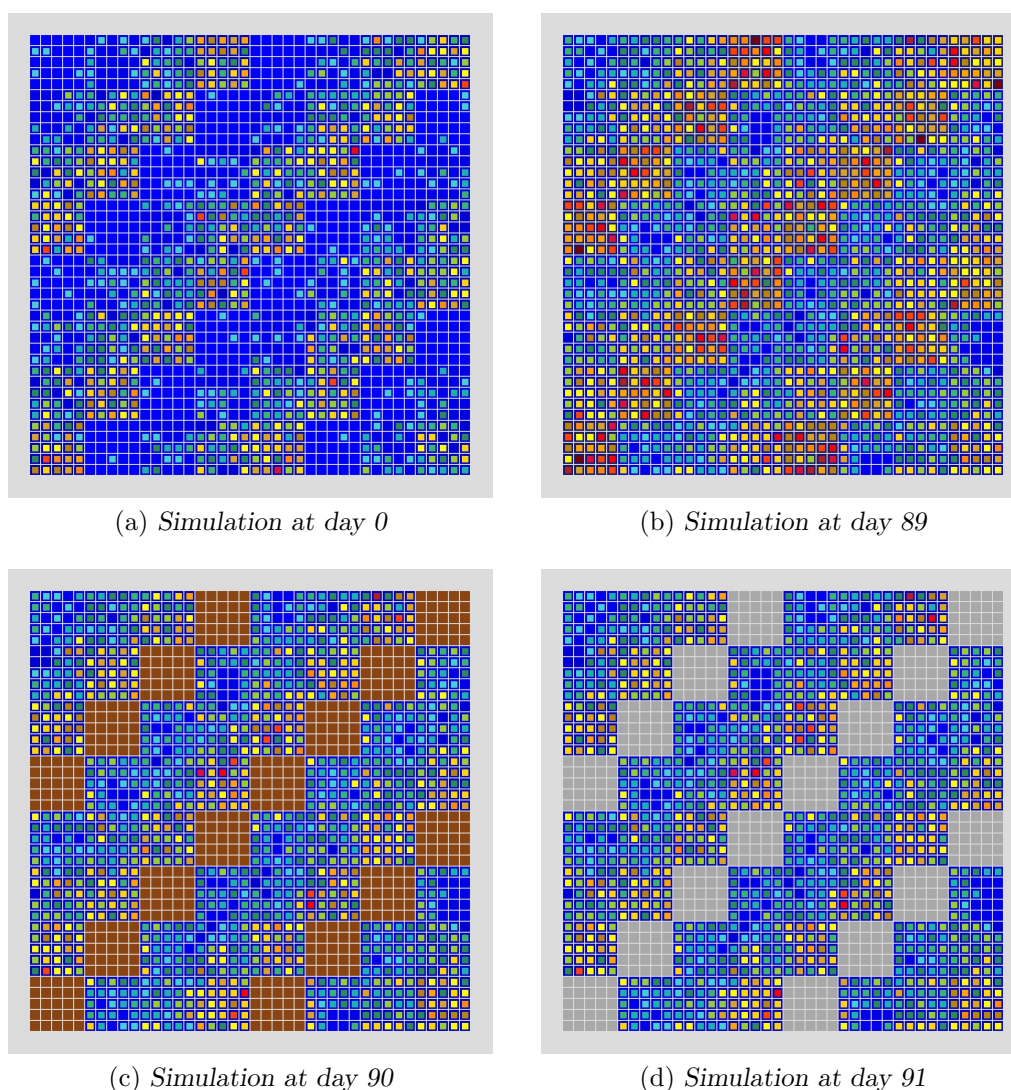


FIGURE 3.8: Visualisation of the harvesting process, showing the harvesting event at day 90 of the simulation.

The initial field configuration is given in Figure 3.8(a), and clearly shows the four age groups of which the oldest crop was initialised with 9 months old cane and thus will be ready for harvesting at day 90, after 3 months have passed in the simulation. The simulation one day before, the day of harvesting and one day after harvesting may be seen in Figure 3.8(b), 3.8(c) and 3.8(d) respectively, with the old and highly infested cane replaced by the brown cells representing harvested cane and later changing to the grey cells that are ready to be planted.

The process for planting is shown in Figure 3.9. A cell becomes planted on the first of the next month after harvesting took place, in this case that is day 119 of the simulation. The simulation one day before, the day of planting and one day after planting may be seen in Figure 3.9(a), 3.9(b) and 3.9(c) respectively, with the ready to plant cells replaced by the cells representing planted cane and later changing to the blue cells that represent growing sugarcane. In Figure 3.9(d), the final day of the simulation is shown, indicating that this process has continued throughout the entire simulation period. It is thus safe to say that the harvesting and planting process behaves as expected and is accurately implemented in the simulation model.

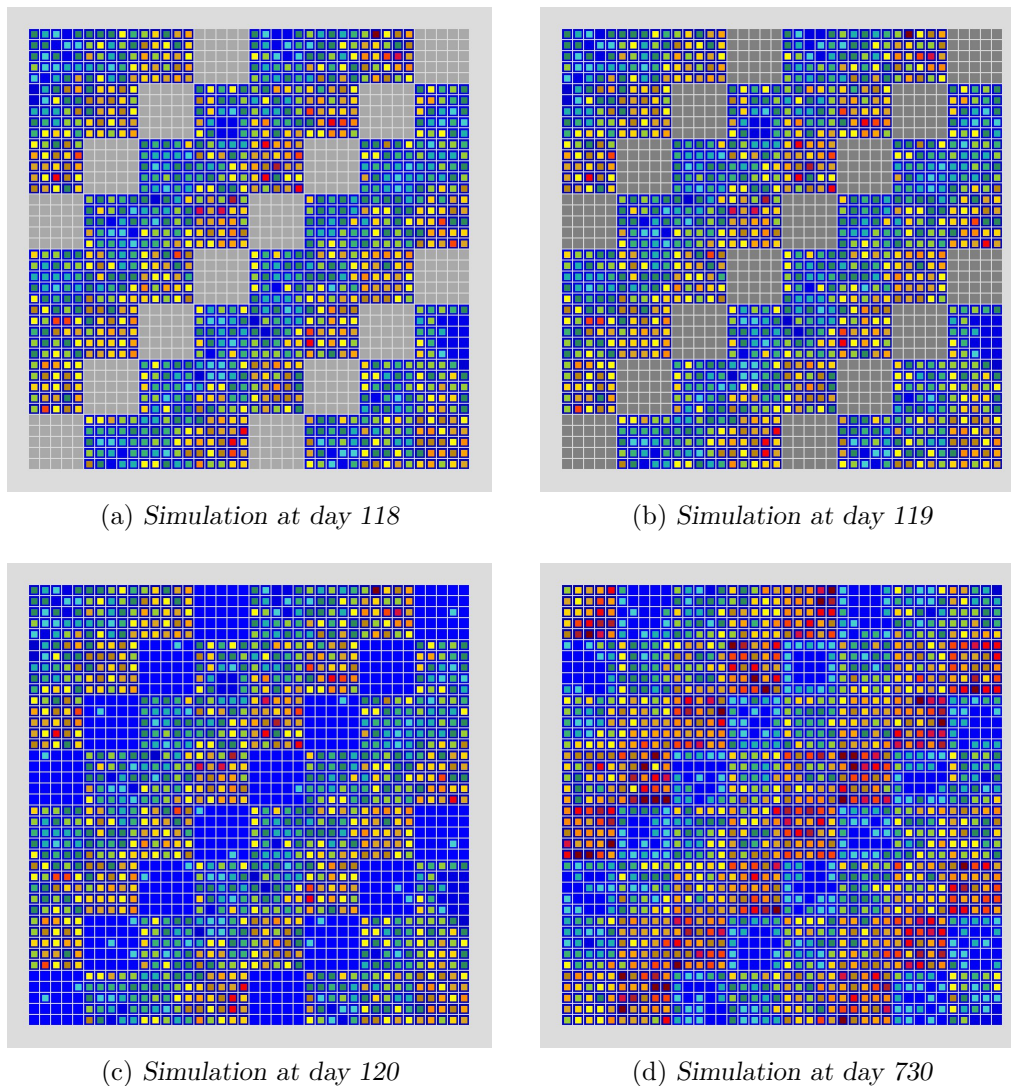


FIGURE 3.9: Visualisation of the planting process, showing the planting event at day 119 of the simulation.

3.9 Chapter Summary

In this chapter, the simulation model was presented, including the model description, formulation and implementation. The various assumptions pertaining to the model were explained together with all the parameters the model requires as inputs and those parameters that the model provided as outputs. The process of implementing the model in the programming language Python, including the different phases of the simulation and the flow between them, was shown schematically.

The chapter then concluded with the verification of the model, showing that the model acts in accordance to the assumptions made.

CHAPTER 4

Results

Contents

4.1	Statistical validation	33
4.2	Agricultural landscape structures	34
4.3	Simulation results	36
4.4	Sensitivity Analysis	46
4.5	Recommendations	48
4.6	Chapter Summary	49

In this chapter, a statistical validation is done in §4.1, followed by a description of the landscape structures that were considered in this study in §4.2. In §4.3, the results of the simulations are presented, followed by additional sensitivity analysis in §4.4. Recommendations for industry, based on the simulation results, are presented in §4.5, after which the chapter is concluded in §4.6.

4.1 Statistical validation

As stated earlier, to determine a solution value for an agricultural landscape structure, multiple simulations are required for each structure. The question then arises of how many simulations are required. This was determined based on the calculation of the half-width using the formula

$$h = Z_{1-\frac{\alpha}{2}} \times \frac{S}{\sqrt{n}} \quad (4.1)$$

where h denotes the half-width, Z denotes the standard normal quantile, S the sample standard deviation and n the number of simulations. For this study, a half-width of 5 was deemed acceptable and a 95% confidence interval was used. Equation (4.1) is thus simplified to

$$h = 1.96 \times \frac{S}{\sqrt{n}} \quad (4.2)$$

where $Z_{1-\frac{\alpha}{2}}$ has a value of 1.96 at the 95% confidence interval.

To obtain information for the half-width calculations, a hundred simulations were run for each of the four maturity probability functions while assuming a 40×40 grid initialised with only

newly planted sugarcane. A fixed harvesting age of 12 months was used and each simulation was run for a duration of 5 years. The results of these simulations are provided in Tables 4.1 & 4.2.

Data Points	Linear			Decreasing		
	Average	St.Dev	Half-width	Average	St.Dev	Half-width
5	5093.132	5.515422	4.83448	5074.029	4.205858	3.686597
10	5092.245	4.476128	2.774333	5074.527	3.277427	2.03137
25	5092.307	4.149392	1.626562	5075.719	3.249477	1.273795
50	5091.86	3.944244	1.093289	5076.351	3.463925	0.960151
100	5091.838	4.03008	0.789896	5076.192	3.35929	0.658421

TABLE 4.1: *Statistical validation results for the Linear and Decreasing probability functions*

Data Points	Increasing			Shaped		
	Average	St.Dev	Half-width	Average	St.Dev	Half-width
5	5104.42	4.555919	3.993439	5097.214	3.499433	3.067388
10	5109.733	7.689097	4.765752	5096.047	5.817464	3.605702
25	5108.657	6.216478	2.436859	5095.781	6.108568	2.394559
50	5108.689	5.76228	1.597222	5095.013	5.881935	1.630389
100	5108.56	5.500106	1.078021	5095.007	6.013323	1.178611

TABLE 4.2: *Statistical validation results for the Increasing and Shaped probability functions*

The results indicate that 5 simulations are sufficient to determine the value of a solution, as the half-width is below 5 for all four test cases. However, for both the increasing and shaped functions, the half-width increased when increasing the number of simulations to 10, indicating that the initial five simulation results may have been tightly clustered and not a complete accurate representation of reality. Therefore 10 simulations were chosen as the appropriate number instead, with all four test cases still yielding a half-width less than five.

4.2 Agricultural landscape structures

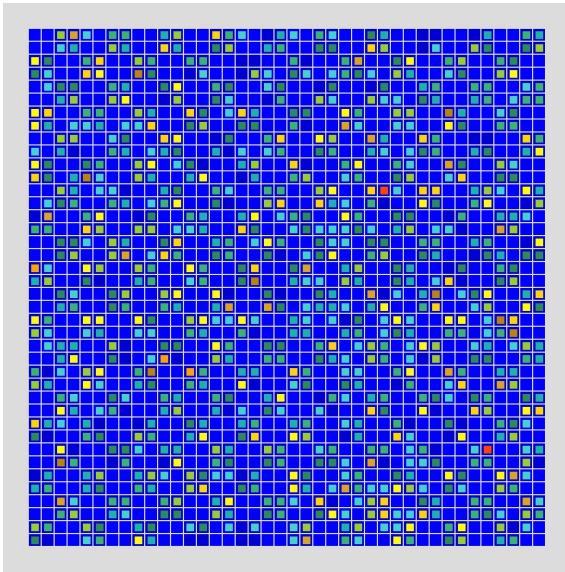
Various pre-determined agricultural landscape structures were considered, differentiated on number of different ages of sugarcane at initialisation, the size of the fields within the simulated area, as well as the configuration pattern used. In this thesis, the column and checkers configuration patterns are considered, in accordance with Potgieter [29]. All landscape structures were compared using a 40×40 grid of cells, with each cell representing a $10\text{m} \times 10\text{m}$ area and thus the total simulated area was 16 hectares per simulation run.

4.2.1 Harvesting age

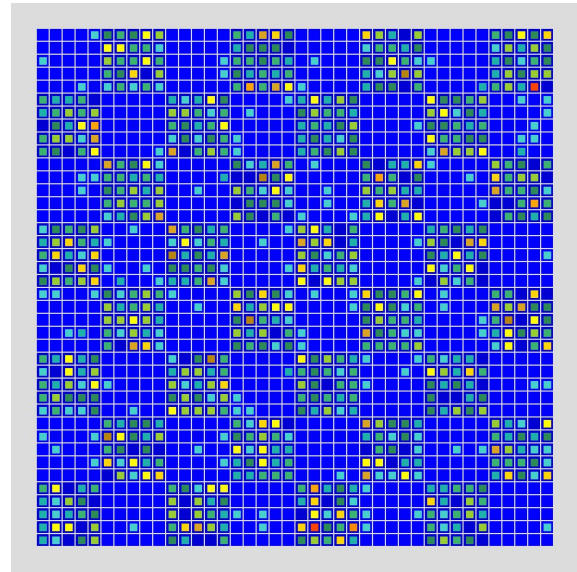
Harvesting ages ranging from 8 to 18 months were considered, with every even number of months included. As stated in the previous chapter, it was assumed that harvesting before 8 months or after 18 months would not be acceptable.

4.2.2 Field sizes

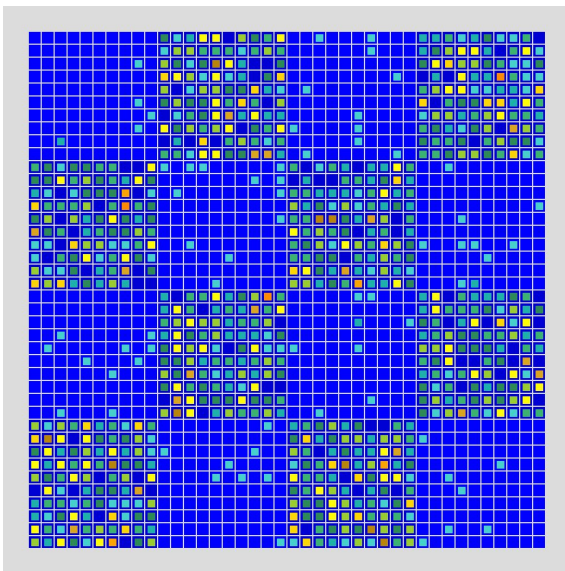
The field size determines how many same aged cells must be grouped to form a single field in the landscape structure considered. The field sizes considered were with width 1, 2, 5, 10 and 20, with all of these fitting into the 40×40 grid multiple times. An example of the different field sizes is provided in Figure 4.1 where four different field sizes are shown. For demonstration purposes, only two age groups are used in all four examples with a checkers type distribution.



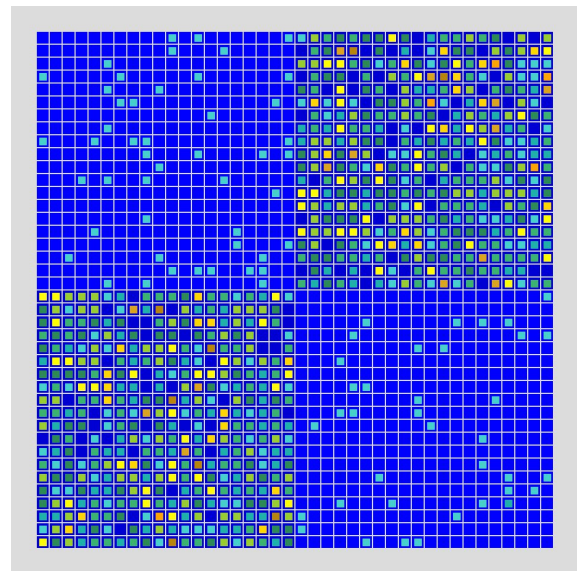
(a) Field size = 2



(b) Field size = 5



(c) Field size = 10



(d) Field size = 20

FIGURE 4.1: An illustration of different field sizes using a checkers configuration with 2 age groups.

4.2.3 Age groups

For each landscape structure, a number of age groups were considered. Age groups indicate same-age fields in the simulation area, and form the basis of the configuration pattern. The age

groups considered in the simulation runs were 2, 4, 8, 12 & 16, with the number of age groups dependant on the harvesting age. Four different examples of age groups are shown in Figure 4.2, with each example making use of a field width of 2 in a column configuration. In Table 4.3, the age groups considered for each corresponding harvesting age and age at initialisation of a simulation run are shown.

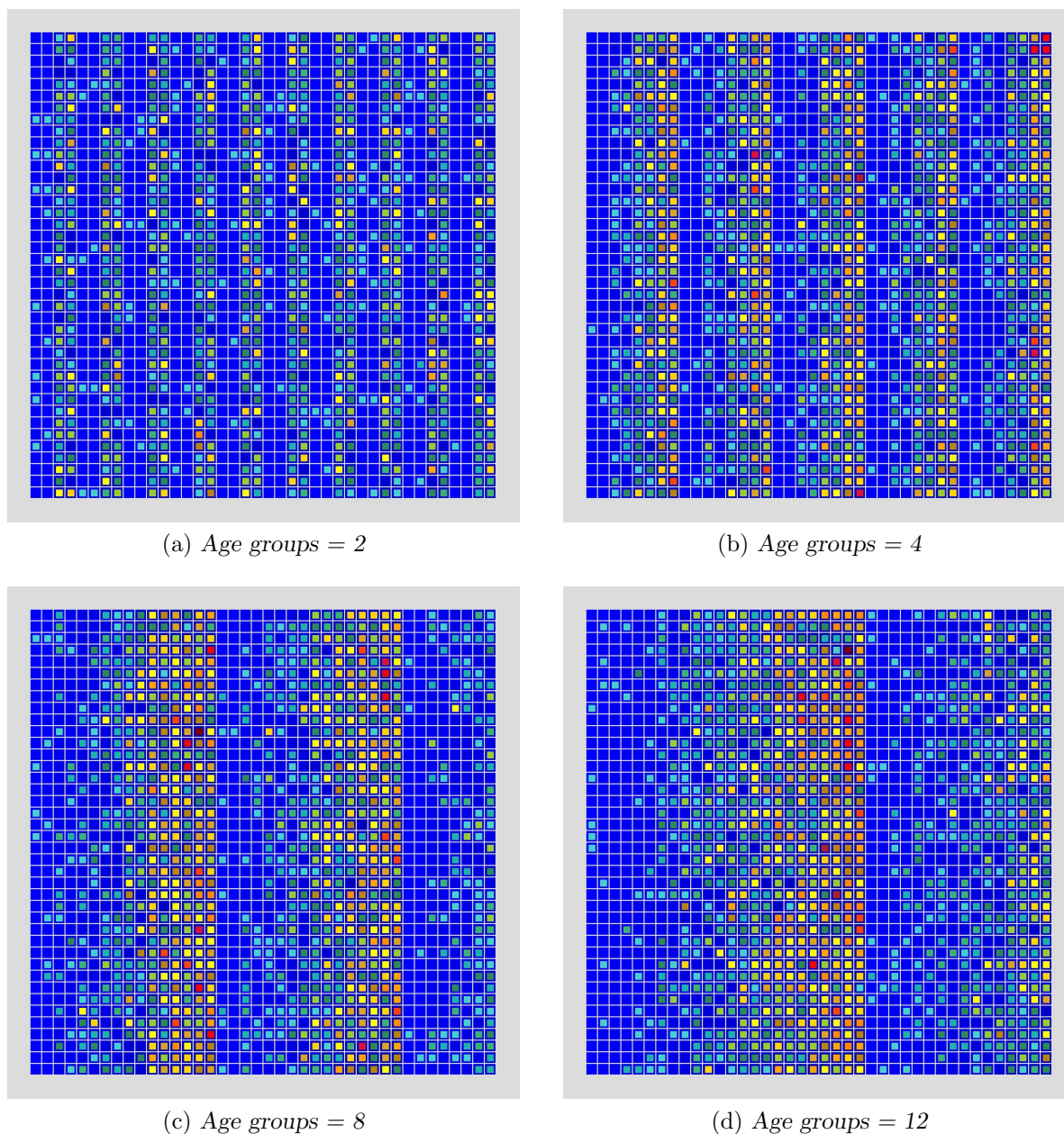


FIGURE 4.2: An illustration of different numbers of age groups using a column configuration of width 2.

4.3 Simulation results

This section provides all the results obtained for the various agricultural landscape structures tested. Analysis was done on each parameter to determine it's effect on sucrose yield. The period of each simulation was 5 years, with each simulation started on the 1st of January. A

Harvesting Age	Age Groups	Ages at initialisation
8	2	0 & 4
8	4	0, 2, 4 & 6
8	8	0, 1, 2, 3, 4, 5, 6 & 7
10	2	0 & 5
10	4	0, 3, 5 & 8
10	8	0, 1, 3, 4, 5, 6, 8 & 9
12	2	0 & 6
12	4	0, 3, 6 & 9
12	8	0, 2, 3, 5, 6, 8, 9 & 11
12	12	0, 1, 2, 3, 4, 5, 6, 7, 8, 9, 10 & 11
14	2	0 & 7
14	4	0, 4, 7 & 11
14	8	0, 2, 4, 5, 7, 9, 11 & 12
14	12	0, 1, 2, 4, 5, 6, 7, 8, 9, 11, 12 & 13
16	2	0 & 8
16	4	0, 4, 8 & 12
16	8	0, 2, 4, 6, 8, 10, 12 & 14
16	12	0, 1, 3, 4, 5, 7, 8, 9, 11, 12, 13 & 15
16	16	0, 1, 2, 3, 4, 5, 6, 7, 8, 9, 10, 11, 12, 13, 14 & 15
18	2	0 & 9
18	4	0, 5, 9 & 14
18	8	0, 2, 5, 7, 9, 11, 14 & 16
18	12	0, 2, 3, 5, 6, 8, 9, 11, 12, 14, 15 & 17
18	16	0, 1, 2, 3, 5, 6, 7, 8, 9, 10, 11, 12, 14, 15, 16 & 17

TABLE 4.3: Sugarcane ages at model initialisation for each harvesting age and number of age groups

total of 10 simulation runs were done for each landscape structure, after which the average of those 10 results was taken as the yield obtained by the corresponding landscape structure.

A summary of the results is provided in Table 4.4, where information regarding the highest yielding landscape structure for each maturity function and harvesting age combination is presented. The effect of each variable in the simulation results were also analysed.

4.3.1 Maturity functions

Four maturity functions were defined in this study, with the variation in the yield results obtained based of the chosen function shown in Figure 4.3. The *Decreasing* maturity function performs the best with the highest average yield values, while the *Increasing* and *Shaped* maturity functions perform the worst.

This indicates that the probability of infestation increase during the later months of the crop cycle has a greater impact than the probability of increase during the earlier months. This seems logical as there are less infected cells in the earlier months, which leads to less impact of a higher infestation probability. When the crop has already matured, it is usually infected and the probability of increase in infestation has a much larger impact.

Maturity Function	Harvesting Age	Highest yielding scenario			
		Pattern	Field Size	Age Groups	Yield
Linear	8	Column	5	8	6267
Linear	10	Column	20	2	6084
Linear	12	Checkers	2	12	5787
Linear	14	Column	20	2	5480
Linear	16	Checkers	2	12	5230
Linear	18	Checkers	2	16	4914
Increasing	8	Column	5	8	6309
Increasing	10	Column	20	2	6114
Increasing	12	Checkers	2	12	5765
Increasing	14	Column	20	2	5475
Increasing	16	Checkers	2	12	5207
Increasing	18	Checkers	1	16	4902
Decreasing	8	Column	5	8	6232
Decreasing	10	Column	20	2	6055
Decreasing	12	Checkers	2	12	5790
Decreasing	14	Column	20	2	5478
Decreasing	16	Checkers	2	12	5257
Decreasing	18	Checkers	2	16	4937
Shaped	8	Column	5	8	6303
Shaped	10	Column	20	2	6102
Shaped	12	Checkers	2	12	5751
Shaped	14	Column	20	2	5467
Shaped	16	Checkers	2	12	5214
Shaped	18	Checkers	2	16	4907

TABLE 4.4: *The best yield obtained for each maturity function and harvesting age combination*

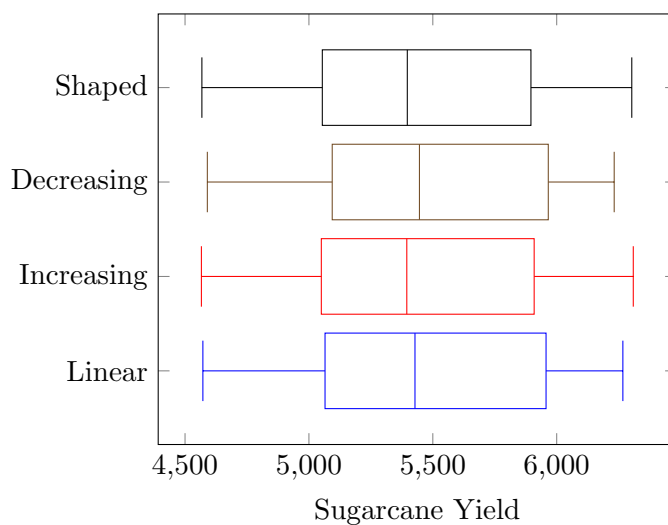
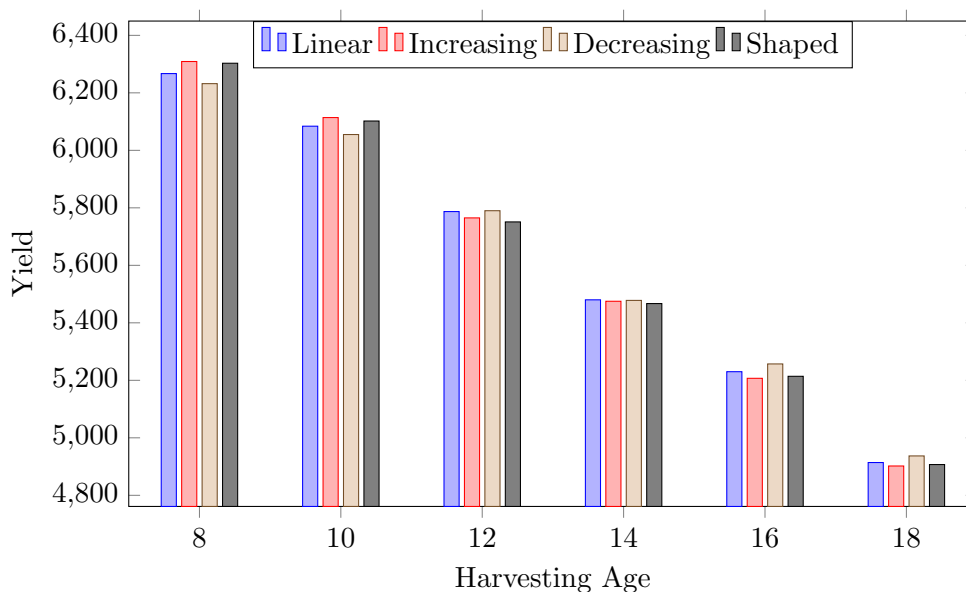
4.3.2 Harvesting age

The harvesting age was compared by considering the best obtained yield for each maturity function for the various harvesting ages tested. The results may be seen in Figure 4.4.

It is clear that there is an inverse relationship between sucrose yield and harvesting age, with an increase in harvesting age leading to a reduction in sucrose yield. Therefore it would be best to harvest as soon as the sugarcane is mature enough, with current industry recommendations are to harvest between 12 and 15 months. This difference might be due to the assumed Eldana maturity functions being too aggressive and leading to any increase in sucrose yield due to prolonged growth being less than the expected increase in sucrose loss caused by increased Eldana infestation. In §4.4, results of sensitivity analyses performed are presented, that shows the effect of decreasing the growth assumed in the Eldana maturity functions.

4.3.3 Initial allocation pattern

If only the best yield structure is taken for each function and harvesting age scenario, then both the Column and Checkers allocation patterns are equal with both performing the best in 12 out of the 24 scenarios. However, this might not be enough and a further comparison is done based on the percentage of results for which one pattern outperforms the other.

FIGURE 4.3: *Maturity function comparison.*FIGURE 4.4: *Best yield for each maturity function by harvesting age.*

A detailed comparison between the Column and Checker allocation patterns can be found in Table 4.5. The comparison is done by comparing the yield obtained by both patterns for the same field size and number of age groups and counting the number of times each one outperforms the other for each combination of maturity function and harvesting age. The total count indicates how many different combinations of maturity function and harvesting age are considered.

A pattern was deemed to outperform the other if it performed best in 80 % or more of the landscape structures tested for each combination of maturity function and harvesting age. The results shown in Table 4.5 indicates that the Column allocation pattern is the best in 10 out of the 24 scenarios, while in the other 14 scenarios there is no clear winner between the Column and Checkers patterns. The Checkers pattern never outperforms the Column allocation although it sometimes does have the best yielding structure.

Maturity Function	Harvesting Age	Total Count	Column Count	Checkers Count	Column %	Checkers %	Best Pattern
Linear	8	12	11	1	92%	8%	Column
Linear	10	12	10	2	83%	17%	Column
Linear	12	14	10	4	71%	29%	Undecided
Linear	14	14	13	1	93%	7%	Column
Linear	16	16	9	6	56%	38%	Undecided
Linear	18	16	6	5	38%	31%	Undecided
Increasing	8	12	11	1	92%	8%	Column
Increasing	10	12	9	3	75%	25%	Undecided
Increasing	12	14	10	4	71%	29%	Undecided
Increasing	14	14	13	0	93%	0%	Column
Increasing	16	16	7	5	44%	31%	Undecided
Increasing	18	16	7	6	44%	38%	Undecided
Decreasing	8	12	11	1	92%	8%	Column
Decreasing	10	12	10	2	83%	17%	Column
Decreasing	12	14	9	3	64%	21%	Undecided
Decreasing	14	14	13	1	93%	7%	Column
Decreasing	16	16	9	5	56%	31%	Undecided
Decreasing	18	16	9	5	56%	31%	Undecided
Shaped	8	12	11	1	92%	8%	Column
Shaped	10	12	9	2	75%	17%	Undecided
Shaped	12	14	10	4	71%	29%	Undecided
Shaped	14	14	13	0	93%	0%	Column
Shaped	16	16	9	5	56%	31%	Undecided
Shaped	18	16	6	5	38%	31%	Undecided

TABLE 4.5: Comparison of best initial allocation pattern for each maturity function and harvesting age combination.

4.3.4 Field size

The effect of field size on the expected yield were inspected, with the results provided in Figures 4.5 to 4.10. In each figure, the results for a certain harvesting age divided into two graphs for the two landscape configuration patterns considered, are shown. Only the results for the linear maturity function are discussed, however, similar results were obtained for the other maturity functions and can be seen in Appendix B.

In Figure 4.5, the results for a harvesting age of 8 months are given, where the maximum number of age groups are 8. It can be seen that an increase in the field size leads to increased yields for all number of age groups considered, indicating that for a given number of age groups the largest possible field size should be used.

A similar results is observed for a harvesting age of 10 months, as provided in Figure 4.6, with an increase in field size leading to increased yields. However, there was a reduction in yields obtained when increasing the field size from 1 to 2 for the Column configuration and 8 age groups. This seems to be an outlier and might be an unfortunate result that occurred due to the randomness applied within the simulation. The benefit from increasing the field size from 1 to 2 is also much less than other increases in field size, which when considered along side the outlier described could indicate that there is not much benefit in increasing to a field size of 2.

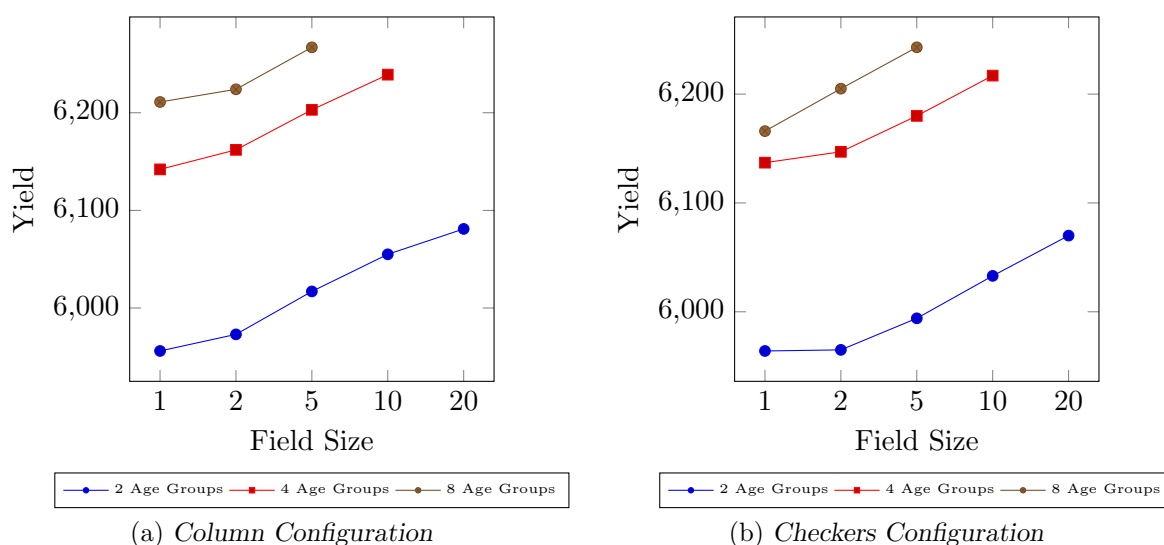


FIGURE 4.5: Yield trend based of field size for harvesting age of 8 months and linear maturity function.

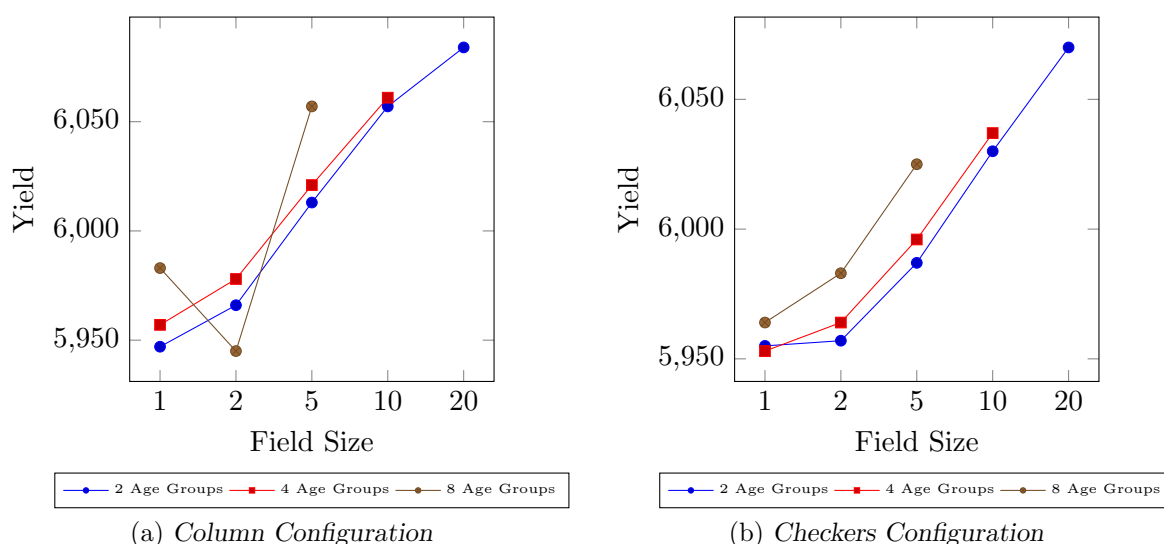


FIGURE 4.6: Yield trend based of field size for harvesting age of 10 months and linear maturity function.

For a harvesting age of 12 months, similar results can be observed once again. Figure 4.7 also has the same outlier as Figure 4.6, which indicates that it is unlikely to be due to randomness within the simulation. The option of 12 age groups are also included since the harvesting age of 12 months allows it. For 12 age groups the only field sizes possible are 1 and 2, with field size 2 obtaining the higher yields.

In Figure 4.8, the results for a harvesting age of 14 months are presented. For this harvesting age and all number of age groups, an increase in field size provides higher yields.

As the harvesting age increased to 16 months, 16 age groups were also considered. These results are seen in Figure 4.9, where more examples of reduced yields are observed for a field size of 2. It is also seen that the yields for 16 age groups are lower than for 12 age groups for the same field size, differing from previous results that indicated more age groups always increased the yield obtained for the same field size.

The results for the final harvesting age of 18 months is provided in Figure 4.10, where the 16

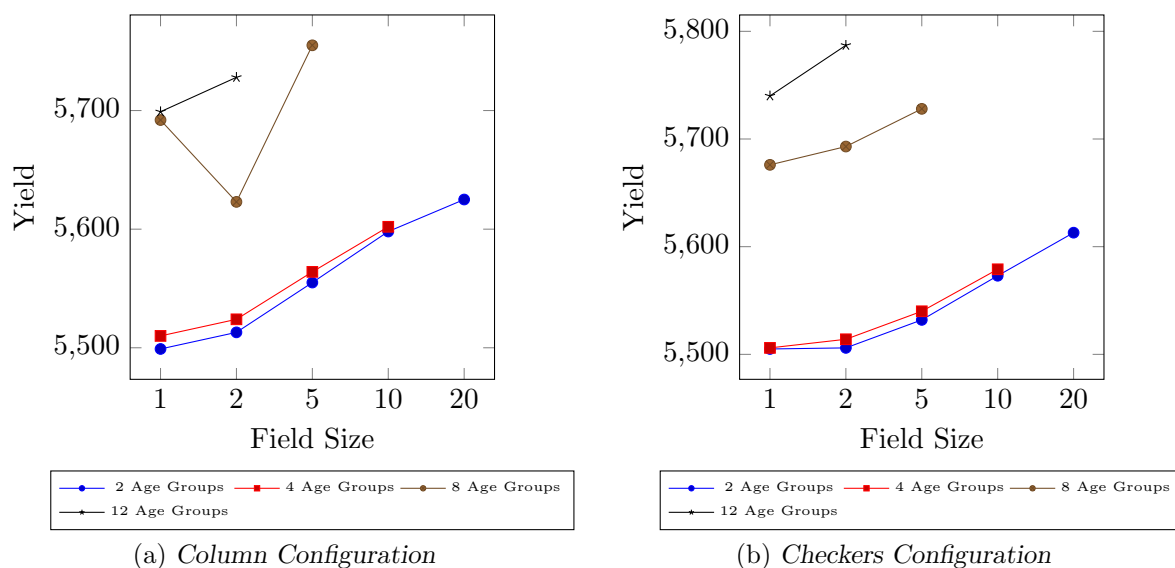


FIGURE 4.7: Yield trend based of field size for harvesting age of 12 months and linear maturity function.

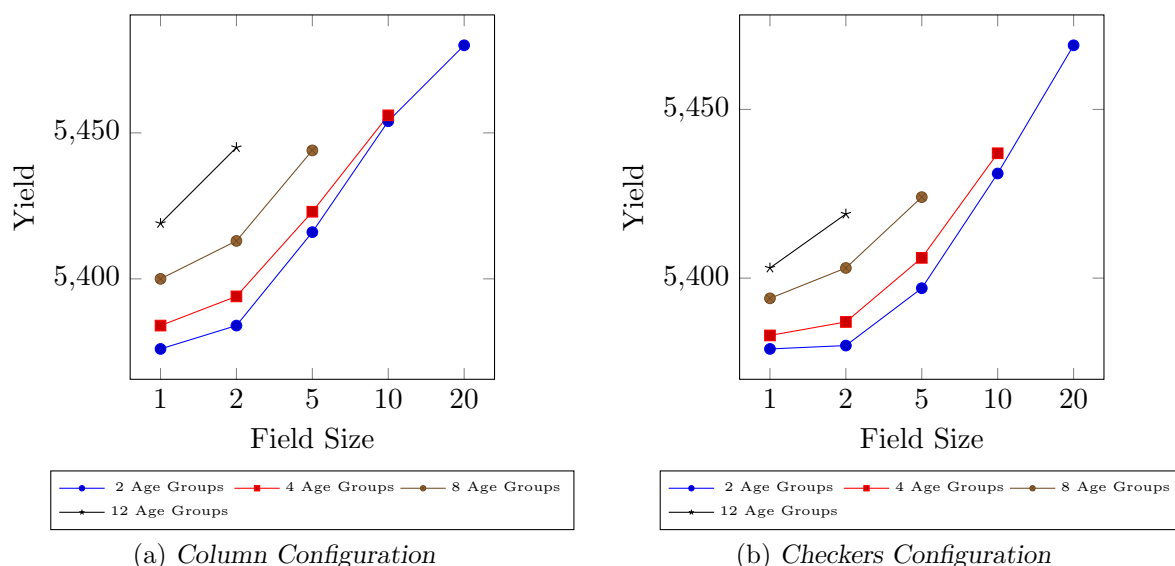


FIGURE 4.8: Yield trend based of field size for harvesting age of 14 months and linear maturity function.

age groups are now performing better than 12 age groups.

From the graphs it is clear that the general trend indicates that an increase in field size leads to an increase in the estimated yield. These results are similar to that of Potgieter [29], where it was found that same-aged patches of sugarcane should be grouped together into larger fields.

4.3.5 Age groups

The impact of the number of age groups are also examined, with Figures 4.11 to 4.16 showing the results. Each figure shows results for a different harvesting age, considers multiple field sizes and compares the Column and Checkers configuration patterns. The results obtained using the linear maturity function are discussed in this section, with the results using the other maturity functions discussed in Appendix C in a similar way.

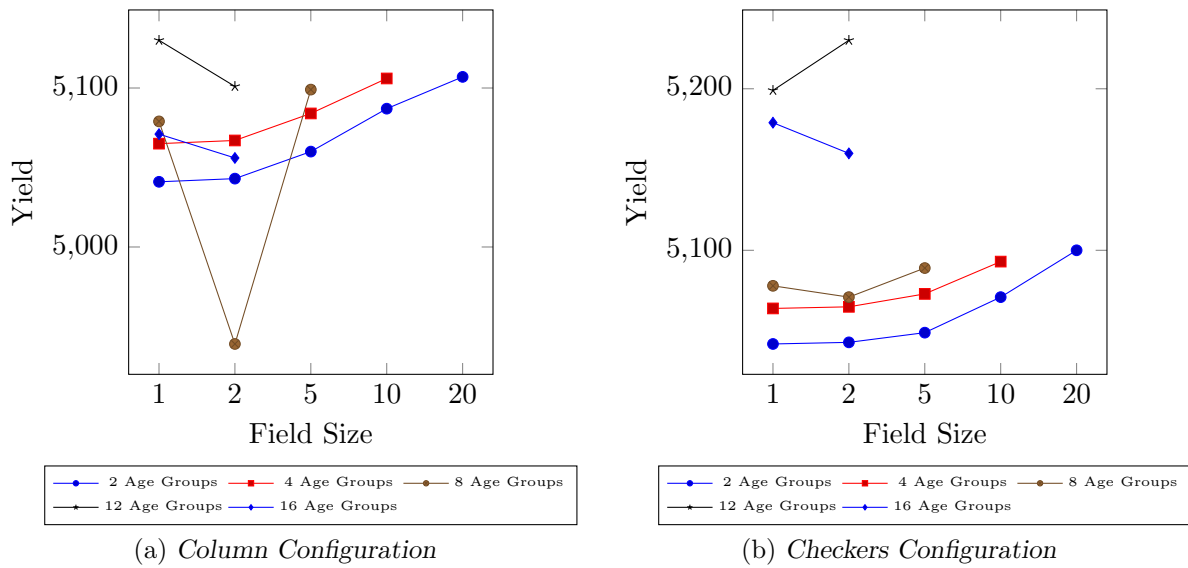


FIGURE 4.9: Yield trend based of field size for harvesting age of 16 months and linear maturity function.

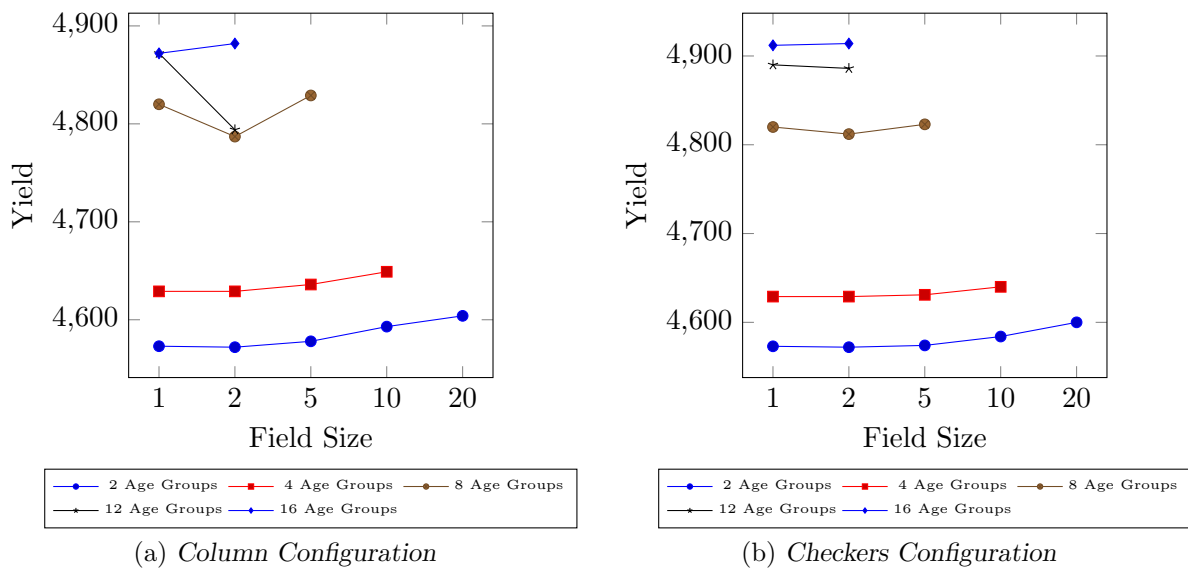


FIGURE 4.10: Yield trend based of field size for harvesting age of 18 months and linear maturity function.

In Figure 4.11, the impact of age groups for a harvesting age of 8 months are presented. For all the field sizes and both configurations, an increase in the age groups leads to increased yields. The largest field size also performs best for each age group, providing the same insight as the previous section.

The results for a harvesting age of 10 months are provided in Figure 4.12. The benefit in increasing the number of age groups seems to have reduced when compared to 4.11, with some cases where increasing the number of age groups led to a decrease in yield.

In Figure 4.13, the results for a harvesting age of 12 months are given. This once again follows the trend that more age groups leads to higher yields, however the additional benefit from each increase in the number of age groups varies drastically. Increasing from 2 to 4 age groups only increases the estimated yield by a small amount, while the increase to 8 age groups has a much larger benefit. When increasing further to 12 age groups, the benefits reduces again but

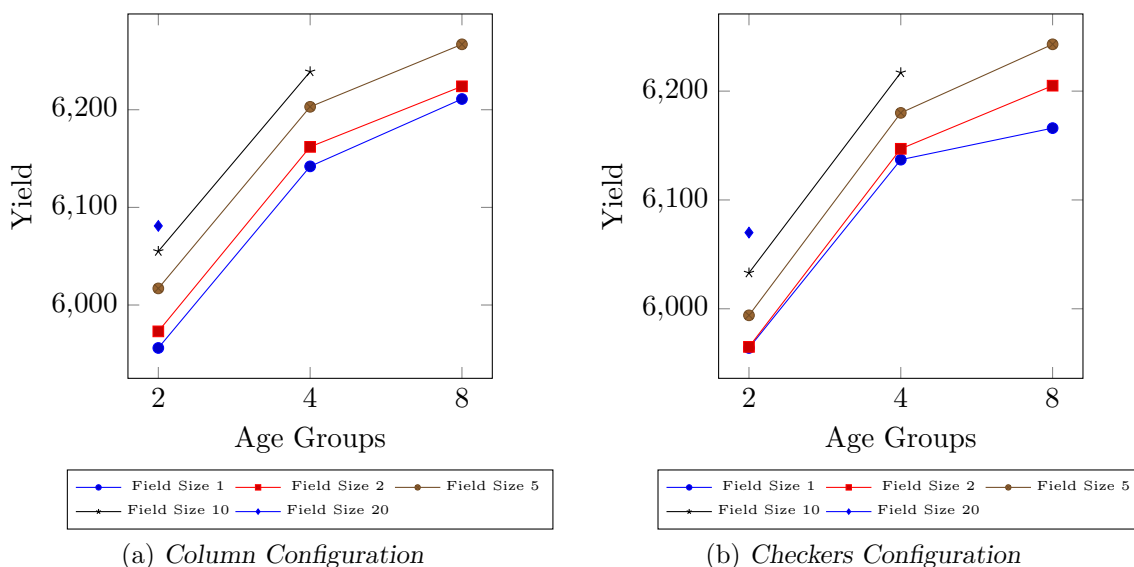


FIGURE 4.11: Yield trend based on number of age groups for harvesting age of 8 months and linear maturity function.

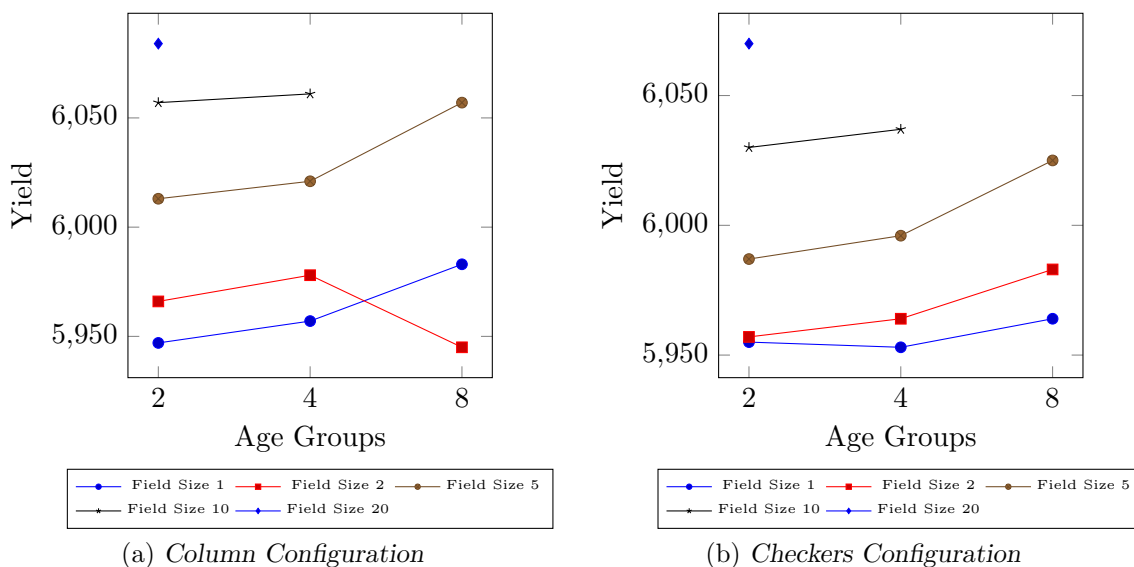


FIGURE 4.12: Yield trend based on number of age groups for harvesting age of 10 months and linear maturity function.

still leads to increase yields. This could indicate that there might be an optimal number of age groups after which the yields might potentially start decreasing if age groups are increased further.

The results for a harvesting age of 14 months are presented in Figure 4.14, providing an example where every increase in the number of age groups increases the estimated yields.

The increased harvesting age of 16 months has given some interesting results, as shown in Figure 4.15. The normal trend is seen from age groups 2 till 12, with the exception of 8 age groups for the *column* configuration and a field size of 2. However, a decrease in yield is seen when increasing the age groups to 16, indicating that there does exist an optimal number of age groups and increasing the age groups passed that optimal point could lead to reduced yields.

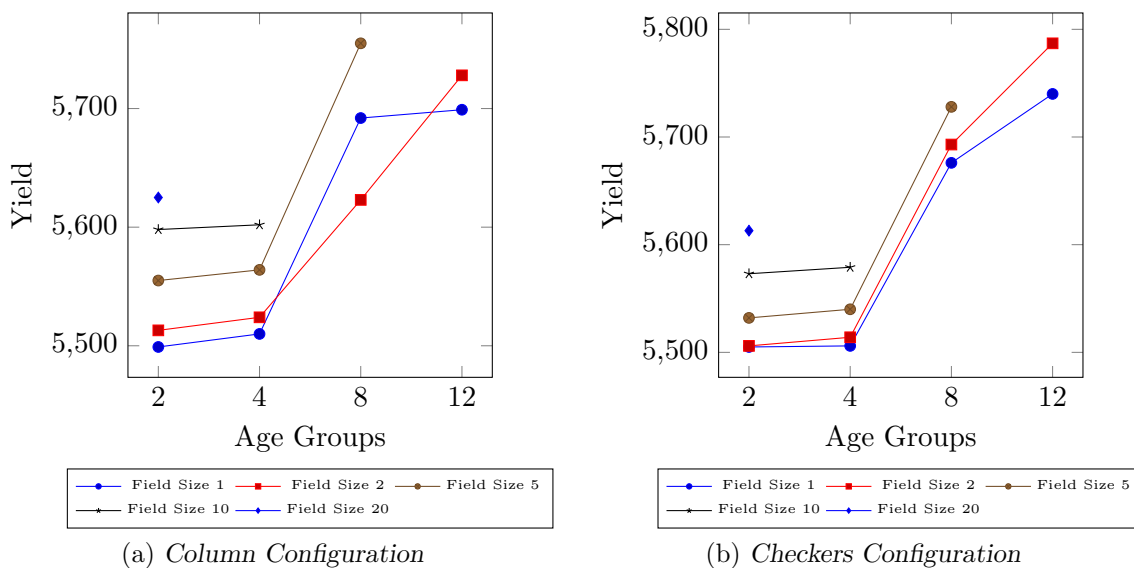


FIGURE 4.13: Yield trend based of number of age groups for harvesting age of 12 months and linear maturity function.

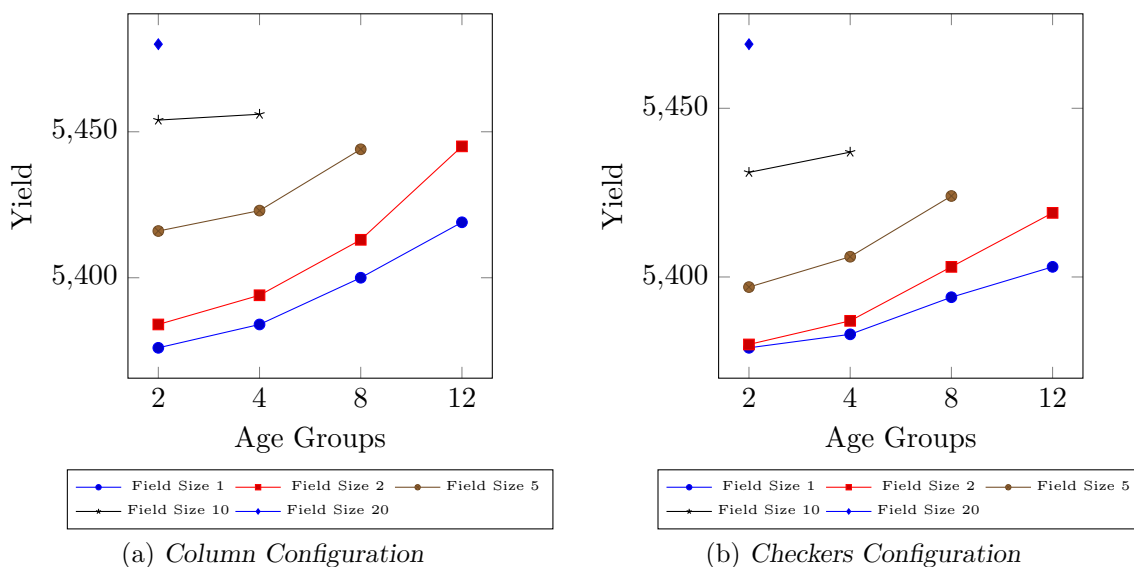


FIGURE 4.14: Yield trend based of number of age groups for harvesting age of 14 months and linear maturity function.

The results for a harvesting age of 18 months are provided in Figure 4.16 and shows that, for this harvesting age, 16 age groups performs better than 12 age groups. This is different from the 16 month harvesting age results seen in Figure 4.15, indicating that the optimal number of age groups is dependant on the chosen harvesting age.

In general, the results clearly show that an increase in number of age groups tends to lead to an increase in the expected yield obtained. This is once again similar to results obtained by Potgieter [29], which stated that more diversified domains in terms of crop age is deemed to be better. The rate of increase varied for each harvesting age considered and between each increase in number of age groups, indicating that there is for each field size and harvesting age an optimal number of age groups.

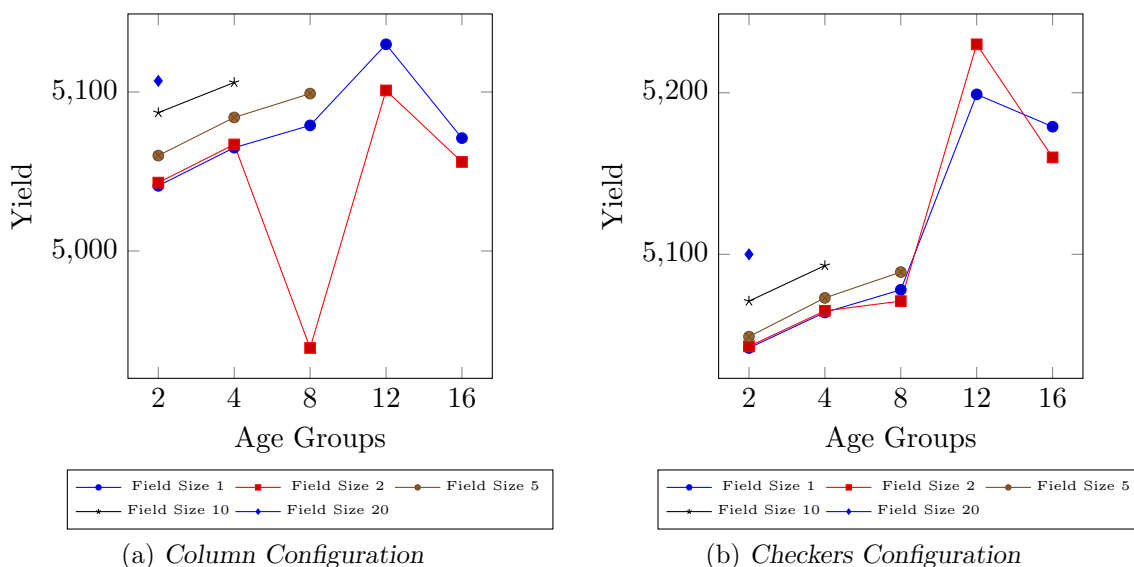


FIGURE 4.15: Yield trend based on number of age groups for harvesting age of 16 months and linear maturity function.

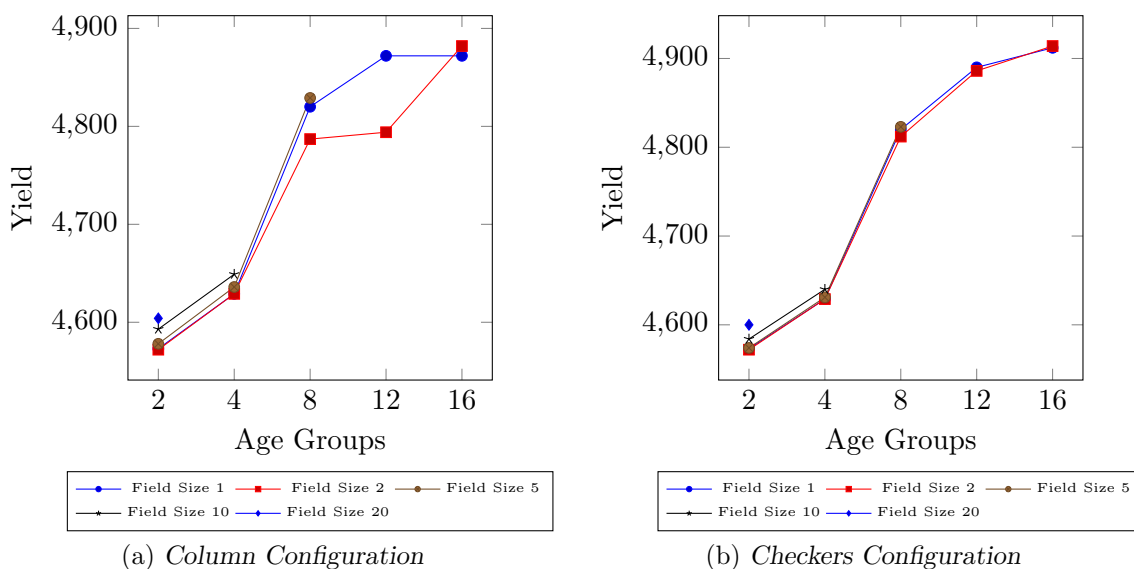


FIGURE 4.16: Yield trend based on number of age groups for harvesting age of 18 months and linear maturity function.

4.4 Sensitivity Analysis

Two parameters were considered for the sensitivity analysis, maturity function value and the value of α . This sensitivity analysis fixed the initial allocation pattern to *Column* and also only considered the linear maturity function.

4.4.1 Maturity function value

Different factors were applied to the Linear maturity function to determine a relationship between speed of Eldana growth and expected sucrose yield. It is assumed that the maturity

function provided in Chapter 3 has a factor of 1, with a factor of 0.5 then halving the obtained value of p_g . In general, the adjusted probability p_g^* is calculated as

$$p_g^* = fp_g, \quad (4.3)$$

where f is the factor applied and p_g is the probability obtained from the maturity functions as described in Chapter 3.

Table 4.6 shows the best yield obtained for each factor applied to the various harvesting ages, with the full set of data provided in Appendix D.

f	Harvesting Age					
	8	10	12	14	16	18
0.1	6354	6208	5912	5650	5280	5043
0.25	6339	6187	5885	5619	5247	5007
0.5	6316	6151	5843	5572	5197	4952
0.75	6292	6120	5799	5523	5150	4907
1	6267	6084	5755	5480	5107	4882

TABLE 4.6: Highest sucrose yield for the various maturity function factors and harvesting ages

As expected, a decrease in maturity probabilities leads to increased sucrose yield.

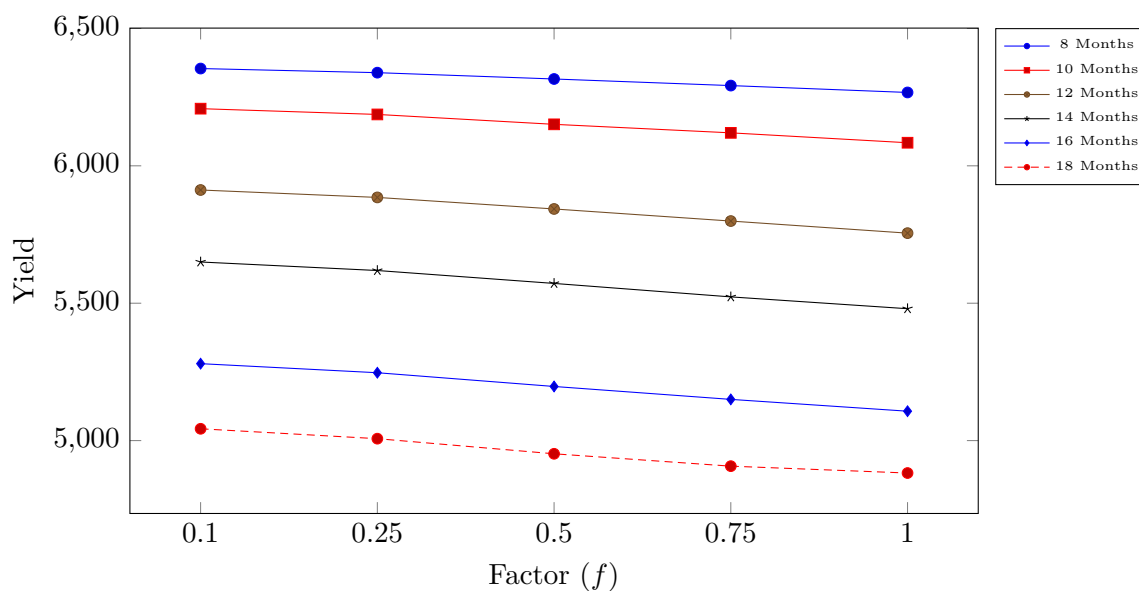


FIGURE 4.17: Best yield for each maturity factor by harvesting age.

4.4.2 Alpha value

The alpha values determines the weighting assigned to the infestation pressure experienced from a cell's neighbourhood compared to the natural increase from population growth within the cell. The effect of changing the alpha value may be seen in Table 4.7, where the highest obtained yield is shown for each alpha value and a fixed harvesting age of 12 months.

Alpha	Harvesting Age					
	8	10	12	14	16	18
0.1	6346	6192	5886	5616	5236	4981
0.2	6305	6132	5808	5535	5154	4915
0.3	6267	6084	5755	5480	5107	4882
0.4	6233	6047	5716	5440	5080	4867
0.5	6202	6013	5682	5405	5067	4863

TABLE 4.7: Highest sucrose yield for the various alpha values and harvesting age equal to 12 months.

It is clear that a lower alpha values leads to higher yields. This means that the neighbourhood pressure contributes more to the Eldana infestation growth than the natural increase of each cell.

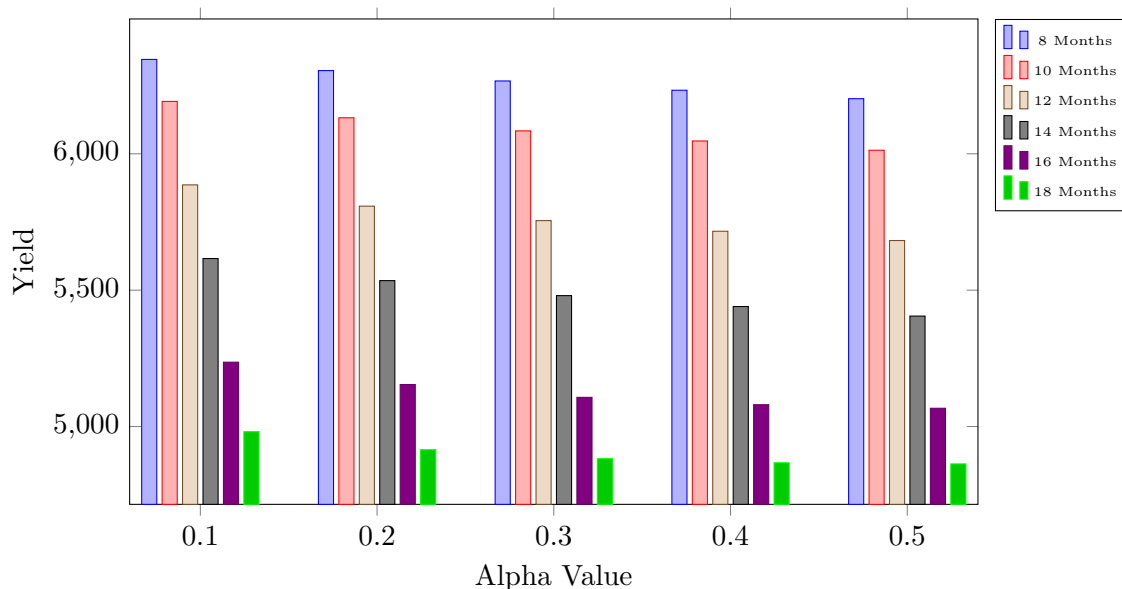


FIGURE 4.18: Best yield for each alpha value by harvesting age.

4.5 Recommendations

From the results obtained it is recommended that harvesting be done at the earliest age that is practically viable, with higher harvesting ages leading to higher infestation levels which then has lower sucrose yields although uninfested sugarcane would have yielded more sucrose with the higher harvesting age. It was observed that larger field sizes leads to increased yields, thus leading to a recommendation that fields should be as large as possible. However, the effect of the number of age groups seems to have a greater impact on the estimated yield than field size has and it is therefore recommended to first determine the number of age groups that will be used. Once the number of age groups to be used is determined, it is recommended to have field sizes as large as possible.

To determine the correct number of age groups, usually it can be assumed that an increase in the number of age groups will lead to increased yields. The optimal number of age groups does however depend on the harvesting age and does not necessarily have to be the maximum

number of age groups allowed. The optimal number of age groups will have to be determined for each unique environment, but for simplicity the general rule of more age groups leads to higher yields can be followed. Lastly, it is recommended to use the *Column* allocation pattern as it outperforms the *Checkers* pattern in the majority of cases.

4.6 Chapter Summary

In the chapter the process of evaluating various agricultural landscape structures is described, including the number of simulation required for each landscape structure. The landscape structures chosen for evaluation are presented, together with the results obtained from simulating these chosen structures.

A detailed analysis is performed on the obtained simulation results, investigating the impact of the various variable aspects considered. Lastly, recommendations are made regarding the best values for these variables investigated based on the finding of the performed analysis.

CHAPTER 5

Decision support tool

Contents

5.1	Description of the decision support tool	51
5.2	GIS incorporation	51
5.3	User interaction	53
5.4	Model output	55
5.5	Chapter Summary	56

In this chapter, the model described in Chapter 3 is expanded upon and GIS information is incorporated. This allows the model to be used as a decision support tool usable by farmers to run a simulation on their unique landscape structure. A description of the tool is provided in §5.1, indicating where adjustments to the underlying model is required. In §5.2, the process of incorporating GIS is presented, followed by the required user interaction explained in §5.3. The obtainable outputs are presented in §5.4 after which the chapter concludes in §5.5.

5.1 Description of the decision support tool

The decision support tool has mostly the same assumptions, model formulation, parameterisation, model outputs, solution evaluation and computer implementation as the model described in Chapter 3. However, some changes and additions were made in the computer implementation of the model.

5.1.1 Initial allocation

If the GIS incorporated model is used, the initial allocation will be dependant on the shapefile provided and the different fields of the simulated area determined by the shapefile. Each field will contain only one age of cane and will be treated similarly to a homogeneous allocation.

5.2 GIS incorporation

The inclusion of GIS information was of great importance to the study. This allowed the simulation model to be run on the layout of a farm instead of just the square grid as with the basic model developed. The use of shapefiles (.shp) was employed to obtain the GIS information

required. A visualisation of the shapefile data is given in Figure 5.1, as generated with free shapefile viewing software.

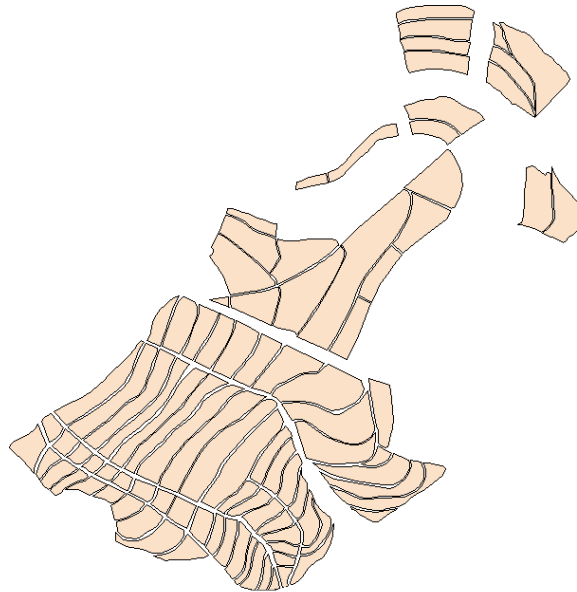


FIGURE 5.1: *Visualisation of shapefile generated by a shapefile viewer.*

The data was extracted from the shapefile using the Python package PyShp, where it was possible to obtain data relating to the different sugarcane fields. This data includes the points that make up the polygon of each field. To construct the cellular automaton, the simulated area is covered with a grid as shown in Figure 5.2. The coordinate points of importance need to be determined based on the size of each cell, with each point the centre of a cell.

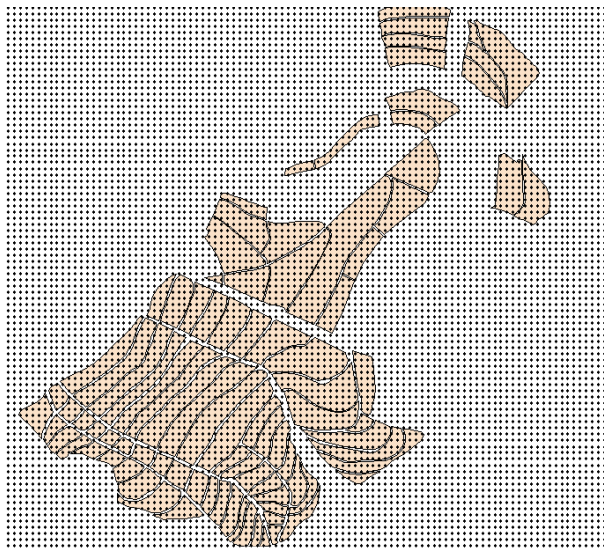


FIGURE 5.2: *Shapefile covered by a grid to determine point of importance.*

A bounding box of the shapefile is used to determine the size of the overlain grid, from which the number of cells are calculated according to the cell size. The coordinate points indicating the centre point of each cell is determined. These coordinate points are then used to determine if the cell should contain a patch of sugarcane, and then also to which sugarcane field that patch would belong to. This field allocation makes use of Algorithm 5.1, where the polygon of each

field is inspected to see if the point is within the polygon. The algorithm accomplishes this in 3 steps:

1. Checks if the point is one of the points used to define the polygon. If one of the points, then return “IN”, else continue algorithm.
2. Checks if the point is on the boundary of the polygon. If on the boundary, then return “IN”, else continue algorithm.
3. Lastly, checks if the point is within the area closed off by the polygon. If within the polygon area, then return “IN”, else return “OUT”.

Once each cell has been assigned to a field, the simulation can be initialised with the provided crop ages for each field in the simulated area. A visual representation of the shapefile structure within the simulation model is provided in Figure 5.3 where it is possible to identify individual fields and infer that each field is initialised with a single crop age.

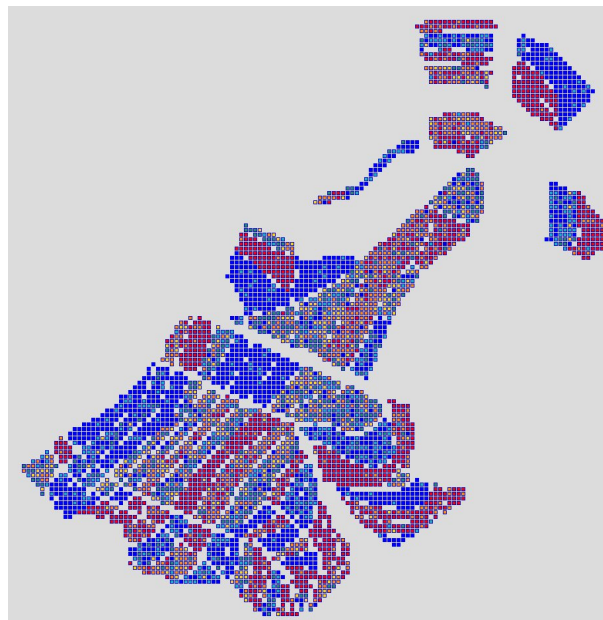


FIGURE 5.3: *Visual of the simulation model with the underlying structure based of a shapefile.*

The colour representation is the same as described in Chapter 3, with the blue indicating none or low levels of infestation and red indicating high infestation levels.

5.3 User interaction

To initialise the simulation model, some user interaction is required to provide the necessary model inputs. This requires the user to access the Python script used by the model and input the required parameters.

5.3.1 Shapefile

It is required that the user provides the model with the file path of where the shapefile is stored. It is important that the shapefile contains the required GIS information regarding the layout

Algorithm 5.1: Determines if a given point is within a specified polygon

Input : *point*, *polygon*

Output: Statement on whether point is in the polygon

```

1 if point in polygon then
2   | return "IN"
3 end
4  $x, y = \text{point}[0], \text{point}[1]$ 
5  $n = \text{length of } \textit{polygon}$ 
6 for  $i \leftarrow 0$  to  $n$  do
7   |  $p_1 = \text{None}$ 
8   |  $p_2 = \text{None}$ 
9   | if  $i == 0$  then
10  |   |  $p_1 = \text{polygon}[0]$ 
11  |   |  $p_2 = \text{polygon}[1]$ 
12  |   | else
13  |   |   |  $p_1 = \text{polygon}[i - 1]$ 
14  |   |   |  $p_2 = \text{polygon}[i]$ 
15  |   | end
16  |   | if  $p_1[1] == p_2[1]$  and  $p_1[1] == y$  and  $x > \min(p_1[0], p_2[0])$  and  $x < \max(p_1[0], p_2[0])$ 
17  |   |   | then
18  |   |   |   | return "IN"
19  |   |   | end
20  |   | end
21  |   |  $\text{inside} = \text{False}$ 
22  |   |  $p_1 = \text{polygon}[0]$ 
23  |   | for  $i \leftarrow 0$  to  $n + 1$  do
24  |   |   |  $p_2 = \text{polygon}[i \bmod n]$ 
25  |   |   | if  $y > \min(p_1[1], p_2[1])$  then
26  |   |   |   | if  $y \leq \max(p_1[1], p_2[1])$  then
27  |   |   |   |   | if  $x \leq \max(p_1[0], p_2[0])$  then
28  |   |   |   |   |   | if  $p_1[1] \neq p_2[1]$  then
29  |   |   |   |   |   |   |  $z = (y - p_1[1]) \times (p_2[0] - p_1[0]) \div (p_2[1] - p_1[1]) + p_1[0]$ 
30  |   |   |   |   |   |   | end
31  |   |   |   |   |   |   | if  $p_1[0] == p_2[0]$  or  $x \leq z$  then
32  |   |   |   |   |   |   |   |  $\text{inside} = \text{not inside}$ 
33  |   |   |   |   |   |   | end
34  |   |   |   |   |   | end
35  |   |   |   |   | end
36  |   |   |   |  $p_1 = p_2$ 
37  |   |   | end
38  |   | end
39  |   |  $\text{inside} = \text{False}$ 
40  |   | end
41  |   |  $p_1 = p_2$ 
42 end

```

of each field on the farm so that Algorithm 5.1 can be applied. Each field also requires a field number, which will be used in the initialisation of the model to assign the correct initial crop age.

5.3.2 Initial structure

The GIS landscape consists of various fields, with all cells in a field initialised with the same properties. The initial structure refers to the unique information required for each field during the initialisation phase of the simulation model, such as the crop age of each field.

If we assume that the number of fields are f , then to be able to represent the agricultural landscape structure we need a list of size f where position l in the list provides the required parameter info of field l at the initialisation of the simulation. Therefore the landscape structure S is represented by

$$S = (h, (a_1, a_2, \dots, a_l, \dots, a_f)) \quad (5.1)$$

if only the age of the crops are required and the harvesting age is fixed at h . The number of variables per field can be increased, for example

$$S = ((a_1, h_1), (a_2, h_2), \dots, (a_l, h_l), \dots, (a_f, h_f)) \quad (5.2)$$

where h_l once again provides the harvesting age for field l . This will allow the user to test different age allocations to fields and compare various landscape structures.

5.4 Model output

During each time step, data pertaining to Eldana infestation and sugarcane growth is recorded. Due to the potential of the number of cells to be quite large, the data is only captured for the entire grid of cells and not recorded for each cell individually.

5.4.1 Infestation state

The following data is captured:

- Minimum infestation state
- Maximum infestation state
- Average infestation state
- Proportional distribution of infestation states

The minimum, maximum and average infestation levels provides the user with a good overview of the infestation across the sugarcane area simulated. More detailed results can be seen from the proportional distribution of the infestation levels, which is the proportion of cells that are in each infestation state at each time step.

5.4.2 Sugarcane growth

Data regarding the growth of the sugarcane is captured as a proportional distribution of cane age. This allows the user to see the available sugarcane at each time step and is captured similarly to the distribution of the infestation states.

5.4.3 Sugarcane yield

Information regarding the sucrose yield accumulated from harvesting is also collected. This data indicates how many cells are harvested each time period and categorises it by infestation level. An aggregated view of total sucrose yield by month is also provided, which is also used to provide the user with a total yield value over the entire simulation period.

5.5 Chapter Summary

The GIS implementation was described, showing how the model can be applied to actual farms with the use of shapefiles. The required adjustments to the simulation model described in Chapter 3 was discussed, indicating where the decision support tool differs. The interaction needed by the user was provided and potential model outputs was presented.

CHAPTER 6

Conclusion

Contents

6.1 Thesis Summary	57
6.2 Main Contributions	58
6.3 Possible Future work	59

A summary of the research presented in this thesis is given in §6.1, followed by a short description of the main contributions of the study in §6.2. The thesis is finally concluded with a list of potential future research that may emanate from this study.

6.1 Thesis Summary

In the introduction of this thesis, the importance of more environmentally friendly pest management strategies were briefly discussed followed by the introduction of Eldana and its history as a pest species in the sugarcane industry. A brief problem description as well as the scope and objectives for this study also formed part of this chapter.

A literature review was presented in Chapter 2, including the necessary biological background of sugarcane and Eldana, and the way they influence each other. A physical description of sugarcane was provided, together with information regarding the growth, harvesting and expected yields of the crop. The life cycle of Eldana was presented, explaining the host-pest relationship with sugarcane and the resulting losses in sucrose yield. Research regarding various pest management strategies were discussed, along with the current strategies that are being implemented in the industry. The chapter also familiarised the reader with the Cellular Automaton simulation methodology that was used in the study.

A detailed description of the CA simulation model was presented in Chapter 3. The simplifying assumptions required to model and simulate Eldana infestation in sugarcane were discussed in §3.2, after which the mathematical formulation of the CA simulation model was presented in §3.3. Two main aspects influence progression to different infestation states in the model, namely the probability of natural increase in infestation due to a cells own infestation state and the probability of increase in infestation due to pressure from neighbouring infested cells. Model input parameters and model output are discussed in detail in §3.4 and §3.5 respectively. The model was implemented using the programming language Python and this implementation along with the iterative process followed during the simulation was described in §3.6. Finally,

various simulations were performed in an attempt to verify and validate the model outputs and compare the results to expected outcomes.

In Chapter 4, the results of numerous simulations were provided. The process of evaluation was discussed along with the number of simulations required for valid evaluation. A number of agricultural landscape structures were defined on which an Eldana infestation was simulated. These results were then analysed, considering the effect of each variable on the quality of the landscape structure in terms of yield and infestation levels. Practical recommendations were made based on the results, which may act as guidelines for the sugarcane industry and help with the decisions regarding how to diversify sugarcane farms with respect to crop age. The main results obtained indicated that larger groupings of same aged crops performed better, while also diversifying the harvest by increasing the number of age groups. An earlier harvesting age also led to higher sucrose yields, recommending the cane should not be carried over during the period that the mills are closed.

A decision support tool is presented in Chapter 5, showing how the GIS information was incorporated into the model as the underlying spatial space that the simulation was run on. The required adjustments to the model described in Chapter 3 was provided along with the required user interaction and possible model outputs obtainable from the model.

6.2 Main Contributions

The main contributions made by this study with regards to the biological modelling of the pest Eldana on sugarcane are discussed in this section.

1. *The development of a cellular automaton simulation model for Eldana infestation in sugarcane*

A cellular automaton model was developed to model the interactions between the pest Eldana and its agricultural host sugarcane. The model incorporated simplified growth functions for Eldana and sugarcane, with these assumptions allowing the simulation to consider larger spatial areas compared to other simulation methods. This study has indicated that the CA simulation methodology can be used successfully to simulate the infestation of Eldana on sugarcane.

2. *The inclusion of GIS information in the form of shapefiles for the underlying environment to be simulated*

The incorporation of shapefiles into the simulation model allows the user to simulate the infestation on a specific field or a collection of fields. Farmers are then able to obtain results calibrated to their own farm and providing a platform to test various what-if scenarios.

3. *Practical recommendations for sugarcane landscape structures to minimise Eldana infestation*

The results obtained in the study can be used to construct guidelines on which agricultural landscapes should lead to reduced Eldana infestation. Various parameters of the configurations were analysed, with higher yielding configurations obtained by increasing the field size, having more age groups and mainly applying an earlier harvesting age strategy. The column pattern performed slightly better than the Checkers, but the effect was not one of the main contributing factors to increased sucrose yield. The slight improvement experienced with the column configuration pattern, once again indicating that it is better to group same aged crops together.

6.3 Possible Future work

Various suggestions are made of possible future research that can be done based on the work done in this study. There are multiple aspects of the simulation model that can be improved upon, including some of the simplifying assumptions made and the incorporation of additional variables.

Consider climate effects

The effect of temperature was not included in the growth of Eldana. The inclusion of daily temperatures might provide a more accurate representation of the growth of Eldana, however, it will increase the complexity of the model, making analysis of the results more challenging.

There are many weather conditions that could impact the growth of both the sugarcane and Eldana. The effect of these can be incorporated like a drought or water logged cane resulting in reduced sucrose yields.

Incorporate push and pull plants

A main part of habitat management is the use of push and pull plants, referring to other crops that can be planted within or around the sugarcane field to either attract the pest (pull plants) or to repel the pest (push plants). The placement of such plants could have a meaningful effect on the spreading of Eldana infestation.

Differentiate between various sugarcane varieties

The study did not consider the variety of sugarcane being used, with each variety having different levels of resistance towards Eldana. However, the more resistant varieties tend to yield less sucrose, thus leading to decisions regarding which varieties would be best suited to plant and what should the distribution of those varieties be.

Effect of soil composition

With the use of GIS information it might be possible to incorporate information regarding the soil composition. Different soil compositions could lead to variability in soil quality which in turn could lead to slower or weaker growth of sugarcane. This information could be used in conjunction with the sugarcane varieties to determine the best place to plant each variety on a farm.

Consider more landscape structures

This study only considered a small percentage of the solution space, with only certain landscape structures identified for comparison. Various other landscape structures can be considered, which might potentially provide improved results.

Other allocation structures

The study only considered a column and checkers allocation. There are many other possible allocations that could be inspected in the future, including some variations on the checkers pattern used.

Optimisation methods

No optimisation was done in this study, with all recommendations based on a set of pre-determined landscape structures. These structures were chosen to be a good representation of the solution space, however, many more possible configurations exist. There might be much more to gain by applying optimisation techniques to find optimal landscape structure.

GIS optimisation

With the use of optimisation techniques, each GIS implementation of the simulation could be optimised independently. This means results could be specified for a user instead of the general guidelines that are provided in this study.

Improve on sucrose yield formula

The formula for sucrose yield used by the model was acquired from the study of Stray [32] and was an estimate of a single variety of sugarcane. Further research and data to estimate sucrose yield for each potential variety may improve the validity of the simulation results and could also incorporate various other factors that influence the expected yield.

Alternative maturity probability functions

The maturity probability functions used in this study were theoretical functions based on the assumption that Eldana infestation would cause a 5% loss of sucrose yield if cane was infested for 12 months. Maturity functions based on validated models or captured data will provide more accurate results.

Additional sensitivity analysis

Sensitivity analysis was performed using the Column allocation pattern and the Linear maturity function. Additional sensitivity analysis can be done with other allocation pattern and maturity function combinations.

References

- [1] A ADAMATZKY ALE R ALONSO-SANZ, 2008, *Automata-2008: Theory and Applications of Cellular Automata*, Luniver Press, Available from <http://gen.lib.rus.ec/book/index.php?md5=21B90C1EFBA5322A362C87D82C7BA780>.
- [2] ARAI K & BASUKI A, 2011, *Gis based two dimensional cellular automata approach for prediction of forest fire spreading*, International Journal of Research and Reviews in Computer Science, **2(6)**, p. 1305.
- [3] ATKINSON P, 1979, *Distribution and natural hosts of eldana saccharina walker in natal, its oviposition sites and feeding patterns*, Proceedings of the Proceedings of the South African Sugar Technologists Associatio.
- [4] ATKINSON P, CARNEGIE A, SMAILL R *et al.*, 1981, *A history of the outbreaks of eldana saccharina walker in natal*, Proc. S. Afr. Sugar Technol. Assoc, **55**, pp. 111–115.
- [5] ATKINSON P & NUSS K, 1989, *Associations between host-plant nitrogen and infestations of the sugarcane borer, eldana saccharina walker (lepidoptera: Pyralidae)*, Bulletin of Entomological Research, **79(3)**, pp. 489–506.
- [6] ATKINSON P *et al.*, 1980, *On the biology, distribution and natural host-plants of eldana saccharina walker (lepidoptera: Pyralidae)*., Journal of the Entomological Society of Southern Africa, **43(2)**, pp. 171–194.
- [7] CARNEGIE A, 1974, *A recrudescence of the borer eldana saccharina walker (lepidoptera: Pyralididae)*, Proceedings of the Proceedings of the South African Sugar Technologists Association, volume 48, pp. 107–110.
- [8] CARNEGIE A & SMAILL R, 1982, *Pre-trashing of sugarcane as a means of combating the borer eldana saccharina walker*, Proceedings of the Proceedings of the South African Sugar Technologists Association, volume 56, pp. 78–81.
- [9] CHOPARD B & DROZ M, 1998, *Cellular Automata Modeling of Physical Systems*, Cambridge University Press, Available from <http://gen.lib.rus.ec/book/index.php?md5=B1D5FAA1206D1C05DB87242FBD6D4376>.
- [10] COCKBURN JJ, 2013, *Implementation of the push-pull strategy for eldana saccharina control on sugarcane in kwazulu-natal, south africa*, Doctoral Dissertation, North-West University.
- [11] CONLONG D, 2001, *Biological control of indigenous african stemborers: What do we know?*, International Journal of Tropical Insect Science, **21(4)**, pp. 267–274.
- [12] COOK SM, KHAN ZR & PICKETT JA, 2007, *The use of push-pull strategies in integrated pest management*, Annu. Rev. Entomol., **52**, pp. 375–400.

- [13] DENT D, 2000, *Insect pest management*, Cabi.
- [14] EHLER L, 1998, *Conservation biological control: past, present, and future*, pp. 1–8 in *Conservation biological control*, pp. 1–8. Elsevier.
- [15] ENCYCLOPEDIA BRITANNICA, *Sugarcane*, Available from <https://www.britannica.com/plant/sugarcane/Diseases>, [Online; accessed 19 December 2019].
- [16] ERMENTROUT GB & EDELSTEIN-KESHET L, 1993, *Cellular automata approaches to biological modeling*, *Journal of theoretical Biology*, **160**(1), pp. 97–133.
- [17] GOEBEL FR & WAY M, 2003, *Investigation of the impact of eldana saccharina (lepidoptera: Pyralidae) on sugarcane yield in field trials in zululand*, *Proceedings of the Proc S Afr Sug Technol Ass*, volume 77, pp. 256–265.
- [18] GURR GM, SCARRATT S, WRATTEN SD, BERNDT L & IRVIN N, 2004, *Ecological engineering, habitat manipulation and pest management*, *Ecological engineering for pest management: Advances in habitat manipulation for arthropods*, pp. 1–12.
- [19] HAWICK KA & SCOGINGS C, 2010, *A minimal spatial cellular automata for hierarchical predatory prey simulation of food chains.*, *Proceedings of the CSC*, pp. 75–80.
- [20] HEATHCOTE R, 1984, *Insecticide testing against eldana saccharina walker*, *Proceedings of The South African Sugar Technologists' Association-June*, p. 155.
- [21] KARAFYLLIDIS I & THANAILAKIS A, 1997, *A model for predicting forest fire spreading using cellular automata*, *Ecological Modelling*, **99**(1), pp. 87–97.
- [22] KING A, 1989, *An assessment of the loss in sucrose yield caused by the stalk borer eldana saccharina in swaziland*, *Proceedings of the Proceedings of the South African Sugar Technologists Association*, volume 63, pp. 197–201.
- [23] KOGAN M, 1998, *Integrated pest management: historical perspectives and contemporary developments*, *Annual review of entomology*, **43**(1), pp. 243–270.
- [24] LESLIE G, 1993, *Dispersal behaviour of neonate larvae of the pyralid sugarcane borer eldana saccharina*, *Proc. S. Afr. Sug. Technol. Assn.*, **67**, pp. 122–126.
- [25] METCALFE J, 1969, *The estimation of loss caused by sugar cane moth borers*, *Pests of sugar cane*. Elsevier, Amsterdam, pp. 61–79.
- [26] OGUNWOLU E, REAGAN T, FLYNN J & HENSLEY S, 1991, *Effects of diatraea saccharalis (f.)(lepidoptera: Pyralidae) damage and stalk rot fungi on sugarcane yield in louisiana*, *Crop Protection*, **10**(1), pp. 57–61.
- [27] PACKARD NH & WOLFRAM S, 1985, *Two-dimensional cellular automata*, *Journal of Statistical physics*, **38**(5-6), pp. 901–946.
- [28] POTGIETER L, 2013, *A mathematical model for the control of eldana saccharina walker using the sterile insect technique*, *Doctoral Dissertation*, Stellenbosch: Stellenbosch University.
- [29] POTGIETER L, VAN VUUREN J & CONLONG D, 2015, *The role of heterogeneous agricultural landscapes in the suppression of pest species following random walk dispersal patterns*, *Ecological Modelling*, **306**, pp. 240–246.

-
- [30] RUTHERFORD R, 2015, *An integrated pest management (ipm) approach for the control of the stalk borer eldana saccharina walker (lepidoptera: Pyralidae)*, The South African Sugarcane Research Institute.
- [31] SOUTH AFRICA, *Sugar cane*, Available from <http://southafrica.co.za/sugar-cane.html>, [Online; accessed 1 December 2019].
- [32] STRAY BJ, 2010, *Tactical sugarcane harvest scheduling*, Doctoral Dissertation, Stellenbosch: University of Stellenbosch.
- [33] VAN VUUREN BJ, 2016, *An agent-based model of eldana saccharina walker*, Doctoral Dissertation, Stellenbosch: Stellenbosch University.
- [34] WAY M, 1995, *Developmental biology of the immature stages of eldana saccharina walker (lepidoptera: Pyralidae)*, Proceedings of the Proceedings of the South African Sugar Technologists Association, volume 69, pp. 83–86.
- [35] WIKIPEDIA THE FREE ENCYCLOPEDIA, *Eldana*, Available from <https://en.wikipedia.org/wiki/Eldana>, [Online; accessed 1 December 2019].
- [36] WIKIPEDIA THE FREE ENCYCLOPEDIA, *Sugarcane*, Available from <https://en.wikipedia.org/wiki/Sugarcane>, [Online; accessed 1 December 2019].
- [37] WOLFRAM S, 1986, *Minimal cellular automaton approximations to continuum systems*, Cellular Automata and Complexity, pp. 329–358.

APPENDIX A

Initial infestation probabilities

In Chapter 3, the probability lookup table for the linear maturity function was given, with the tables for the other maturity functions presented in this Appendix. These probability lookup tables are required to determine which initial infestation state to assign, with each maturity function having its own lookup table.

The probability lookup table for the decreasing maturity function is provided in Table A.1 along with the probability lookup tables for the increasing and shaped maturity functions given in Table A.2 and Table A.3 respectively.

Age	Initial infestation state ($g_{i,j,0}$)																
	0	1	2	3	4	5	6	7	8	9	10	11	12	13	14	15	16
0	0.9	0.1	0.0	0.0	0.0	0.0	0.0	0.0	0.0	0.0	0.0	0.0	0.0	0.0	0.0	0.0	0.0
1	0.818	0.095	0.059	0.022	0.005	0.001	0.0	0.0	0.0	0.0	0.0	0.0	0.0	0.0	0.0	0.0	0.0
2	0.665	0.13	0.102	0.062	0.028	0.009	0.003	0.001	0.0	0.0	0.0	0.0	0.0	0.0	0.0	0.0	0.0
3	0.469	0.153	0.145	0.111	0.069	0.034	0.013	0.004	0.001	0.0	0.0	0.0	0.0	0.0	0.0	0.0	0.0
4	0.278	0.142	0.162	0.154	0.12	0.079	0.041	0.017	0.006	0.002	0.0	0.0	0.0	0.0	0.0	0.0	0.0
5	0.14	0.099	0.141	0.165	0.161	0.129	0.087	0.046	0.02	0.007	0.002	0.001	0.0	0.0	0.0	0.0	0.0
6	0.06	0.057	0.097	0.139	0.167	0.165	0.137	0.093	0.051	0.023	0.008	0.003	0.001	0.0	0.0	0.0	0.0
7	0.023	0.026	0.054	0.094	0.136	0.167	0.169	0.142	0.097	0.055	0.025	0.009	0.003	0.001	0.0	0.0	0.0
8	0.008	0.01	0.025	0.052	0.091	0.136	0.168	0.173	0.145	0.099	0.055	0.025	0.01	0.002	0.001	0.0	0.0
9	0.003	0.004	0.01	0.024	0.052	0.092	0.138	0.17	0.175	0.144	0.099	0.054	0.024	0.008	0.002	0.0	0.0
10	0.001	0.001	0.004	0.01	0.025	0.054	0.095	0.142	0.175	0.174	0.142	0.095	0.05	0.022	0.007	0.002	0.0
11	0.0	0.0	0.001	0.004	0.011	0.027	0.057	0.101	0.15	0.178	0.172	0.14	0.089	0.044	0.018	0.005	0.002
12	0.0	0.0	0.0	0.001	0.004	0.012	0.031	0.063	0.11	0.155	0.181	0.172	0.133	0.081	0.037	0.013	0.005
13	0.0	0.0	0.0	0.001	0.002	0.005	0.014	0.035	0.072	0.121	0.166	0.186	0.167	0.123	0.068	0.028	0.014
14	0.0	0.0	0.0	0.0	0.001	0.002	0.006	0.018	0.042	0.083	0.135	0.178	0.188	0.16	0.107	0.051	0.031
15	0.0	0.0	0.0	0.0	0.0	0.001	0.002	0.008	0.022	0.051	0.098	0.151	0.187	0.188	0.146	0.083	0.062
16	0.0	0.0	0.0	0.0	0.0	0.0	0.001	0.004	0.011	0.029	0.064	0.117	0.168	0.199	0.179	0.118	0.111
17	0.0	0.0	0.0	0.0	0.0	0.0	0.001	0.001	0.005	0.015	0.039	0.082	0.139	0.189	0.199	0.151	0.179
18	0.0	0.0	0.0	0.0	0.0	0.0	0.001	0.001	0.002	0.007	0.022	0.054	0.105	0.165	0.203	0.176	0.265

TABLE A.1: Probability lookup table for the Decreasing maturity function with $N = 17$.

Age	Initial infestation state ($g_{i,j,0}$)																
	0	1	2	3	4	5	6	7	8	9	10	11	12	13	14	15	16
0	0.9	0.1	0.0	0.0	0.0	0.0	0.0	0.0	0.0	0.0	0.0	0.0	0.0	0.0	0.0	0.0	0.0
1	0.833	0.135	0.027	0.004	0.001	0.0	0.0	0.0	0.0	0.0	0.0	0.0	0.0	0.0	0.0	0.0	0.0
2	0.731	0.183	0.063	0.017	0.005	0.001	0.0	0.0	0.0	0.0	0.0	0.0	0.0	0.0	0.0	0.0	0.0
3	0.598	0.228	0.108	0.043	0.015	0.005	0.002	0.001	0.0	0.0	0.0	0.0	0.0	0.0	0.0	0.0	0.0
4	0.446	0.253	0.159	0.08	0.037	0.015	0.006	0.002	0.001	0.0	0.0	0.0	0.0	0.0	0.0	0.0	0.0
5	0.301	0.244	0.196	0.124	0.068	0.035	0.018	0.008	0.004	0.002	0.001	0.0	0.0	0.0	0.0	0.0	0.0
6	0.184	0.204	0.204	0.16	0.108	0.064	0.037	0.02	0.01	0.005	0.003	0.001	0.001	0.0	0.0	0.0	0.0
7	0.101	0.145	0.183	0.172	0.141	0.099	0.065	0.04	0.024	0.014	0.008	0.004	0.002	0.001	0.001	0.0	0.0
8	0.051	0.092	0.138	0.16	0.153	0.126	0.095	0.068	0.044	0.029	0.018	0.011	0.007	0.004	0.002	0.001	0.002
9	0.024	0.051	0.091	0.127	0.141	0.135	0.117	0.095	0.07	0.05	0.035	0.023	0.015	0.01	0.007	0.004	0.006
10	0.011	0.026	0.053	0.086	0.112	0.124	0.122	0.11	0.093	0.075	0.055	0.041	0.03	0.021	0.015	0.01	0.019
11	0.004	0.012	0.028	0.051	0.076	0.098	0.108	0.11	0.103	0.09	0.077	0.062	0.048	0.036	0.028	0.02	0.049
12	0.002	0.005	0.013	0.028	0.047	0.065	0.082	0.095	0.099	0.097	0.087	0.077	0.066	0.054	0.044	0.035	0.105
13	0.001	0.002	0.006	0.013	0.025	0.04	0.055	0.07	0.08	0.087	0.088	0.083	0.077	0.069	0.06	0.05	0.194
14	0.0	0.001	0.003	0.006	0.012	0.021	0.033	0.045	0.058	0.067	0.075	0.077	0.079	0.074	0.069	0.062	0.316
15	0.0	0.0	0.001	0.003	0.006	0.011	0.018	0.026	0.036	0.046	0.056	0.063	0.069	0.07	0.069	0.067	0.458
16	0.0	0.0	0.0	0.001	0.003	0.005	0.009	0.014	0.021	0.029	0.037	0.045	0.052	0.058	0.061	0.063	0.604
17	0.0	0.0	0.0	0.001	0.001	0.002	0.004	0.007	0.011	0.016	0.022	0.029	0.035	0.042	0.047	0.052	0.732
18	0.0	0.0	0.0	0.0	0.0	0.001	0.002	0.003	0.005	0.008	0.012	0.017	0.022	0.027	0.031	0.038	0.833

TABLE A.2: Probability lookup table for the Increasing maturity function with $N = 17$.

APPENDIX A. INITIAL INFESTATION PROBABILITIES

Age	Initial infestation state ($g_{i,j,0}$)																
	0	1	2	3	4	5	6	7	8	9	10	11	12	13	14	15	16
0	0.9	0.1	0.0	0.0	0.0	0.0	0.0	0.0	0.0	0.0	0.0	0.0	0.0	0.0	0.0	0.0	0.0
1	0.833	0.135	0.027	0.004	0.001	0.0	0.0	0.0	0.0	0.0	0.0	0.0	0.0	0.0	0.0	0.0	0.0
2	0.734	0.18	0.064	0.017	0.004	0.001	0.0	0.0	0.0	0.0	0.0	0.0	0.0	0.0	0.0	0.0	0.0
3	0.603	0.225	0.112	0.04	0.013	0.005	0.002	0.001	0.0	0.0	0.0	0.0	0.0	0.0	0.0	0.0	0.0
4	0.455	0.251	0.161	0.077	0.032	0.013	0.006	0.003	0.001	0.001	0.001	0.0	0.0	0.0	0.0	0.0	0.0
5	0.309	0.244	0.201	0.121	0.062	0.03	0.015	0.007	0.004	0.003	0.002	0.001	0.001	0.0	0.0	0.0	0.0
6	0.19	0.203	0.213	0.159	0.097	0.055	0.032	0.018	0.011	0.009	0.006	0.004	0.002	0.001	0.0	0.0	0.0
7	0.105	0.147	0.191	0.175	0.129	0.085	0.054	0.034	0.022	0.02	0.016	0.011	0.007	0.003	0.001	0.0	0.0
8	0.053	0.092	0.147	0.163	0.142	0.108	0.078	0.053	0.037	0.036	0.033	0.027	0.017	0.009	0.003	0.001	0.0
9	0.025	0.052	0.098	0.129	0.132	0.114	0.092	0.071	0.053	0.056	0.054	0.05	0.036	0.022	0.011	0.004	0.001
10	0.011	0.027	0.057	0.087	0.104	0.103	0.093	0.076	0.063	0.072	0.079	0.076	0.066	0.046	0.025	0.011	0.005
11	0.005	0.012	0.03	0.053	0.071	0.079	0.078	0.072	0.063	0.077	0.092	0.102	0.098	0.078	0.05	0.025	0.015
12	0.002	0.005	0.014	0.028	0.043	0.053	0.056	0.057	0.053	0.071	0.092	0.115	0.125	0.115	0.085	0.049	0.038
13	0.001	0.002	0.006	0.013	0.023	0.031	0.037	0.039	0.039	0.055	0.079	0.108	0.135	0.144	0.123	0.082	0.081
14	0.0	0.001	0.003	0.006	0.011	0.017	0.02	0.023	0.025	0.038	0.059	0.092	0.126	0.154	0.154	0.121	0.15
15	0.0	0.0	0.001	0.003	0.005	0.008	0.011	0.013	0.014	0.023	0.039	0.065	0.104	0.147	0.168	0.152	0.247
16	0.0	0.0	0.001	0.001	0.002	0.004	0.005	0.007	0.007	0.013	0.022	0.042	0.076	0.122	0.163	0.17	0.364
17	0.0	0.0	0.0	0.0	0.001	0.002	0.002	0.003	0.004	0.006	0.012	0.024	0.049	0.092	0.143	0.171	0.49
18	0.0	0.0	0.0	0.0	0.0	0.001	0.001	0.001	0.002	0.003	0.006	0.013	0.03	0.062	0.113	0.156	0.612

TABLE A.3: Probability lookup table for the Shaped maturity function with $N = 17$.

APPENDIX B

Field size analysis

The size of fields within the agricultural landscape has an impact on the spreading of Eldana infestations. This impact was discussed in §4.3, where the results for the linear maturity function was presented. In this Appendix, the results for the other maturity functions are presented and discussed.

Similar results are obtained for all maturity functions. This indicates that the recommendations made should hold for any maturity function.

B.1 Increasing maturity function

The results for the increasing maturity function and a harvesting age of 8 months are provided in Figure B.1. A general trend of an increase in fields size leading to an increase in yields, can be seen.

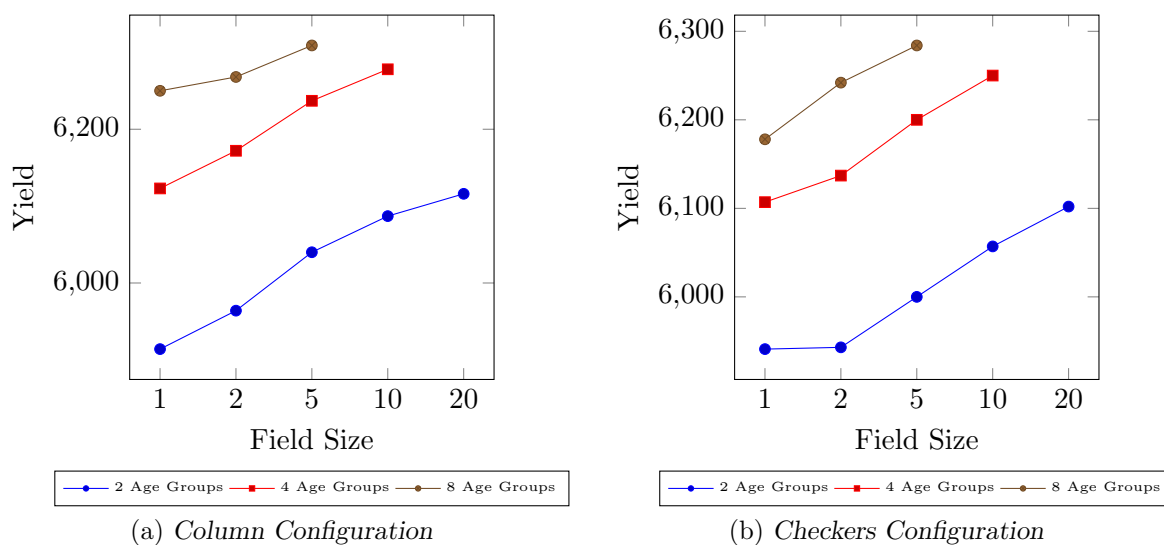


FIGURE B.1: Field size comparison for increasing function and 8 months harvesting age.

The results for the increasing maturity function and a harvesting age of 10 months are provided in Figure B.2. A general trend of an increase in fields size that leads to an increase in yields can be seen. There is an exception where the yield reduced when the field size increased from 1 to 2 for the *column* configuration and 8 age groups.

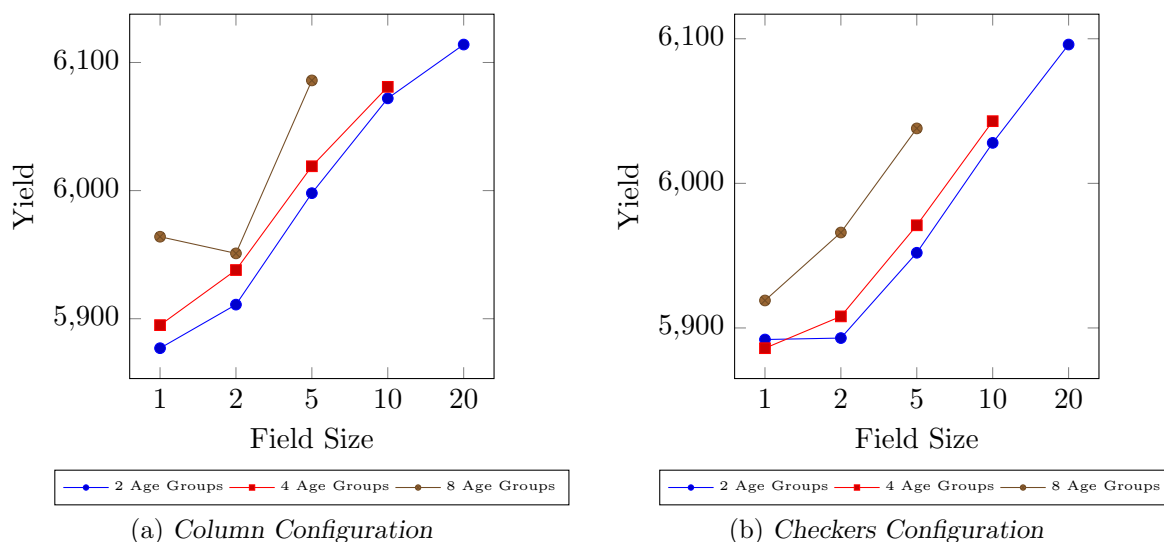


FIGURE B.2: Field size comparison for increasing function and 10 months harvesting age.

The results for the increasing maturity function and a harvesting age of 12 months are provided in Figure B.3. A general trend of an increase in fields size leading to an increase in yields, can be seen. Once again there is an exception where the yield reduced when the field size increased from 1 to 2 for the *column* configuration and 8 age groups.

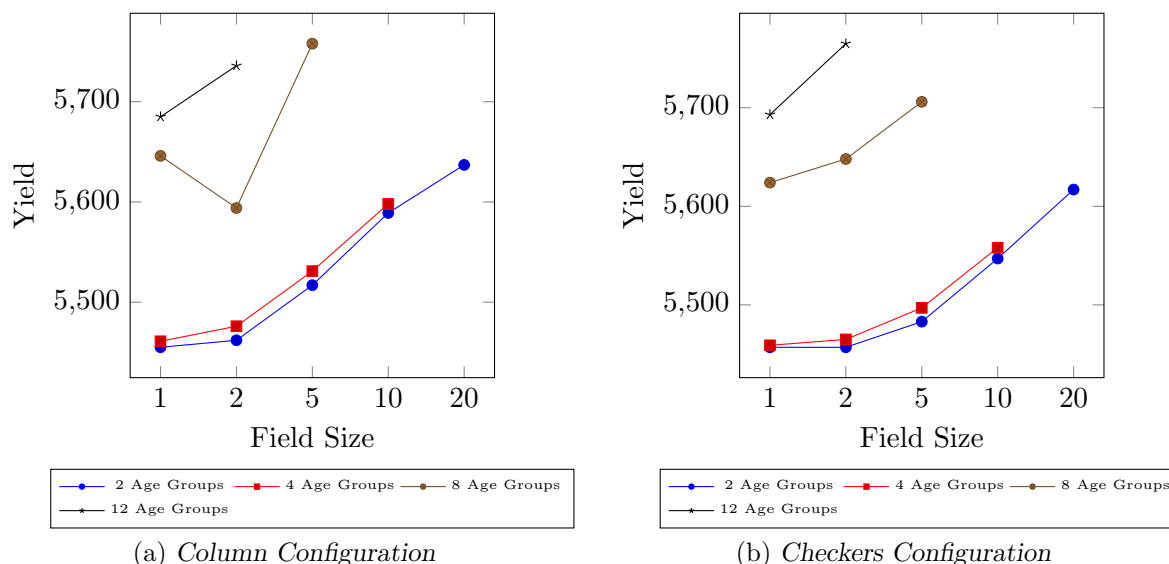


FIGURE B.3: Field size comparison for increasing function and 12 months harvesting age.

The results for the increasing maturity function and a harvesting age of 14 months are provided in Figure B.4. A general trend of an increase in fields size that leads to an increase in yields can be seen.

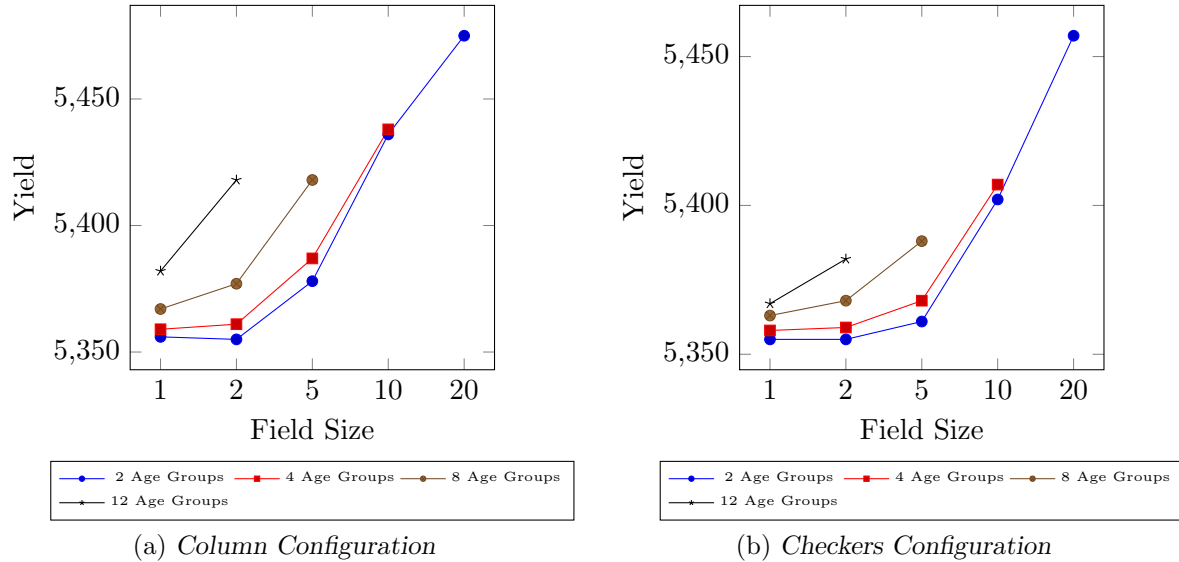


FIGURE B.4: Field size comparison for increasing function and 14 months harvesting age.

The results for the increasing maturity function and a harvesting age of 16 months are provided in Figure B.5. A general trend of an increase in fields size that leads to an increase in yields can be seen, however, a few exceptions are present. The yield reduced when the field size increased from 1 to 2 for the *column* configuration and 8, 12 & 16 age groups. The same reduction in yield is seen for the *checkers* configuration and 16 age groups.

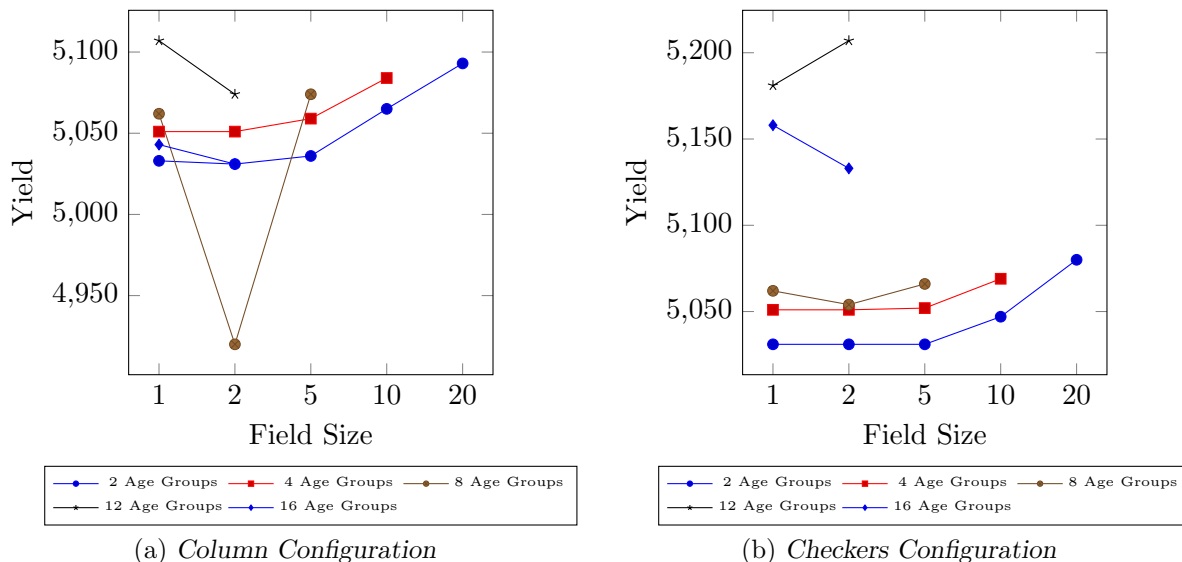


FIGURE B.5: Field size comparison for increasing function and 16 months harvesting age.

The results for the increasing maturity function and a harvesting age of 18 months are provided in Figure B.6. The usual trend of an increase in fields size that leads to an increase in yields does not seem to apply here, with very little benefit obtained from increasing field sizes.

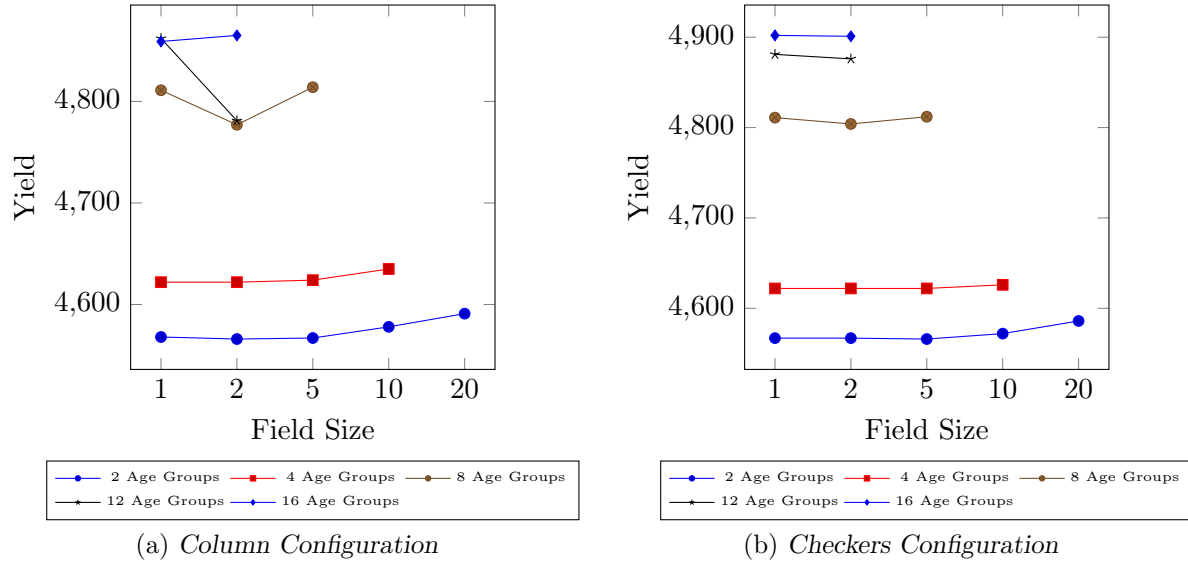


FIGURE B.6: Field size comparison for increasing function and 18 months harvesting age.

B.2 Decreasing maturity function

The results for the decreasing maturity function and a harvesting age of 8 months are provided in Figure B.7. A general trend of an increase in fields size leading to an increase in yields, can be seen.

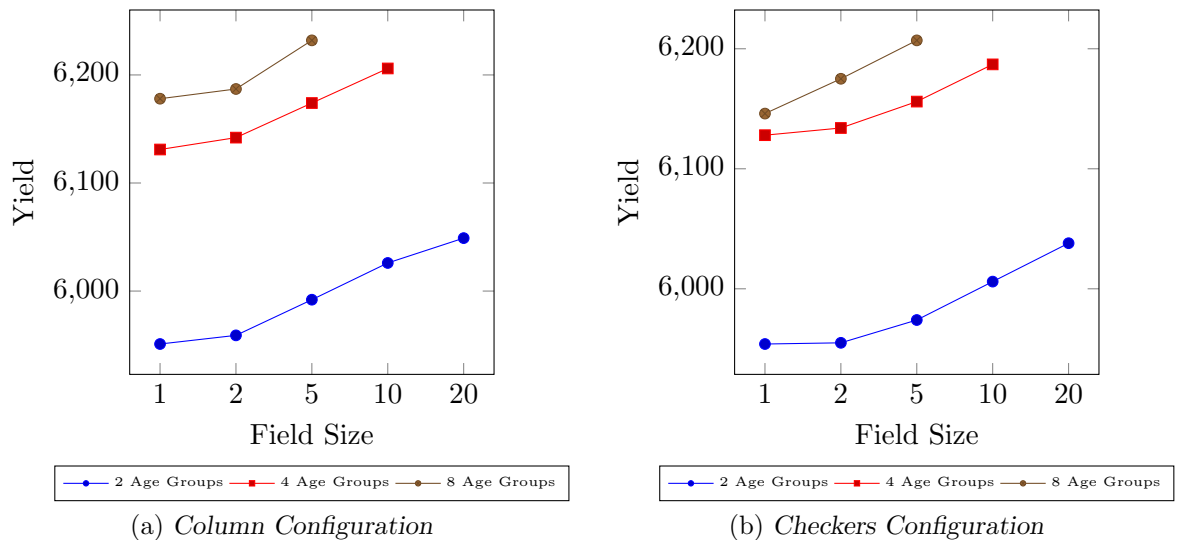


FIGURE B.7: Field size comparison for decreasing function and 8 months harvesting age.

The results for the decreasing maturity function and a harvesting age of 10 months are provided in Figure B.8. A general trend of an increase in fields size that leads to an increase in yields can be seen. There is an exception where the yield reduced when the field size increased from 1 to 2 for the *column* configuration and 8 age groups.

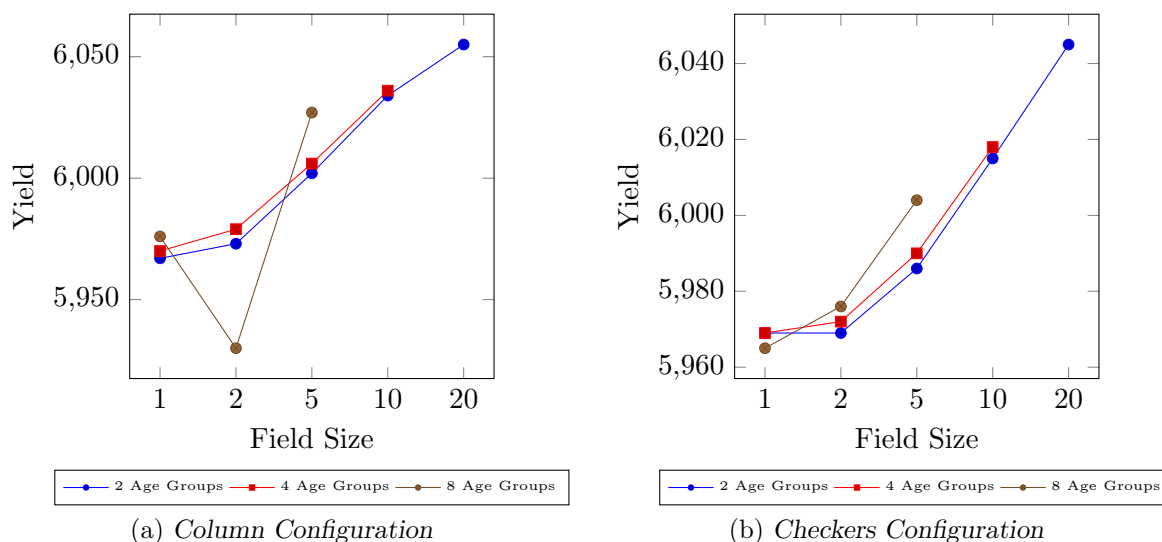


FIGURE B.8: Field size comparison for decreasing function and 10 months harvesting age.

The results for the decreasing maturity function and a harvesting age of 12 months are provided in Figure B.9. A general trend of an increase in fields size leading to an increase in yields, can be seen. Once again there is an exception where the yield reduced when the field size increased from 1 to 2 for the *column* configuration and 8 age groups.

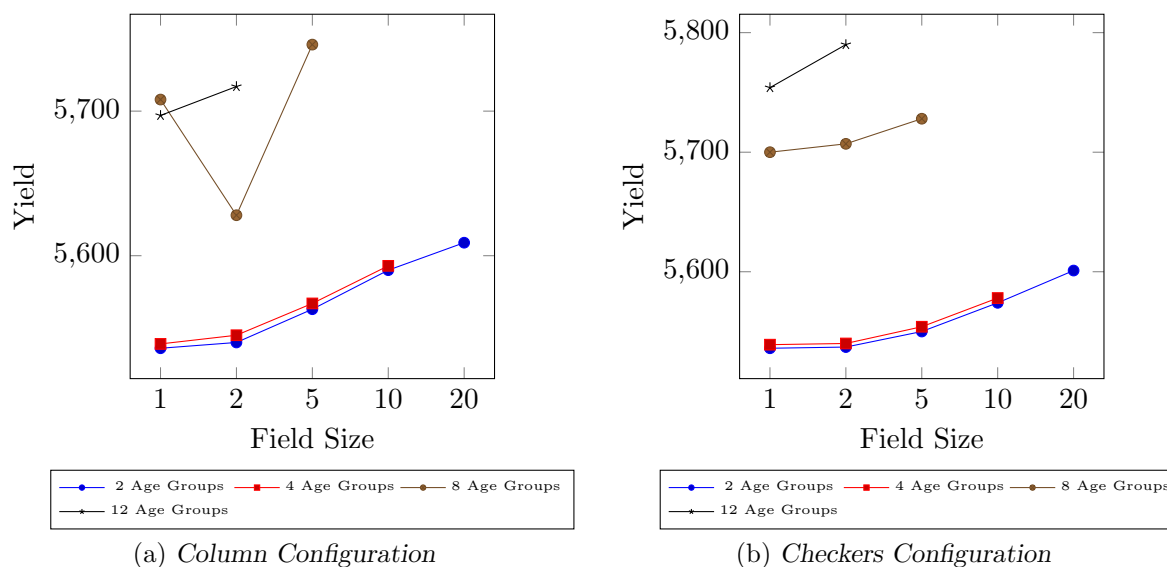


FIGURE B.9: Field size comparison for decreasing function and 12 months harvesting age.

The results for the decreasing maturity function and a harvesting age of 14 months are provided in Figure B.10. A general trend of an increase in fields size that leads to an increase in yields can be seen.

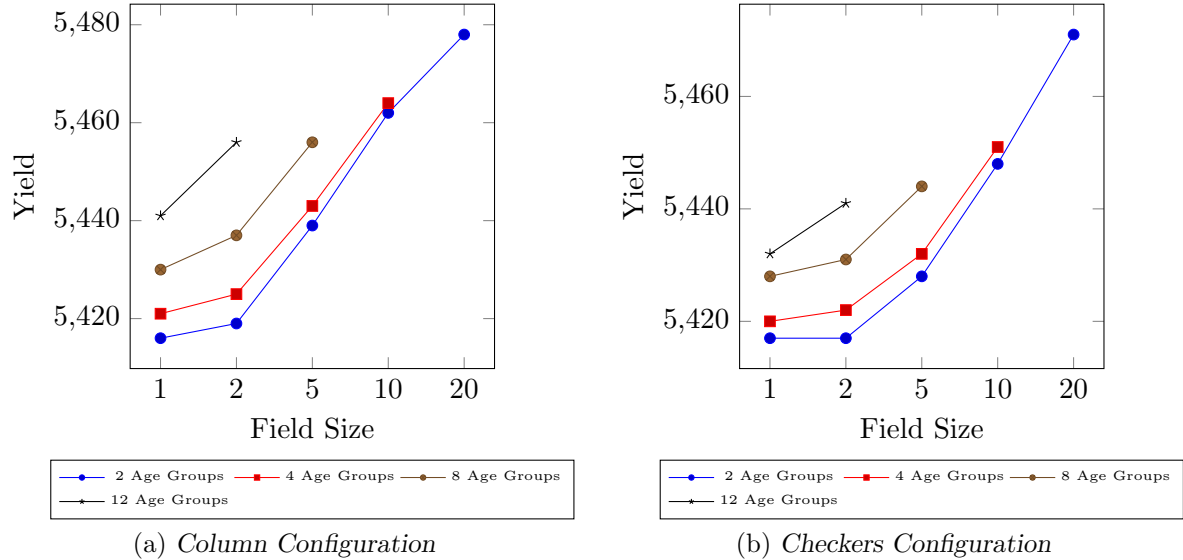


FIGURE B.10: Field size comparison for decreasing function and 14 months harvesting age.

The results for the decreasing maturity function and a harvesting age of 16 months are provided in Figure B.11. A general trend of an increase in fields size that leads to an increase in yields can be seen, however, a few exceptions are present. The yield reduced when the field size increased from 1 to 2 for the *column* configuration and 8, 12 & 16 age groups. The same reduction in yield is seen for the *checkers* configuration and 16 age groups.

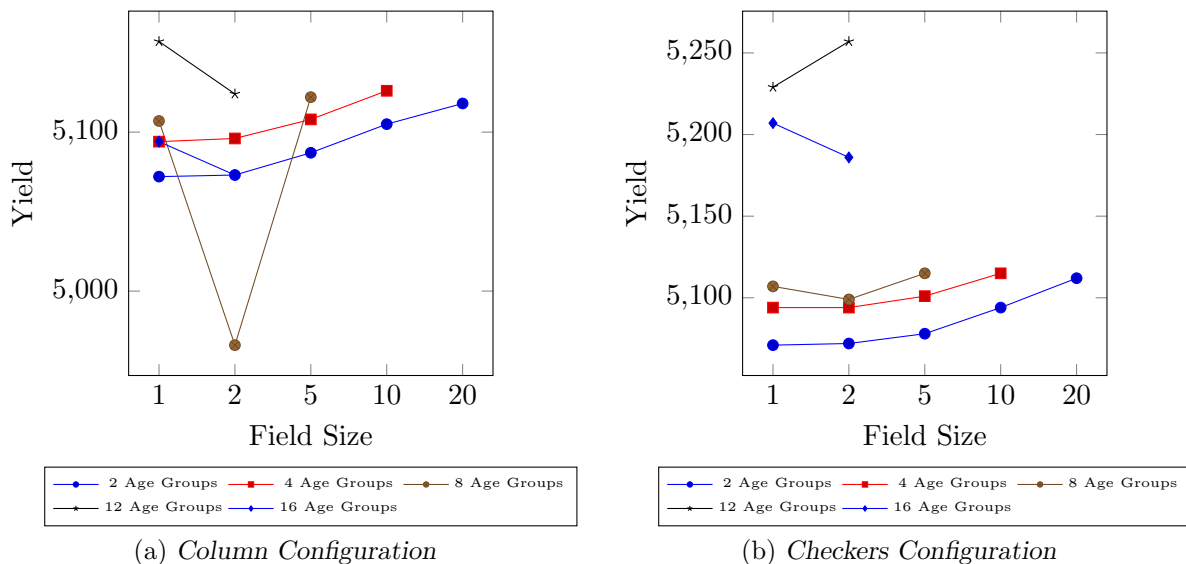


FIGURE B.11: Field size comparison for decreasing function and 16 months harvesting age.

The results for the decreasing maturity function and a harvesting age of 18 months are provided in Figure B.12. The usual trend of an increase in fields size that leads to an increase in yields does not seem to apply here, with very little benefit obtained from increasing field sizes.

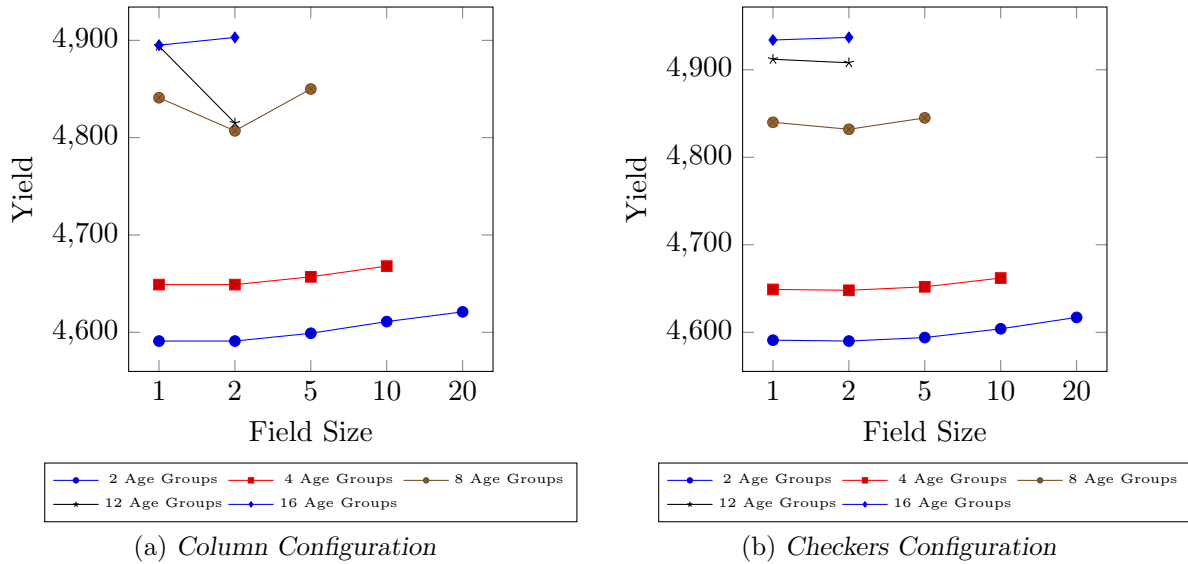


FIGURE B.12: Field size comparison for decreasing function and 18 months harvesting age.

B.3 Shaped maturity function

The results for the shaped maturity function and a harvesting age of 8 months are provided in Figure B.13. A general trend of an increase in fields size leading to an increase in yields, can be seen.

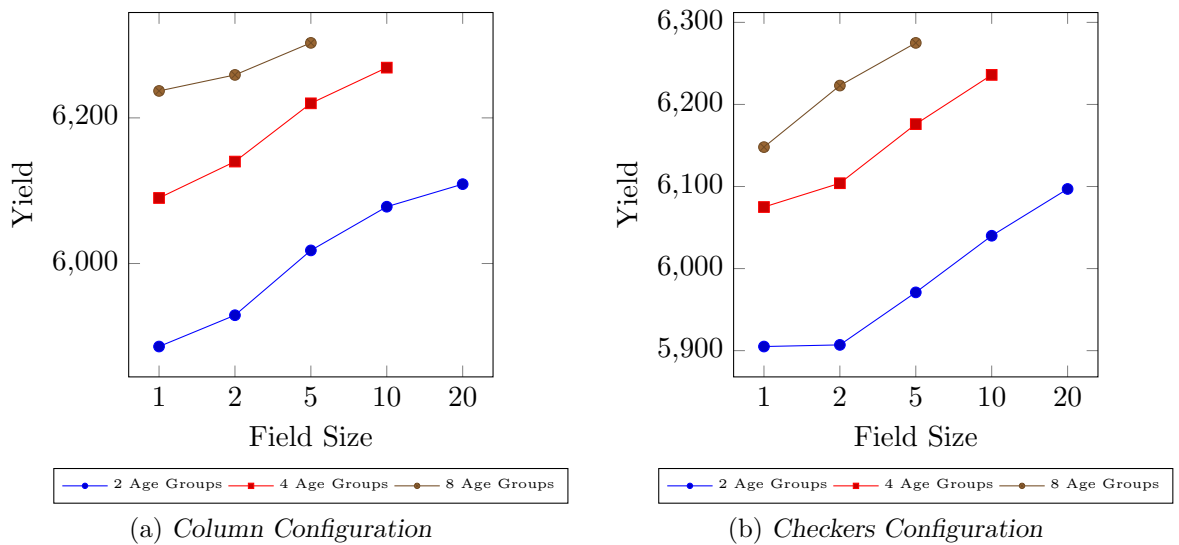


FIGURE B.13: Field size comparison for shaped function and 8 months harvesting age.

The results for the shaped maturity function and a harvesting age of 10 months are provided in Figure B.14. A general trend of an increase in fields size that leads to an increase in yields can be seen. There is an exception where the yield reduced when the field size increased from 1 to 2 for the *column* configuration and 8 age groups.

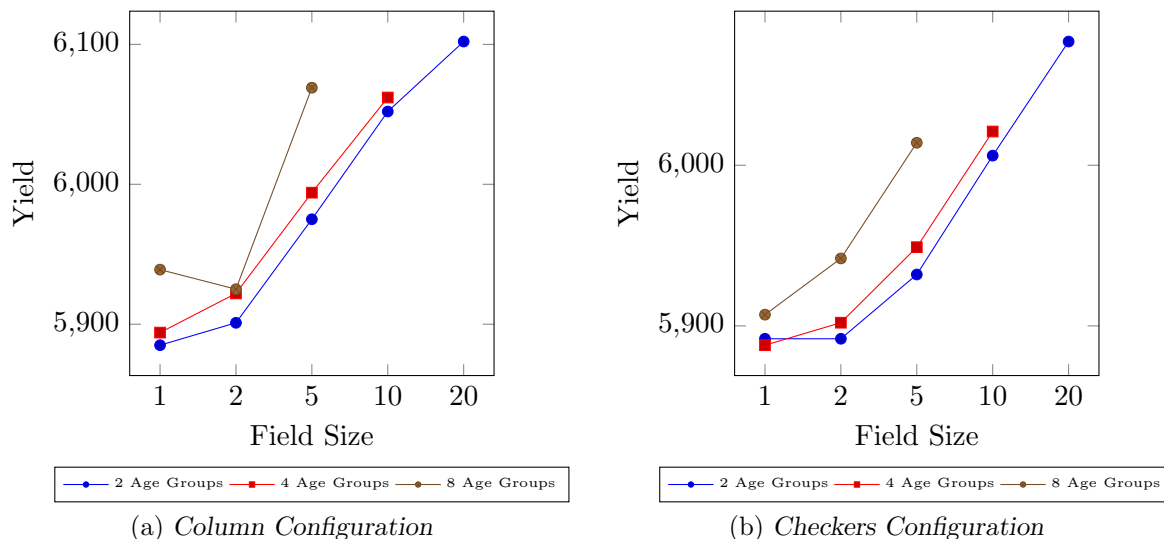


FIGURE B.14: Field size comparison for shaped function and 10 months harvesting age.

The results for the shaped maturity function and a harvesting age of 12 months are provided in Figure B.15. A general trend of an increase in fields size leading to an increase in yields, can be seen. Once again there is an exception where the yield reduced when the field size increased from 1 to 2 for the *column* configuration and 8 age groups.

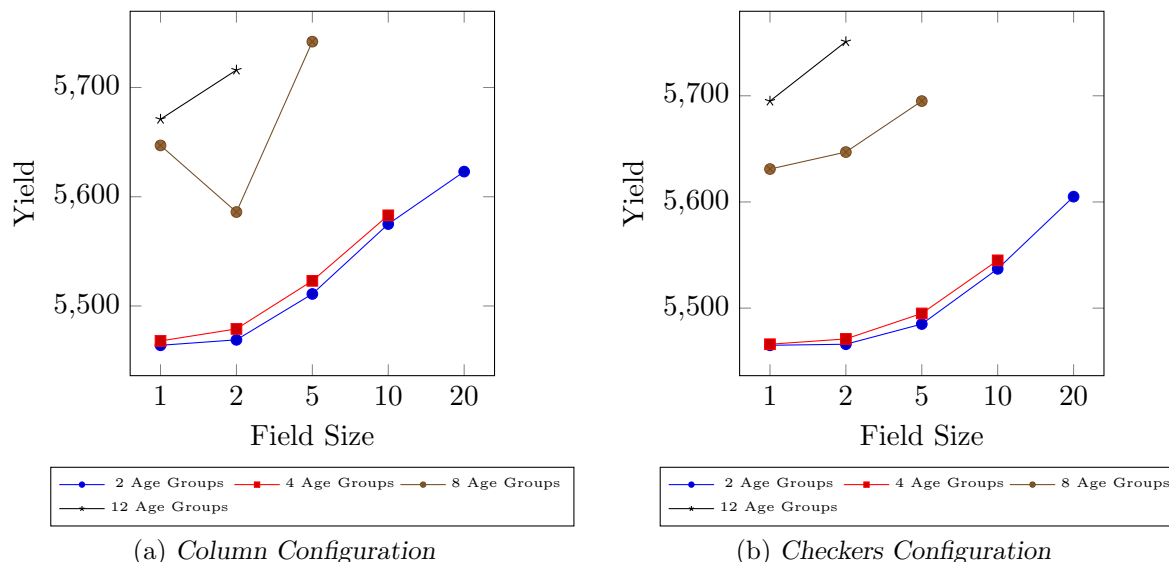


FIGURE B.15: Field size comparison for shaped function and 12 months harvesting age.

The results for the shaped maturity function and a harvesting age of 14 months are provided in Figure B.16. A general trend of an increase in fields size that leads to an increase in yields can be seen.

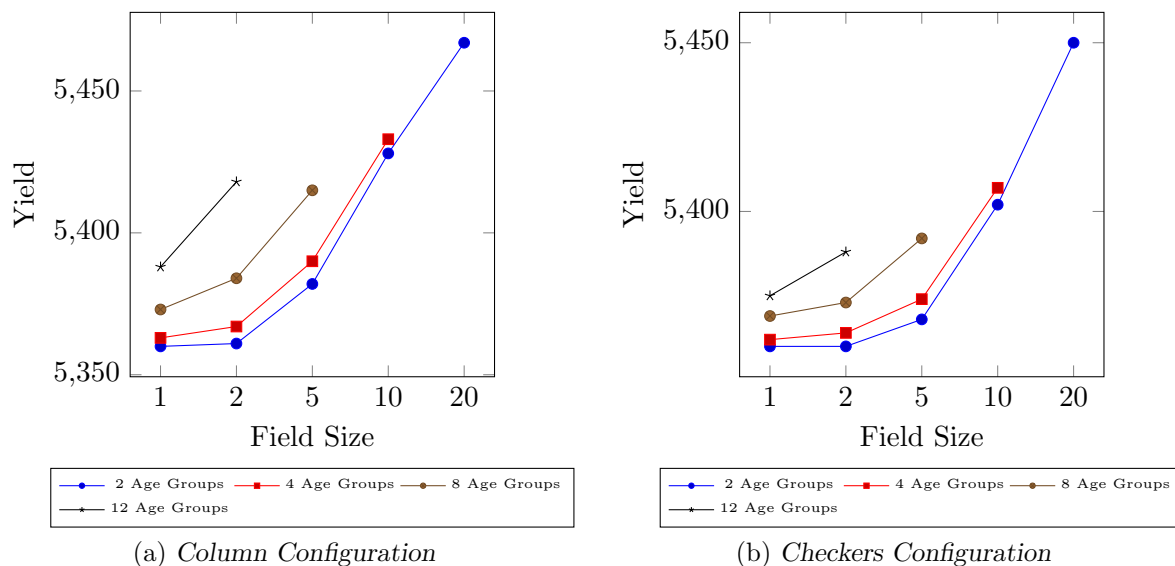


FIGURE B.16: Field size comparison for shaped function and 14 months harvesting age.

The results for the shaped maturity function and a harvesting age of 16 months are provided in Figure B.17. A general trend of an increase in fields size that leads to an increase in yields can be seen, however, a few exceptions are present. The yield reduced when the field size increased from 1 to 2 for the *column* configuration and 8, 12 & 16 age groups. The same reduction in yield is seen for the *checkers* configuration and 16 age groups.

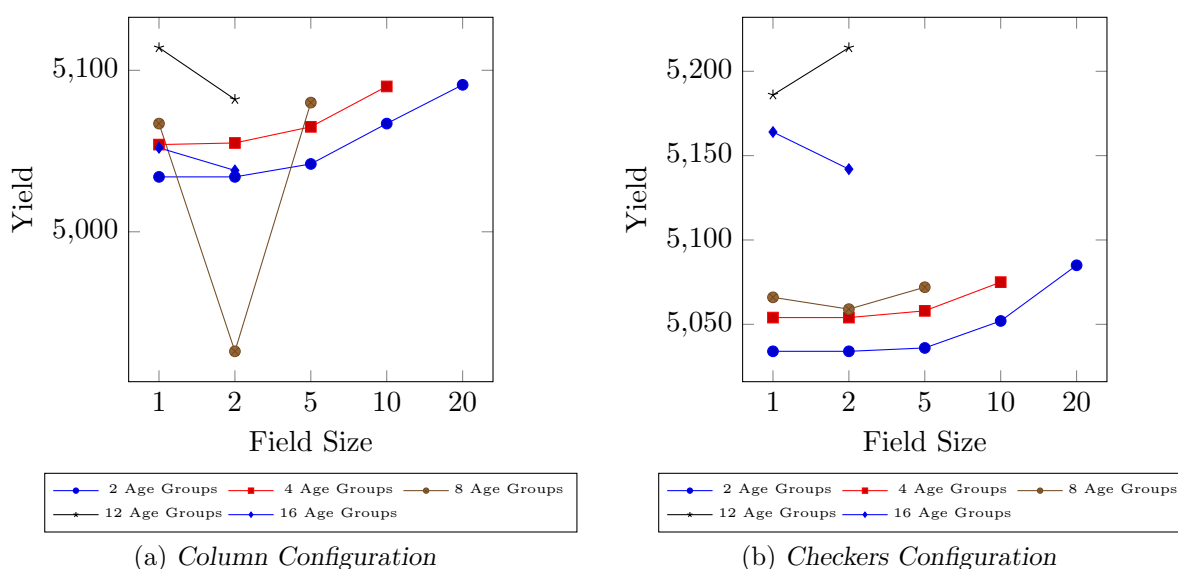


FIGURE B.17: Field size comparison for shaped function and 16 months harvesting age.

The results for the shaped maturity function and a harvesting age of 18 months are provided in Figure B.18. The usual trend of an increase in fields size that leads to an increase in yields does not seem to apply here, with very little benefit obtained from increasing field sizes.

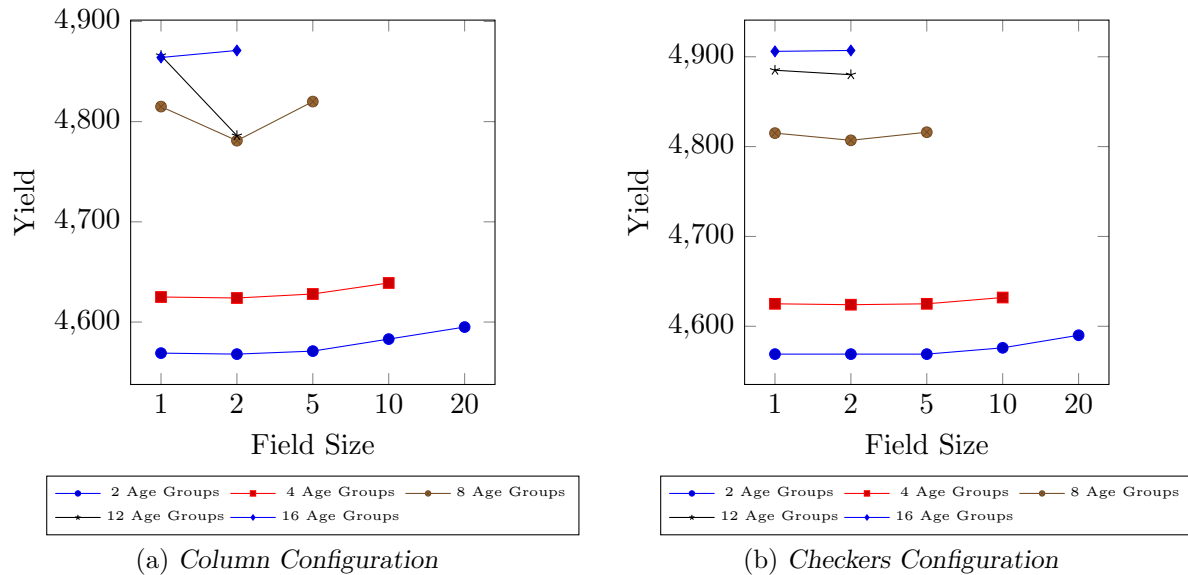


FIGURE B.18: Field size comparison for shaped function and 18 months harvesting age.

APPENDIX C

Age group analysis

The number of age groups within the planted crops has an impact on the spreading of Eldana infestations. This impact was discussed in §4.3, where the results for the linear maturity function was presented. In this Appendix, the results for the other maturity functions are presented and discussed.

Similar results are obtained for all maturity functions. This indicates that the recommendations made should hold for any maturity function.

C.1 Increasing maturity function

In Figure C.1, the results for the increasing maturity function and a harvesting age of 8 months are provided. A general trend of more age groups leading to increased yields, is visible.

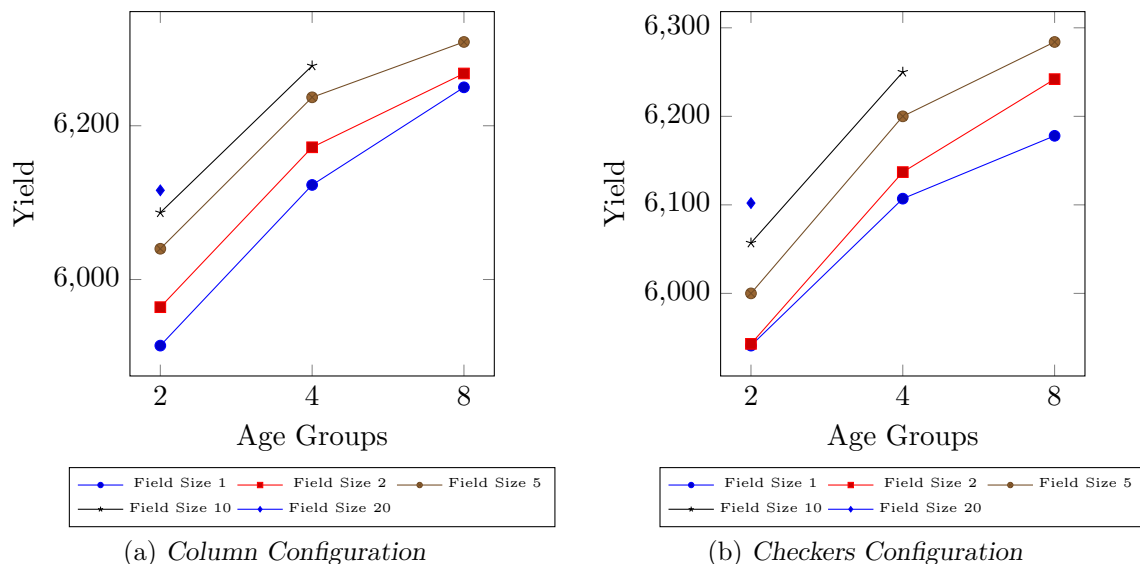


FIGURE C.1: Age group comparison for increasing function and 8 months harvesting age.

In Figure C.2, the results for the increasing maturity function and a harvesting age of 10 months are provided. A general trend that more age groups that leads to increased yields is still visible, but with reduced benefit when compared to the results for a harvesting age of 8 months.

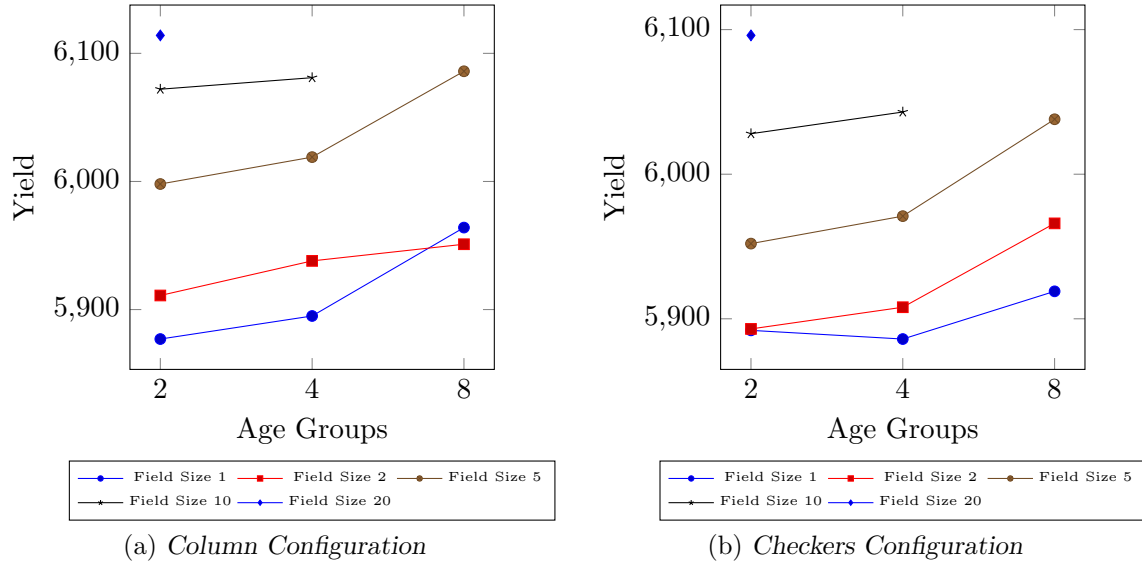


FIGURE C.2: Age group comparison for increasing function and 10 months harvesting age.

In Figure C.3, the results for the increasing maturity function and a harvesting age of 12 months are provided. A general trend of more age groups leading to increased yields, is visible.

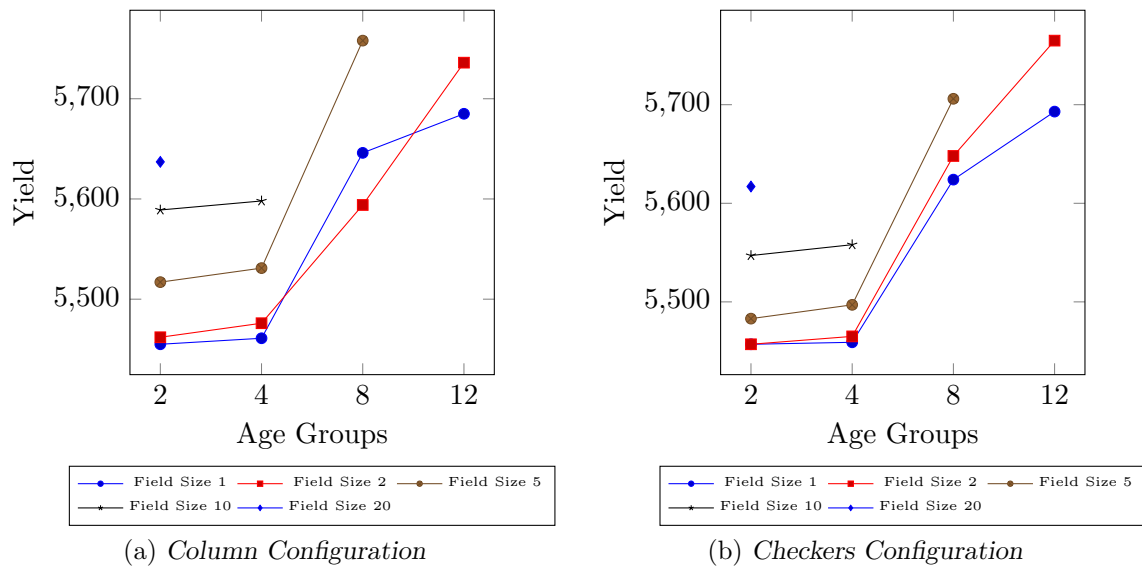


FIGURE C.3: Age group comparison for increasing function and 12 months harvesting age.

In Figure C.4, the results for the increasing maturity function and a harvesting age of 14 months are provided. A general trend of more age groups that leads to increased yields is visible.

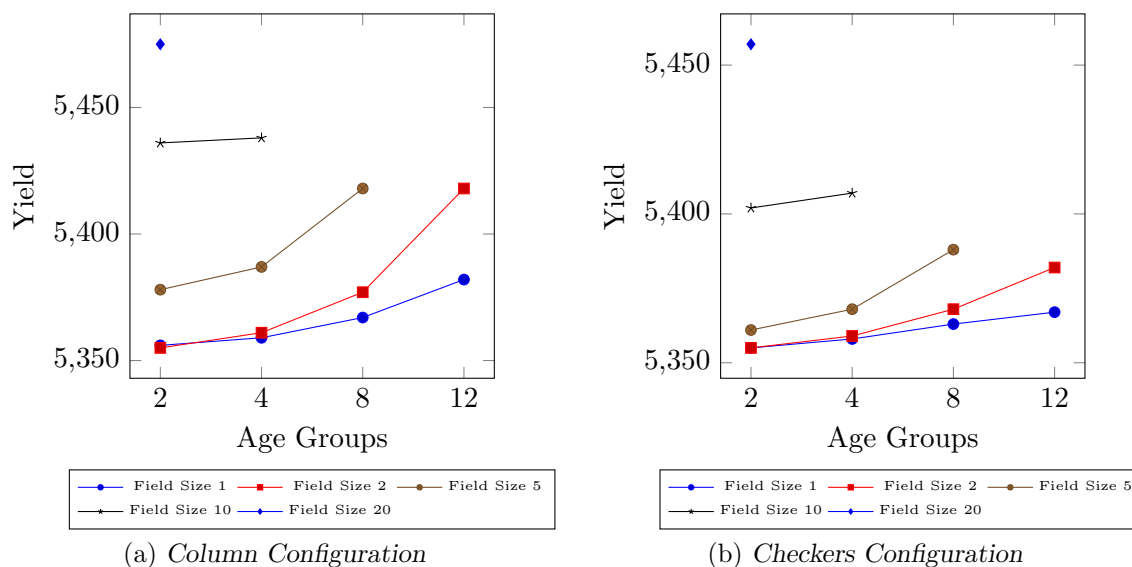


FIGURE C.4: Age group comparison for increasing function and 14 months harvesting age.

In Figure C.5, the results for the increasing maturity function and a harvesting age of 16 months are provided. A general trend that more age groups that leads to increased yields is seen from age groups 2 till 12, with the exception of 8 age groups for the *column* configuration and a field size of 2. However, a decrease in yield are seen when increasing the age groups to 16.

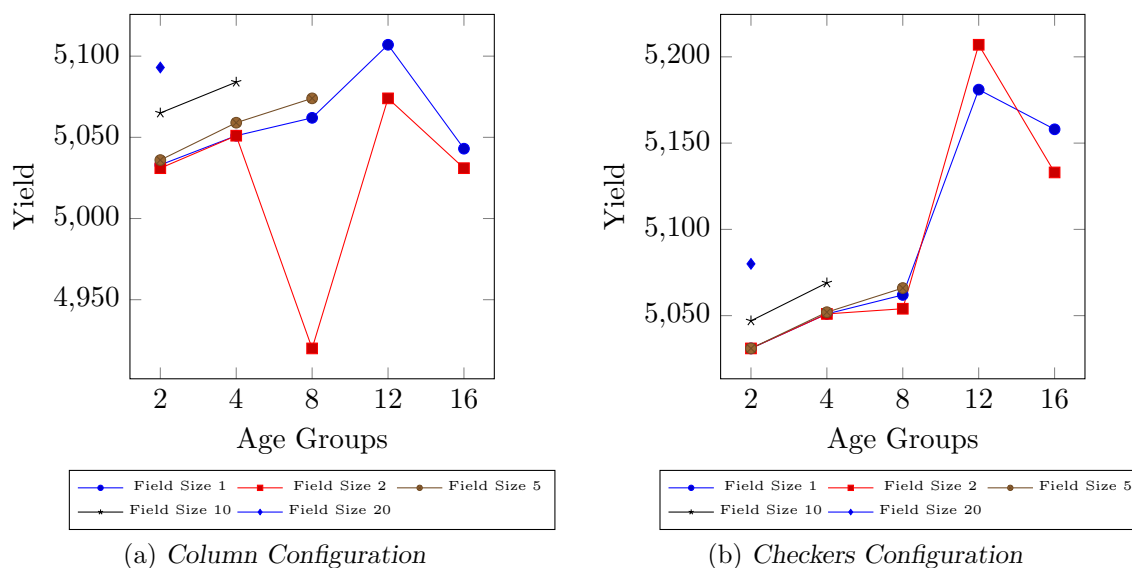


FIGURE C.5: Age group comparison for increasing function and 16 months harvesting age.

In Figure C.6, the results for the increasing maturity function and a harvesting age of 18 months are provided. A general trend of more age groups leading to increased yields, is visible.

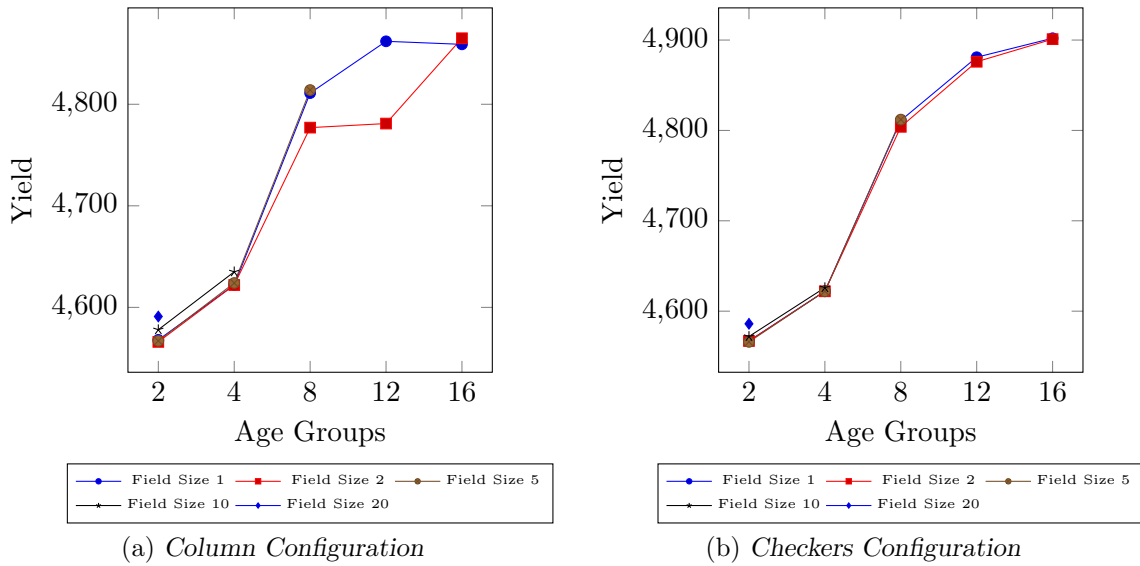


FIGURE C.6: Age group comparison for increasing function and 18 months harvesting age.

C.2 Decreasing maturity function

In Figure C.7, the results for the decreasing maturity function and a harvesting age of 8 months are provided. A general trend of more age groups leading to increased yields, is visible.

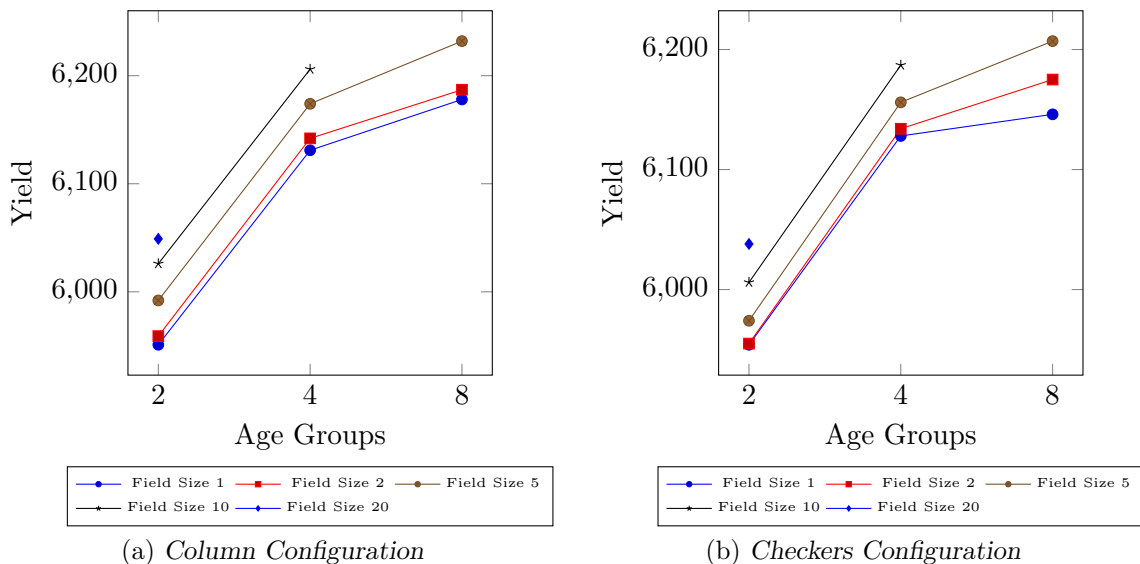


FIGURE C.7: Age group comparison for decreasing function and 8 months harvesting age.

In Figure C.8, the results for the decreasing maturity function and a harvesting age of 10 months are provided. A general trend that more age groups that leads to increased yields is still visible, but with reduced benefit when compared to the results for a harvesting age of 8 months. There is an exception where the yield reduced when the number of age groups increased from 4 to 8 for the *column* configuration and a field size of 2.

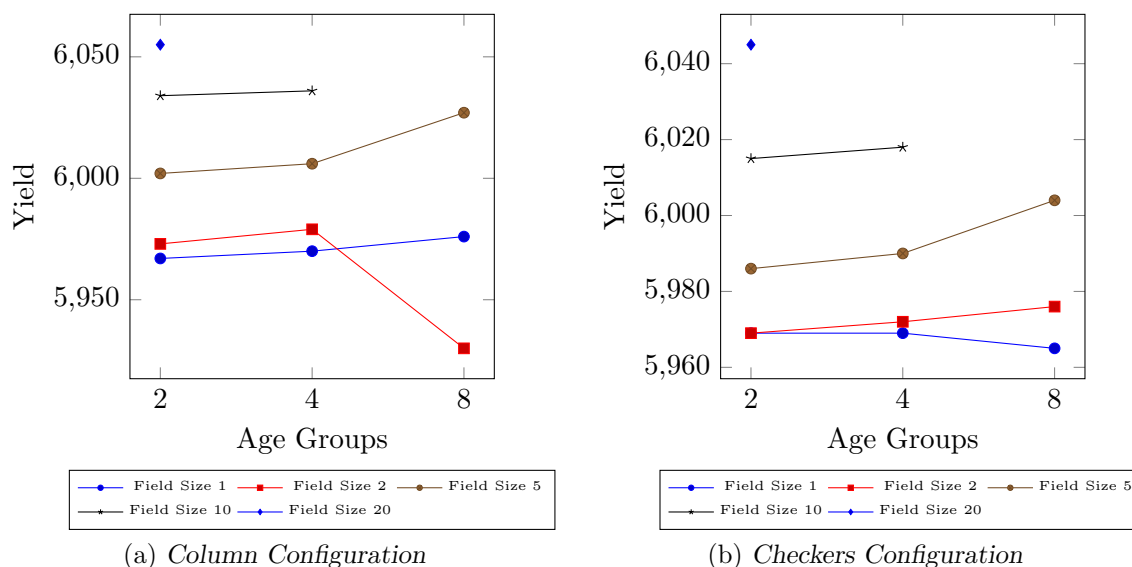


FIGURE C.8: Age group comparison for decreasing function and 10 months harvesting age.

In Figure C.9, the results for the decreasing maturity function and a harvesting age of 12 months are provided. A general trend of more age groups leading to increased yields, is visible. There is an exception where the yield reduced when the number of age groups increased from 8 to 12 for the *column* configuration and a field size of 1.

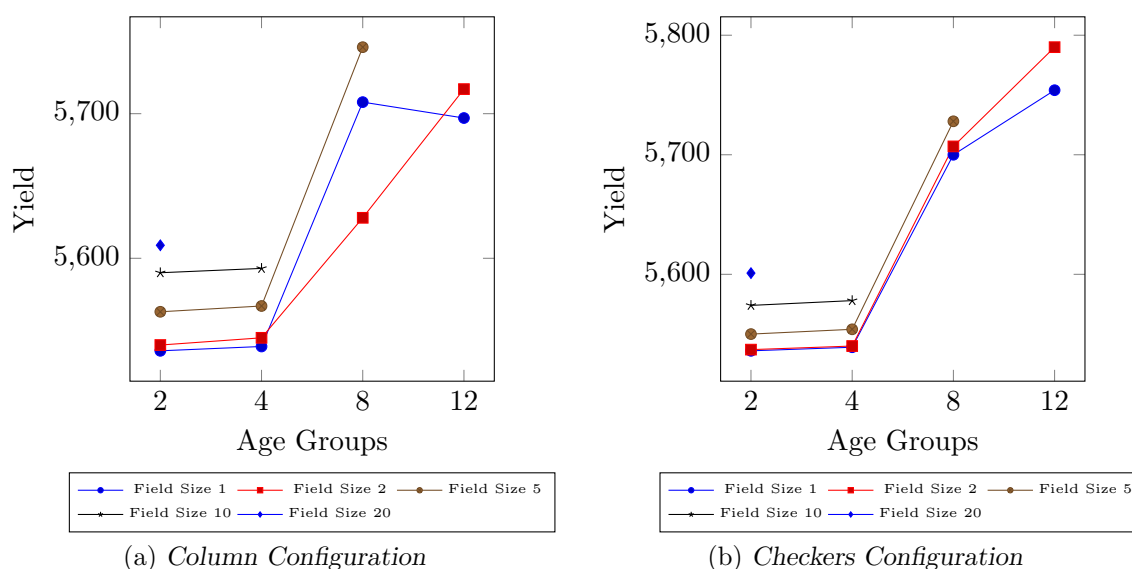


FIGURE C.9: Age group comparison for decreasing function and 12 months harvesting age.

In Figure C.10, the results for the decreasing maturity function and a harvesting age of 14 months are provided. A general trend of more age groups that leads to increased yields is visible.

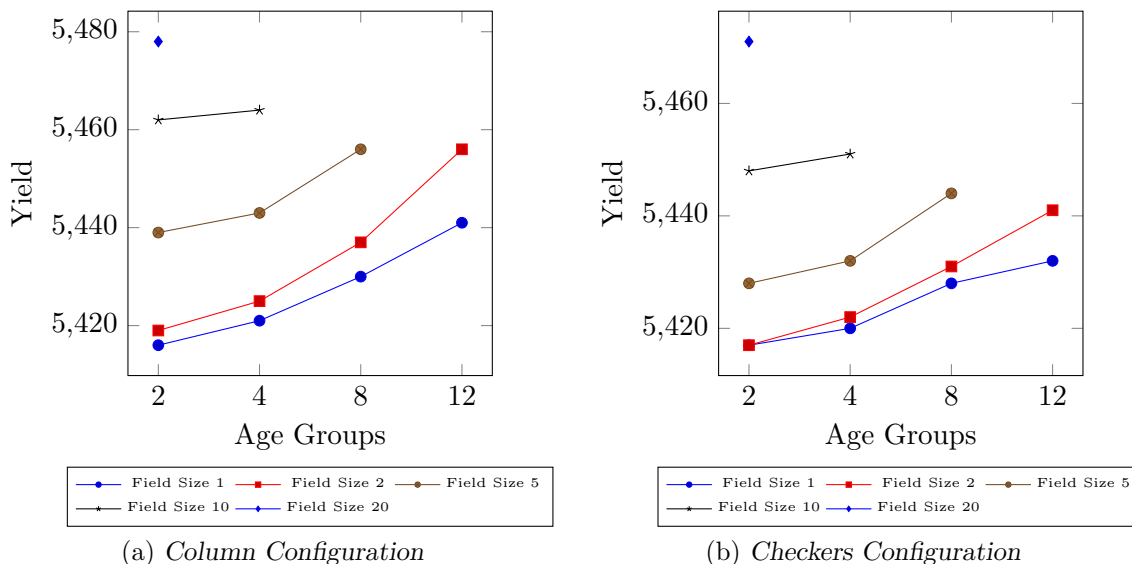


FIGURE C.10: Age group comparison for decreasing function and 14 months harvesting age.

In Figure C.11, the results for the decreasing maturity function and a harvesting age of 16 months are provided. A general trend that more age groups that leads to increased yields is seen from age groups 2 till 12, with the exception of 8 age groups for the *column* configuration and a field size of 2. However, a decrease in yield are seen when increasing the age groups to 16.

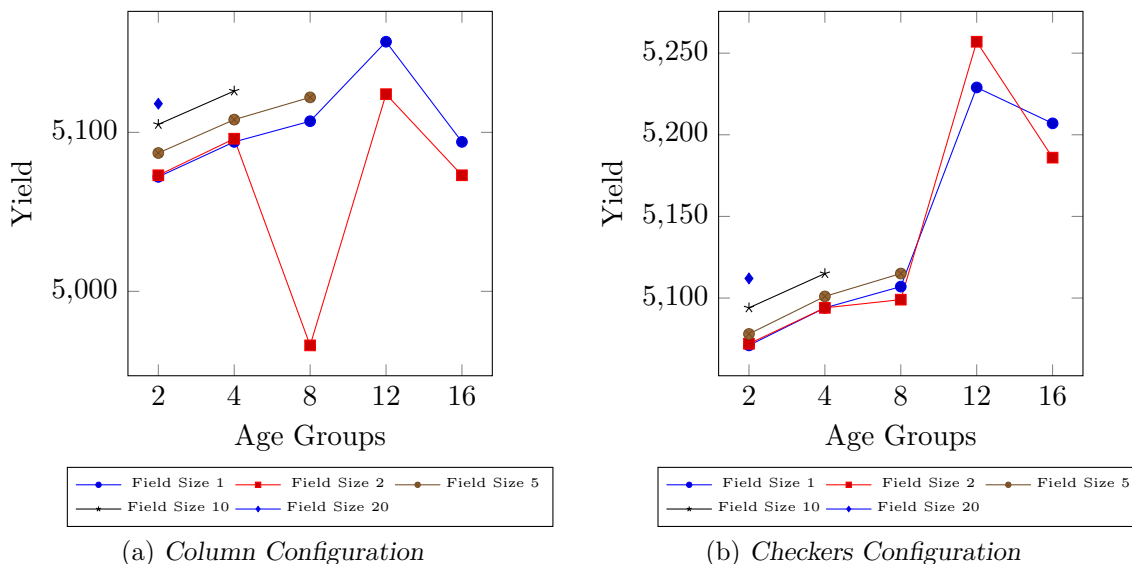


FIGURE C.11: Age group comparison for decreasing function and 16 months harvesting age.

In Figure C.12, the results for the decreasing maturity function and a harvesting age of 18 months are provided. A general trend of more age groups leading to increased yields, is visible.

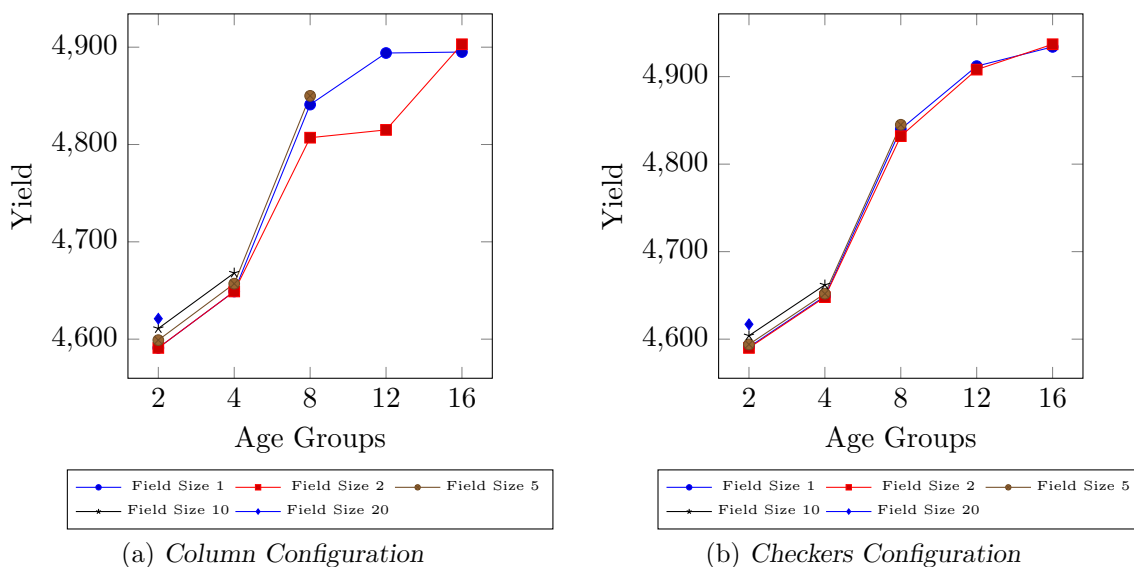


FIGURE C.12: Age group comparison for decreasing function and 18 months harvesting age.

C.3 Shaped maturity function

In Figure C.13, the results for the shaped maturity function and a harvesting age of 8 months are provided. A general trend of more age groups leading to increased yields, is visible.

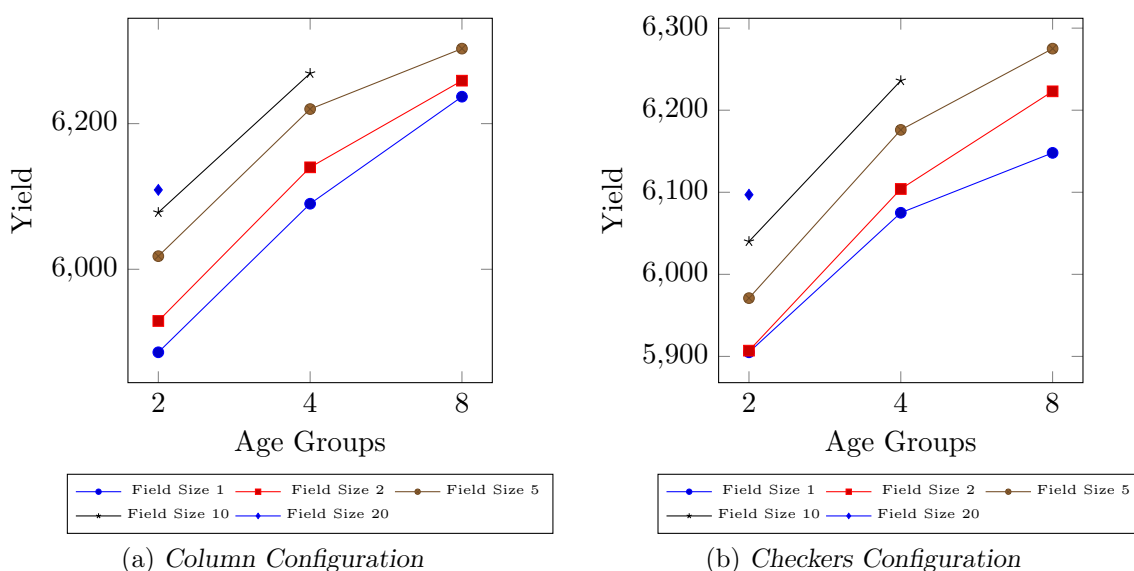


FIGURE C.13: Age group comparison for shaped function and 8 months harvesting age.

In Figure C.14, the results for the shaped maturity function and a harvesting age of 10 months are provided. A general trend that more age groups that leads to increased yields is still visible, but with reduced benefit when compared to the results for a harvesting age of 8 months.

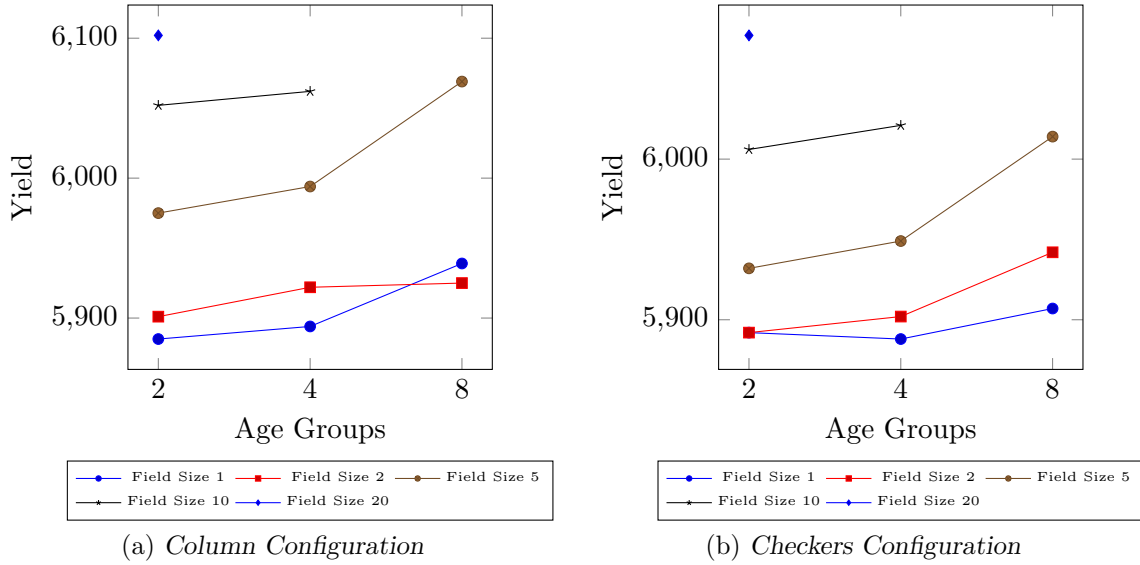


FIGURE C.14: Age group comparison for shaped function and 10 months harvesting age.

In Figure C.15, the results for the shaped maturity function and a harvesting age of 12 months are provided. A general trend of more age groups leading to increased yields, is visible.

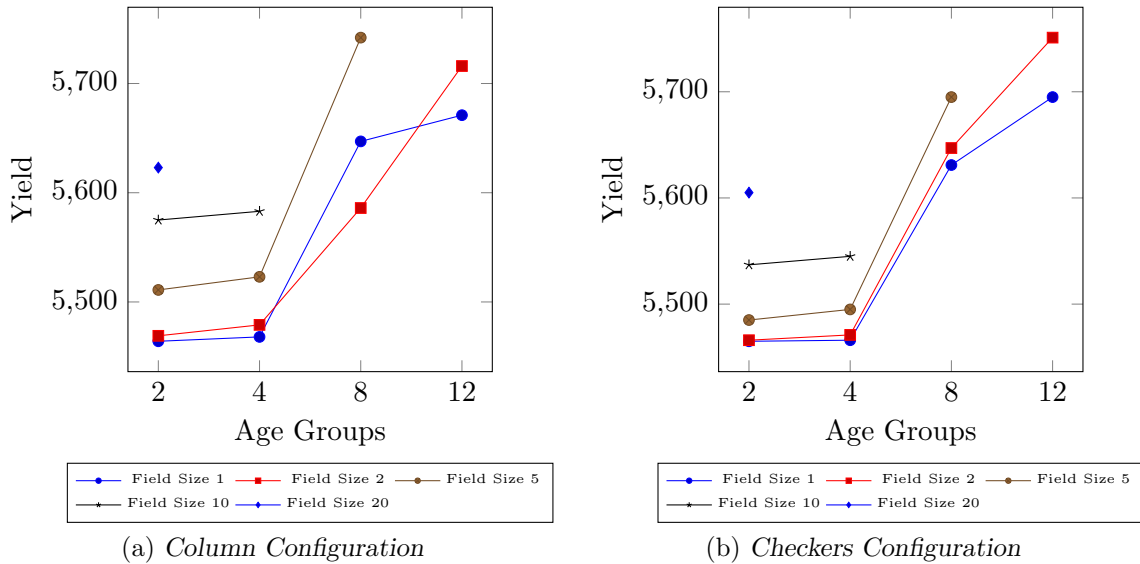


FIGURE C.15: Age group comparison for shaped function and 12 months harvesting age.

In Figure C.16, the results for the shaped maturity function and a harvesting age of 14 months are provided. A general trend of more age groups that leads to increased yields is visible.

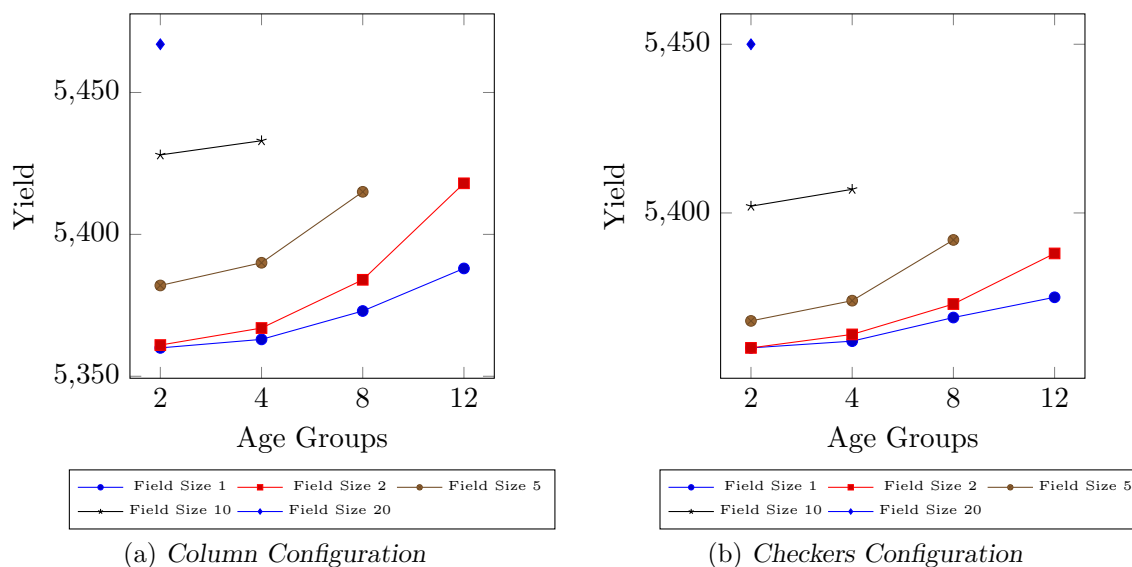


FIGURE C.16: Age group comparison for shaped function and 14 months harvesting age.

In Figure C.17, the results for the shaped maturity function and a harvesting age of 16 months are provided. A general trend that more age groups that leads to increased yields is seen from age groups 2 till 12, with the exception of 8 age groups for the *column* configuration and a field size of 2. However, a decrease in yield are seen when increasing the age groups to 16.

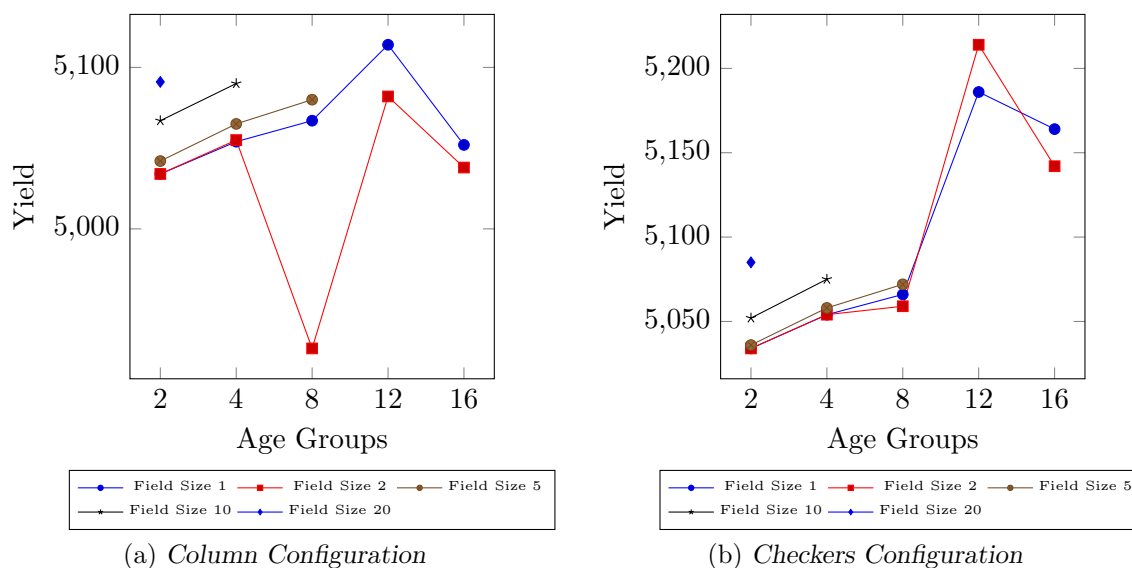


FIGURE C.17: Age group comparison for shaped function and 16 months harvesting age.

In Figure C.18, the results for the shaped maturity function and a harvesting age of 18 months are provided. A general trend of more age groups leading to increased yields, is visible.

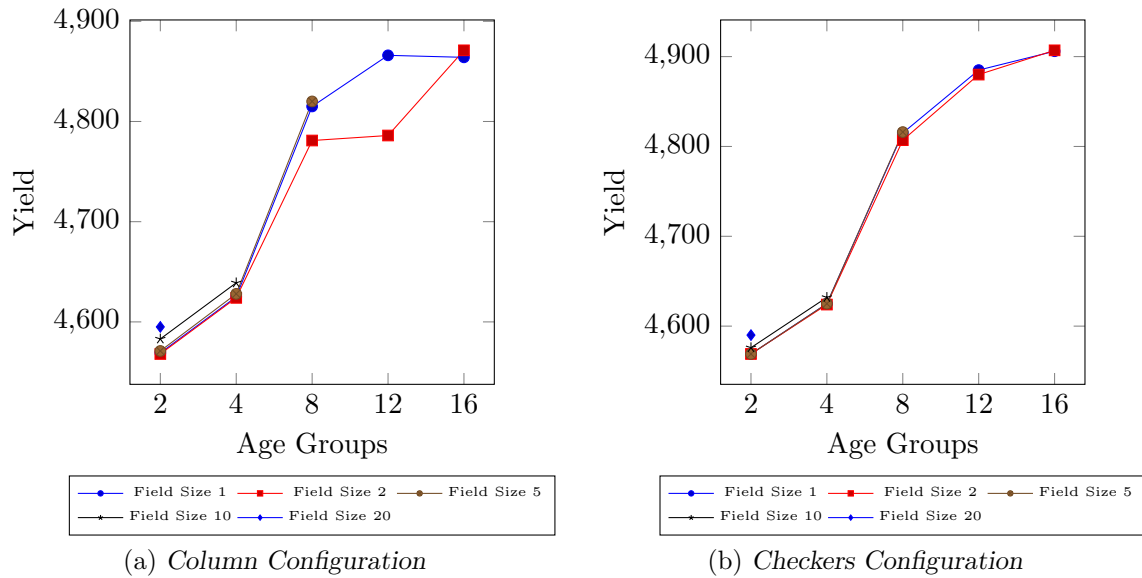


FIGURE C.18: Age group comparison for shaped function and 18 months harvesting age.

APPENDIX D

Sensitivity analysis: Maturity function

As part of sensitivity analysis, different factors were applied to the linear maturity function to determine a relationship between the speed of Eldana growth and expected sucrose yield. The factors applied for this analysis was 0.1, 0.25, 0.5, 0.75 and 1, where 1 would have the default maturity function used in the simulation model. These factors were applied in simulations where the harvesting age was fixed at 12 month, with the results for factors 0.1, 0.25 & 0.5 provided in Table D.1 and the results for factors 0.75 & 1 provided in Table D.2.

Field Size	Factor = 0.1				Factor = 0.25				Factor = 0.5			
	2	4	8	12	2	4	8	12	2	4	8	12
1	5671	5679	5866	5871	5639	5647	5835	5841	5586	5596	5785	5792
2	5686	5695	5792	5890	5655	5664	5761	5864	5602	5614	5714	5818
5	5723	5726	5912	N/A	5692	5697	5885	N/A	5643	5651	5843	N/A
10	5751	5751	N/A	N/A	5725	5726	N/A	N/A	5681	5683	N/A	N/A
20	5768	N/A	N/A	N/A	5744	N/A	N/A	N/A	5704	N/A	N/A	N/A

TABLE D.1: Sucrose yield for the various maturity function factors, assuming fixed harvesting age of 12 months

Field Size	Factor = 0.75				Factor = 1			
	2	4	8	12	2	4	8	12
1	5538	5549	5736	5745	5499	5510	5692	5699
2	5555	5567	5666	5773	5513	5524	5623	5728
5	5598	5606	5799	N/A	5555	5564	5755	N/A
10	5639	5642	N/A	N/A	5598	5602	N/A	N/A
20	5664	N/A	N/A	N/A	5625	N/A	N/A	N/A

TABLE D.2: Sucrose yield for the various maturity function factors, assuming fixed harvesting age of 12 months

The smaller the factor that is applied, the more favourable the obtained results. This is to be expected, as a decrease in maturity probabilities leads lower infestation levels and increased sucrose yields.